

Principles of Protein Group SUMO Modification Substantiated in DNA Repair

Dissertation
zur Erlangung des Doktorgrades
der Fakultät für Biologie der
Ludwig-Maximilians-Universität
München

vorgelegt von
Diplom-Biochemiker
Ivan Psakhye

Juli 2013

Eidesstattliche Erklärung

Hiermit erkläre ich, dass ich die vorliegende Dissertation selbständig und ohne unerlaubte Hilfe angefertigt habe. Ich habe weder anderweitig versucht, eine Dissertation einzureichen oder eine Doktorprüfung durchzuführen, noch habe ich diese Dissertation oder Teile derselben einer anderen Prüfungskommission vorgelegt.

Ivan Psakhye

München, den 04.07.2013

Promotionsgesucht eingereicht:

04.07.2013

Tag der mündlichen Prüfung:

29.10.2013

Erster Gutachter:

Prof. Dr. Stefan Jentsch

Zweiter Gutachter:

Prof. Dr. Peter B. Becker

Die vorliegende Arbeit wurde zwischen September 2007 und Februar 2013 unter Anleitung von Prof. Dr. Stefan Jentsch am Max-Planck-Institut für Biochemie in Martinsried durchgeführt.

Wesentliche Teile dieser Arbeit sind in folgenden Publikationen veröffentlicht:

Psakhye I. and Jentsch S. Protein group modification and synergy in the SUMO pathway as exemplified in DNA repair. *Cell*; 2012 (151, 4, 807-820)

Jentsch S. and **Psakhye I.** Control of nuclear activities by substrate-selective and protein group SUMOylation. *Annual Review of Genetics*; 2013 (47, 185-204)

TABLE OF CONTENTS

I. SUMMARY	1
II. INTRODUCTION	2
II.1 Ubiquitin and Ubiquitin-like Protein Modifiers	2
II.1.1 Comparison of the Ubiquitin and SUMO Modification Pathways	2
II.1.2 Molecular Mechanisms of SUMO Modification	7
II.1.3 SUMO Pathway Enzymes and Substrate Specificity	9
II.2 DNA Damage Repair	14
II.2.1 Homologous Recombination-mediated DNA Double-strand Break Repair	16
II.2.2 DNA Damage Checkpoint	19
II.2.3 SUMO Modification in DNA Repair	21
II.3 Aim of This Study	23
III. RESULTS	25
III.1 Protein Group SUMOylation upon DNA Damage	25
III.1.1 Identification of SUMO Substrates Induced by Specific DNA Damage Types	25
III.1.2 Synchronous Collective SUMOylation of a Whole Set of HR Proteins	27
III.2 Resection and Exposure of ssDNA Triggers SUMOylation Wave in HR	31
III.2.1 Long-range DNA Resection is Required for SUMOylation of HR Proteins	31
III.2.2 Exposure of ssDNA is the Trigger for HR Protein Group SUMOylation	33
III.2.3 Crosstalk between SUMOylation in HR and DNA Damage Checkpoint	35
III.3 DNA-bound SUMO Ligase Siz2 Induces a SUMOylation Wave in HR	38
III.3.1 SUMOylation in HR is Mediated by Sequence-nonspecific DNA-bound Siz2	38
III.3.2 Features of Siz2 Required for Efficient Protein Group SUMOylation in HR	42
III.3.3 Artificial Targeting of HR Proteins to DNA Triggers Their SUMOylation	46
III.4 SUMOylation Promotes Physical Interactions between HR Proteins	49
III.4.1 SUMOylation of HR Proteins on Chromatin Promotes Complex Formation	49
III.4.2 Identification of SUMO-Acceptor Lysine Residues in the Core HR Proteins	54
III.5 HR Protein SUMOylation Accelerates DNA Repair	56
III.5.1 Protein Group SUMOylation Facilitates HR	56
III.5.2 SUMOylation in HR Accelerates DSB Repair by Promoting Rad51 Loading	58

TABLE OF CONTENTS

IV. DISCUSSION	61
IV.1 Protein Group SUMOylation	61
IV.2 Specificity of SUMO Modification	64
IV.3 Synergy in the SUMO Pathway	66
IV.4 Dynamics of SUMO-SIM-assisted Assemblies	67
V. MATERIALS AND METHODS	70
V.1 Computational Analyses	70
V.2 Microbiological and Genetic Techniques	70
V.2.1 <i>E. coli</i> techniques	70
V.2.2 <i>S. cerevisiae</i> techniques	72
V.3 Molecular Biology Techniques	82
V.3.1 Isolation of DNA	82
V.3.2 Molecular cloning	83
V.3.3 Polymerase chain reaction	84
V.4 Biochemistry Techniques	86
V.4.1 Preparation of yeast protein extracts	87
V.4.2 Gel electrophoresis and immunoblot techniques	87
V.4.3 Protein purification and binding experiments	89
V.4.4 Chromatin immunoprecipitation, binding and related assays	90
V.5 Mass Spectrometry Analyses	92
VI. LITERATURE	93
Abbreviations	105
Acknowledgements	108
Curriculum Vitae	109

I. SUMMARY

Posttranslational modifications (PTMs) of proteins by covalent attachment of functional groups (like phosphorylation, acetylation, methylation, glycosylation, etc.) are of key importance for the cell as they regulate various aspects of protein behavior after its synthesis, e.g., dictate protein interaction properties, change catalytic activity of enzymes, induce conformational changes, guide subcellular localization and determine protein stability. A special class of protein PTMs is the conjugation of small proteins of the ubiquitin family to typically acceptor lysine residues of the substrates. The reversible nature of this PTM and the presence of dedicated domains that specifically recognize modified substrates make this type of protein modification instrumental for the regulation of numerous biological pathways. For ubiquitylation, strong substrate selectivity due to the presence of highly diversified conjugation machinery is characteristic and well studied, especially in case of ubiquitin's proteolytic role. On the contrary, much less is known about the principles of substrate specificity and mechanisms of PTM action in the ubiquitin-like protein SUMO modification system.

Despite the fact that SUMOylation specifically targets hundreds of substrates and major conjugation steps are identical with ubiquitin system, strikingly only a handful of enzymes operate in the SUMO pathway, suggesting that other principles of substrate selectivity must apply and perhaps distinct mechanisms of PTM action exist in the SUMO pathway. Moreover, the recognition of SUMO modification is surprisingly simple and relies mainly on a short hydrophobic sequence known as SUMO-interacting motif (SIM), in striking contrast to the ubiquitin system, where numerous ubiquitin-binding domains exist with different interaction specificities. All these, together with the observations that SUMO conjugation machinery seems rather promiscuous *in vitro*, that typically only a small fraction of a protein is being SUMOylated at a given time, and that specific SUMOylation-defective mutants often exhibit no obvious phenotypes, whereas SUMO pathway mutants do, emphasize the question of substrate specificity in the SUMO system and suggest other principles of SUMO action on its substrates.

Here, we address the question of SUMOylation specificity and function using DNA double-strand break (DSB) repair pathway via homologous recombination (HR) as a case study because of its strong ties to the SUMO system. First, using SILAC-based proteomic approach we show that proteins acting in the same DNA repair pathway become collectively SUMOylated upon a specific stimulus (HR factors – upon DSB induction; nucleotide excision repair factors – upon exposure to UV light), suggesting that SUMO machinery often targets protein groups within the same pathway. Then, focusing on the DSB repair we find that DNA-bound SUMO ligase Siz2 catalyzes collective multisite SUMOylation of a whole set of HR factors. Repair proteins are loaded onto resected single-stranded DNA (ssDNA) in the vicinity of the ligase, thus making exposure of ssDNA a precise trigger for modification. Protein group SUMOylation fosters physical interactions between the HR proteins engaged in DNA repair, because not only that they become collectively modified at multiple SUMO-acceptor sites, but they also possess multiple SIMs, which promote SUMO-SIM mediated complex formation. Only wholesale elimination of SUMOylation of the core HR proteins significantly affects the HR pathway by slowing down DNA repair, suggesting that SUMO acts synergistically on several proteins. Thus, we show that SUMOylation collectively targets functionally engaged protein group rather than individual proteins, whereas localization of modification enzymes and specific triggers ensure substrate specificity.

II. INTRODUCTION

II.1 Ubiquitin and Ubiquitin-like Protein Modifiers

Regulation of protein behavior by various posttranslational modifications (PTMs) is vital for the cell. Numerous functional groups (e.g., phosphate, acetyl, alkyl, glycosyl) can be conjugated to proteins, rapidly affecting their physical properties and thus greatly expanding functional assortment and dynamics of the proteome. The covalent attachment of small proteins of the ubiquitin family to substrates is a special PTM class widely used in the cell to direct diverse physiological processes (Kerscher et al., 2006). The first characterized and most well studied member of this protein modifier family is a small globular 76-amino acid (aa)-long protein called ubiquitin, highly conserved among the eukaryotes (Jentsch, 1992). The characteristic feature of ubiquitin is its β -grasp fold – globular three-dimensional core structure, which is being shared by other known ubiquitin-like (Ubl) protein modifiers including Rub1/NEDD8, Atg8, Atg12, Urm1, UFM1, ISG15, FAT10, FUB1/FAU, and Smt3/SUMO (Kerscher et al., 2006; Welchman et al., 2005).

Ubiquitin and SUMO (small ubiquitin-like modifier) both are known to reversibly modify hundreds of substrates affecting numerous cellular processes. For ubiquitylation, the principles of substrate selectivity and mechanistic consequences of the modification are extensively studied and relatively well understood. Highly diversified ubiquitin pathway components and existence of multiple ubiquitin-binding domains (UBDs) that can recognize various ubiquitylation events ensure high substrate specificity (Dikic et al., 2009; Husnjak and Dikic, 2012). For SUMOylation, on the contrary, much less is known regarding how relatively simple organized conjugation machinery recognizes its multiple targets (Gareau and Lima, 2010) and what are the functional outcomes of SUMO modification, especially that in many cases specific SUMOylation-defective mutants barely exhibit any abnormalities, while SUMO pathway mutants do show strong phenotypes.

II.1.1 Comparison of the Ubiquitin and SUMO Modification Pathways

The ubiquitin and SUMO modification pathways might seem very similar at the first sight (**Fig. 1**), however several striking differences exist that will be emphasized below.

INTRODUCTION

Both protein modifiers are being synthesized as inactive precursors, which need to be further processed by dedicated proteases in order to expose carboxyl (C)-terminal double-glycine motifs required for conjugation (Geiss-Friedlander and Melchior, 2007; Johnson, 2004; Kerscher et al., 2006). Covalent conjugation of modifiers to protein substrates involves an elaborate enzymatic cascade that via isopeptide bond formation attaches the modifier typically to the ϵ -amino group of an acceptor lysine (K) residue. This cascade is ATP-dependent and consists of several kinetically distinct steps mediated by the sequential action of specialized enzymes (Capili and Lima, 2007).

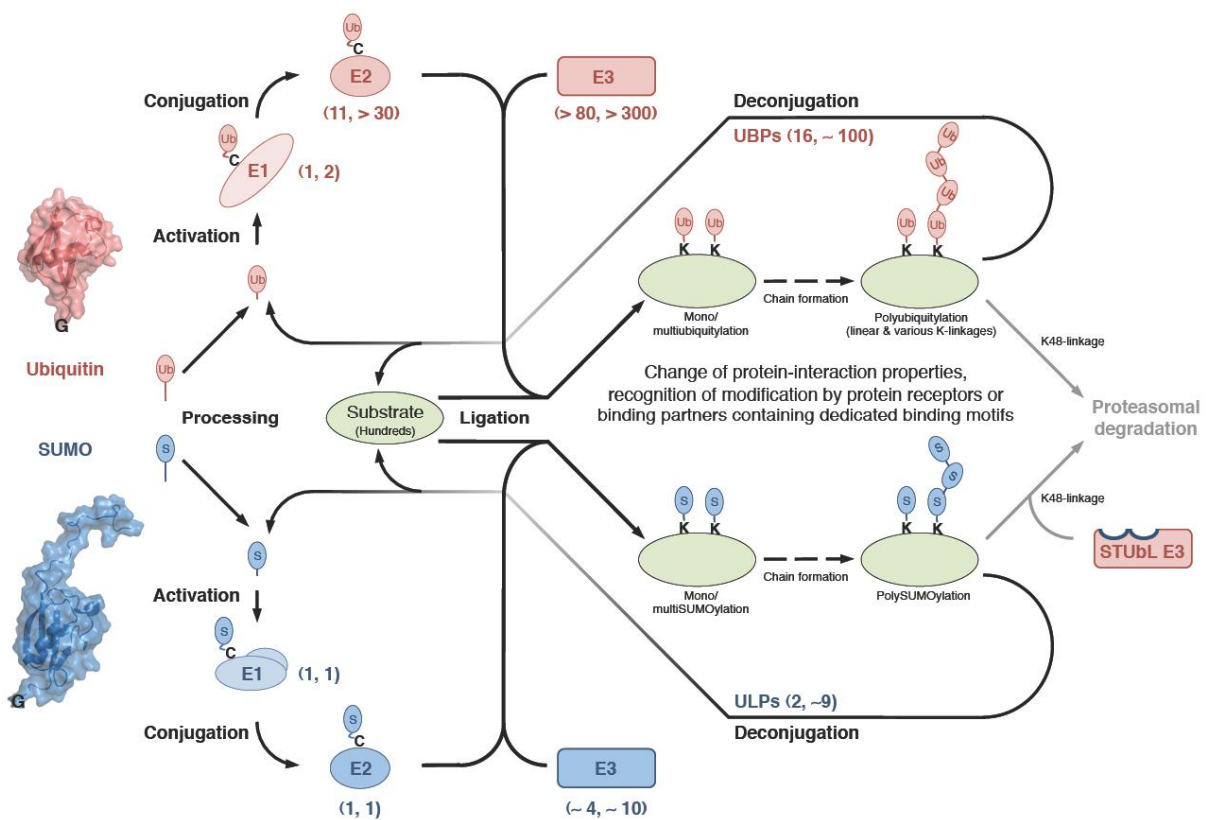


Figure 1. Comparison of the Ubiquitin and SUMO Modification Pathways

Ubiquitin (Ub, top, red) and SUMO (S, bottom, blue) conjugation machinery selectively targets hundreds of substrates (middle, green), despite striking difference in the number of ubiquitin E2 and E3 enzymes compared to the SUMO pathway. Processed modifiers are covalently attached to lysine (K) residues of substrates via their C-terminal glycine (G) residues. Modifiers can target single or multiple acceptor lysines of the substrate, or can form chains mediated by various K-linkages. Modification of the substrate changes its protein-interaction properties and can be recognized by protein receptors containing dedicated binding motifs (e.g., SIMs in the SUMO-targeted ubiquitin ligases). Modifications are reversible due to the presence of a large number of UBPs and relatively small number of ULPs, which mediate deconjugation of ubiquitin and SUMO from substrates, respectively. The major steps (processing, activation, conjugation, ligation and deconjugation) of ubiquitin and SUMO cycles are depicted and the number of involved enzymes in budding yeast and humans, respectively, are shown in parentheses.

INTRODUCTION

The ubiquitin/SUMO conjugation starts with the ATP hydrolysis required for the initial adenylation of the C-terminal glycine residue of the modifiers that has been exposed during processing of the precursors. This first step (termed activation) is catalyzed by modifier-specific activating enzymes (also called E1s). A single protein (Uba1) operates in budding yeast *S. cerevisiae* for the ubiquitin pathway, and a heterodimer (Aos1/Uba2) is utilized for the SUMO pathway (Johnson, 2004). Subsequently, ubiquitin/SUMO-AMP adducts become attached via high-energy thioester bonds to internal catalytic cysteine residues of the dedicated E1 enzymes (Johnson et al., 1997; Lois and Lima, 2005). This reaction requires large conformational changes in E1 and is needed to position the “activated” modifiers in the favorable orientation for their consecutive transfer to the catalytic cysteine residues of the respective conjugating enzymes (termed E2s). Whereas for the ubiquitin pathway 11 E2s exist in *S. cerevisiae* and more than 30 operate in humans, a single enzyme (Ubc9) mediates all SUMOylation events in budding yeast as well as in mammals (Johnson and Blobel, 1997; Tong et al., 1997). As a result of this second catalytic step (termed conjugation) thioester-linked complexes between the modifiers and the E2s are being formed. In case of the SUMO pathway, modifier-charged Ubc9 is capable of direct substrate recognition and modification of correct acceptor lysine residues *in vitro* (Bernier-Villamor et al., 2002; Gareau and Lima, 2010; Ulrich, 2009). Moreover, direct Ubc9 fusion to substrates mediates specific SUMOylation of these targets also *in vivo* (Jakobs et al., 2007). However, for most proteins and especially for ubiquitin targets the substrate modification reaction requires the presence of so-called ligases or E3s. It is important to note that the term “ligase” is operationally defined, as it refers collectively to proteins that stimulate the final transfer of the modifier from the E2 to the substrate (final conjugation step termed ligation), disregarding differences in mechanisms. For instance, in the case of the HECT (Homologous to E6-AP C-terminus) family of ubiquitin ligases the modifier is further transferred from E2s to catalytic cysteines of E3s forming high-energy intermediates prior to substrate modification (Rotin and Kumar, 2009). However, in most other cases, the ligases play non-enzymatic role as adaptors recruiting modifier-charged E2s in close vicinity of their substrates and enhancing the activity of the conjugating enzymes. In the ubiquitin system hundreds of E3s (due to combinatorial complexity) operate and determine high substrate selectivity of ubiquitylation (Woodsmith et al., 2012). However, it is not the case for the SUMO modification pathway, where a

INTRODUCTION

handful of E3s (only 4 in budding yeast) mediate specific SUMOylation of the substrates (Geiss-Friedlander and Melchior, 2007; Ulrich, 2009).

The ubiquitin and SUMO modifications are reversible. Dedicated enzymes mediate their cleavage from substrates. Again, multiple ubiquitin-specific proteases (UBPs) function in the ubiquitin pathway, while just a few ubiquitin-like protein (SUMO)-specific proteases (ULPs) operate in the SUMO system (Hickey et al., 2012). In the budding yeast only 2 SUMO deconjugating enzymes (Ulp1 and Ulp2) exist and are differentially localized in the cell, which seems to determine their substrate specificity. The maturation of the modifiers from their inactive precursors is another duty of the deconjugating enzymes.

The ubiquitin/SUMO conjugation machinery can target substrates for modification not only at individual or multiple acceptor lysine residues (termed mono/multi-ubiquitylation/SUMOylation), but can also generate chains consisting of multiple modifier moieties attached to each other via their internal lysines (poly-ubiquitylation/SUMOylation). For the ubiquitin system, chain formation plays important roles and tremendously increases the versatility of the pathway (Komander and Rape, 2012). In fact, not only all seven internal lysine residues of ubiquitin (K6, K11, K27, K29, K33, K48 and K63) can be used for chain formation, but also the α -amino group of its N-terminal methionine, resulting in poly-ubiquitin chains of different topologies (Kulathu and Komander, 2012). These chains of various lengths and linkages attached to substrates define unique signals that can be recognized by specialized ubiquitin receptors or interaction partners that harbor specific UBDs, many of which were identified in the ubiquitin pathway (Dikic et al., 2009; Finley, 2009; Husnjak and Dikic, 2012; Richly et al., 2005). On the contrary, in the SUMO system much less is known about the function of poly-SUMO chains (Ulrich, 2008). In *S. cerevisiae* mainly first three lysines (K11, K15, K19) located in the N-terminus of SUMO are being used for chain formation most likely due to the fact that they lie within so-called SUMO “consensus” motifs (see below), however all other internal lysines (K27, K38, K40, K41, K54, K58) are also found by mass spectrometry to be SUMOylated *in vitro* and *in vivo* (I. Psakhye & S. Jentsch, unpublished data). The biological functions of these various poly-SUMO chains and their recognition mode remain poorly characterized, especially that in striking difference to the ubiquitin pathway, which utilizes multiple UBDs, SUMOylated substrates are being recognized mainly by the single short hydrophobic SUMO-interacting motif (SIM, see below). Only recently, global analysis of SUMO chain function in budding yeast using SUMO

INTRODUCTION

variant with all nine lysines replaced by arginine was performed, implicating the poly-SUMO chain synthesis in the maintenance of transcriptional repression and higher-order chromatin structure (Srikumar et al., 2013).

High substrate selectivity is characteristic for the ubiquitin system, which can be largely explained by the complexity of its enzymatic repertoire. Ubiquitin E3 ligases specifically recognize and interact with particular protein motifs of individual substrates. These elements are termed degradation signals (degrons) in case of the ubiquitin-proteasome system (UPS), e.g., D-box and KEN-box motifs found in all targets of the APC/C^{Cdc20} and APC/C^{Cdh1} E3 complexes (Pfleger and Kirschner, 2000; Visintin et al., 1997; Wasch and Cross, 2002). In contrast, in the SUMO system the only E2 available (Ubc9) is often on its own able to recognize and correctly SUMOylate appropriate acceptor lysine residues both *in vitro* and *in vivo*, as was mentioned earlier. The validated SUMO-targeted lysines are most frequently found in extended loops or disordered regions of the substrates outside of conserved globular domains. In many cases an acceptor lysine lies within a ψ KX(D/E) motif, where ψ is a large hydrophobic residue (Rodriguez et al., 2001; Sampson et al., 2001). These residues can directly interact with Ubc9; the motif (termed consensus) adopts an extended conformation allowing the acceptor lysine to reach into the catalytic site of E2, while flanking residues within the motif facilitate interaction with Ubc9 (Bernier-Villamor et al., 2002; Gareau and Lima, 2010). In addition, several variants of the SUMO consensus motif were described, e.g., phosphorylation-dependent SUMO motif (PDSM), negatively charged amino acid-dependent SUMO motif (NDSM), N-terminal hydrophobic cluster SUMO motif (HCSM), all of which have additional elements extending interactions with Ubc9, or inverted consensus motif (Matic et al., 2010; Mohideen et al., 2009; Yang et al., 2006). Despite different motif names, it rather seems that SUMO-acceptor lysine simply has to be accessible and flexible enough within its surrounding context in order to fit into catalytic groove of Ubc9 for its modification.

Whereas recognition of different ubiquitin signals is mediated by a large variety of dedicated UBDs (at least 20 known), non-covalent interaction between SUMOylated substrate and its binding partners seems to be mediated by a SIM alone. The SIMs can be largely defined as short stretches of hydrophobic amino acids (typically V/I-X-V/I-V/I or inverted), which are in many, but not all, cases flanked by acidic residues that further support the interaction with basic residues on the surface of SUMO (Kerscher, 2007; Minty et al., 2000; Song et al., 2004). When bound to SUMO, the

INTRODUCTION

hydrophobic residues of the SIM fit into the hydrophobic groove on the SUMO surface extending its β -sheet structure. Many variants of SIMs exist (e.g., SIMa, SIMb, phosphor-SIM), but the hydrophobic core, consisting of just 3-4 aliphatic residues, is their essential component (Kerscher, 2007). In fact, short synthetic SIM-containing peptides carrying the hydrophobic core are fully capable of binding SUMO *in vitro* (Namanja et al., 2012). In essence, the SUMO modification is recognized by proteins harboring simple short “adhesive surfaces” known as SIMs. Not surprisingly, these motifs are found often at multiple copies in a wide range of proteins, including SUMO substrates and especially enzymes of the SUMO pathway, for instance ligases and SUMO-specific proteases (Gareau and Lima, 2010; Hickey et al., 2012).

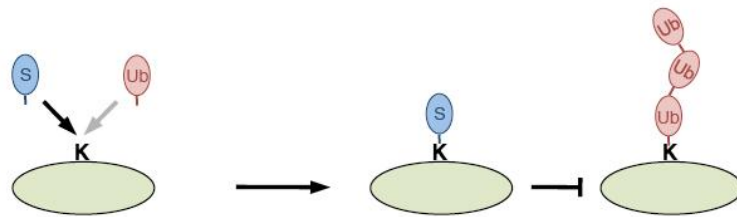
In summary, despite seeming similarity between the ubiquitin and SUMO pathways, the two modification systems have several major differences. First, while the components of the ubiquitin system are highly diversified in order to ensure immense substrate selectivity, the enzymatic apparatus of the SUMO system is surprisingly simple, yet both pathways target hundreds of substrates with high precision. Second, the SUMO conjugation machinery seems rather promiscuous, as *in vitro* Ubc9 (E2) alone is fully capable of substrate modification at correct SUMO-acceptor sites without the need for any ligase. Similarly, *in vivo* Ubc9 fusions to substrates mediate their correct modification in the absence of the ligases. Moreover, if accessible acceptor lysines are introduced (in context of a protein tag, e.g., Myc-tag) into SUMO substrates, they will in most cases also become readily modified *in vivo*. Third, while multiple dedicated UBDs specifically distinguish various types of ubiquitin modifications, the recognition of numerous SUMOylated targets largely depends on the single simple module – SIM. These striking differences suggest that other principles of substrate selectivity must apply and perhaps distinct mechanisms of PTM action exist in the SUMO pathway.

II.1.2 Molecular Mechanisms of SUMO Modification

To better understand the unusual behavior of the SUMO pathway, it is necessary to have a closer look at how SUMOylation affects principal biochemical properties of the modified substrates. There are three basic molecular consequences currently known for SUMO modification (**Fig. 2**).

SUMO modification

Competes for acceptor lysine with other PTMs



Interferes with protein-protein interactions



Fosters inter- and intramolecular protein interactions

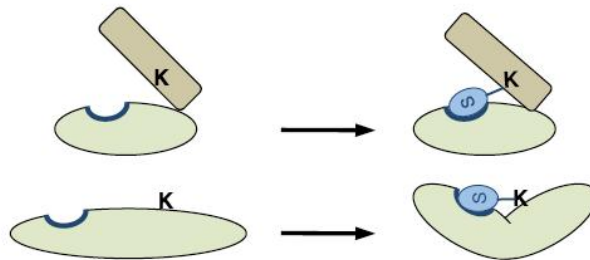


Figure 2. Basic Consequences of SUMO Modification

In principal, SUMO modification affects its substrate properties in three different ways: SUMO can compete for acceptor lysine (K) with other PTMs (e.g., ubiquitylation, acetylation, methylation), preventing their action on the substrate; SUMO is a bulky moiety that can interfere with protein-protein interactions, allowing binding only in the absence of modification; SUMO can bind SUMO to SIMs either inter- or intra-molecularly, thereby fostering physical associations or conformational changes, respectively.

First, SUMO conjugation machinery can compete for the acceptor lysine residue of a substrate with other possible PTMs, such as methylation, acetylation and ubiquitylation, thus preventing their possible effects on the target. The competition between SUMO modification and acetylation can be exemplified in the cases of MEF2A and HIC1 transcription factors, where SUMOylation inhibits their activity, for which acetylation is required (Shalizi et al., 2006; Stankovic-Valentin et al., 2007). Similarly, SUMO antagonizes poly-ubiquitylation of I κ B α and its subsequent degradation via the UPS by blocking the target lysine residue (Desterro et al., 1998).

Second, SUMO modification may alter protein surface of the substrate required for interaction with its binding partners and thus interfere with protein-protein interactions. In such a way, SUMOylation of transcription repressor ZNF76 blocks its binding site for the TATA-box binding protein (Zheng and Yang, 2004). Similarly, SUMO-modified corepressor CtBP cannot longer interact with the PDZ domain of the neuronal nitric-oxide synthase, while the SUMOylated ubiquitin-conjugating enzyme E2-25K loses its ability to bind the ubiquitin E1 (Lin et al., 2003; Pichler et al., 2005).

INTRODUCTION

Another example of SUMO modification inhibiting protein binding is the SUMOylation of the budding yeast proliferating cell nuclear antigen (PCNA) at K127 during S-phase, which was shown to interfere with Eco1 interaction and thus repress Eco1-dependent sister chromatid cohesion establishment (Moldovan et al., 2006, 2007).

The third consequence of the SUMO modification, which seems to be by far the most abundant, is the fostering of protein-protein interactions mediated by SUMO-SIM binding (Geiss-Friedlander and Melchior, 2007). Multiple studies provide evidence that SUMOylation further strengthens weak affinities that exist between the interacting proteins, acting like a molecular glue. One of the most well studied cases of SUMO modification promoting physical interaction between two proteins is the SUMOylation of PCNA at K164, which is crucial for the recruitment of the budding yeast PCNA-interacting anti-recombinogenic enzyme Srs2 (Hoegel et al., 2002; Moldovan et al., 2007; Papouli et al., 2005; Pfander et al., 2005). PCNA becomes SUMOylated during the S-phase of the cell cycle once it is loaded onto chromatin in the vicinity of the dedicated DNA-bound SUMO ligase Siz1. This in turn recruits DNA helicase Srs2 specifically to sites of ongoing replication, where it prevents unwanted aberrant recombination events by removing the recombinase Rad51 from chromatin. For its binding to PCNA Srs2 harbors a so-called PIP (PCNA-interacting protein) box, but the crucial additional affinity for the SUMOylated PCNA engaged in DNA replication comes from the SIM located next to the PIP box in the C-terminal tail of Srs2 (Armstrong et al., 2012; Pfander et al., 2005). Thus, SUMOylation of PCNA at K164 ensures efficient recruitment of the right binding partner (Srs2) at the right time (during replication) and within the right context (replicating chromatin). Interestingly, SUMO modification not only fosters intermolecular protein binding, but was also shown to induce protein conformational changes by stimulating intramolecular SUMO-SIM mediated physical interactions, as in the case of the base excision repair (BER) enzyme thymine DNA glycosylase (TDG). The SUMOylation of TDG results in the binding of the modifier to the SIM located within TDG itself, which changes the conformation of the enzyme allowing DNA release and thereby driving the enzymatic cycle (Steinacher and Schär, 2005).

II.1.3 SUMO Pathway Enzymes and Substrate Specificity

As discussed earlier, the basic mechanisms defining the acceptor lysine selection by the SUMO conjugating enzyme Ubc9 are relatively well understood, however the SUMOylation substrate specificity in general remains largely unresolved, especially

INTRODUCTION

because only a handful of ligases contribute to global SUMO levels and in many cases share overlapping substrate selectivity. This in part can be explained by the fact that the SUMO ligases largely play the role of adaptors that bring SUMO-charged E2 in the vicinity of its targets, which harbor accessible acceptor lysines. Therefore, the localization and local concentration of the SUMO pathway enzymes in the cell seem to be the crucial determinants that guide substrate specificity and define protein pools to be targeted by the SUMO pathway components (Gareau and Lima, 2010; Heun, 2007; Hickey et al., 2012; Takahashi et al., 2008).

The largest group of SUMO ligases identified belongs to the Siz/PIAS family and can be characterized by the presence of the Siz/PIAS-RING (SP-RING) domain that specifically recruits Ubc9 (Hochstrasser, 2001; Johnson and Gupta, 2001; Palvimo, 2007). In fact, in the budding yeast all four known E3s (Siz1, Siz2, Mms21; and the meiosis-specific Zip3) are a part of this SUMO ligase family (**Fig. 3**). The SP-RING is a conserved zinc finger type domain related to the RING (Really Interesting New Gene) domain found in a respective class of ubiquitin ligases (Freemont, 2000; Hershko and Ciechanover, 1998; Weissman, 2001). The RING contains a C_3HC_4 amino acid motif that coordinates two zinc cations and binds charged ubiquitin E2s, whereas the SP-RING domain lacks two key cysteine residues (C_2HC_3), coordinates single zinc ion and binds SUMO-charged Ubc9. A subgroup of SP-RING ligases (yeast Siz1-2, human PIAS1-4), in addition to the described SP-RING domain, harbors a SAP (after SAF-A/B, Acinus and PIAS) domain for sequence nonspecific DNA targeting (Aravind and Koonin, 2000) and a PINIT domain, involved in substrate interaction (Yunus and Lima, 2009). The domain architecture of these canonical Siz/PIAS ligases is largely similar (**Fig. 3**), with the main differences allocated to their C-terminal tails, which additionally guide the subcellular localization of the E3s and thus contribute to their substrate selectivity (Reindle et al., 2006). In contrast, yeast Mms21 (or NSE2 in humans) and Zip3 are different as they lack both PINIT and SAP domains. However, these ligases are also specifically localized in the cell, as Mms21 is the component of the structural maintenance of chromosomes Smc5/6 complex involved in DNA repair and genomic stability (Andrews et al., 2005; Branzei et al., 2006; Potts and Yu, 2005; Zhao and Blobel, 2005), while Zip3 is exclusively recruited to the synaptonemal complexes (SCs) during meiosis (Cheng et al., 2006; de Carvalho and Colaiacovo, 2006). Not surprisingly, the cellular localization largely determines their SUMO substrate specificity, as Zip3 targets specifically proteins involved in SC formation (Eichinger and Jentsch, 2010), whereas Mms21 mediates

INTRODUCTION

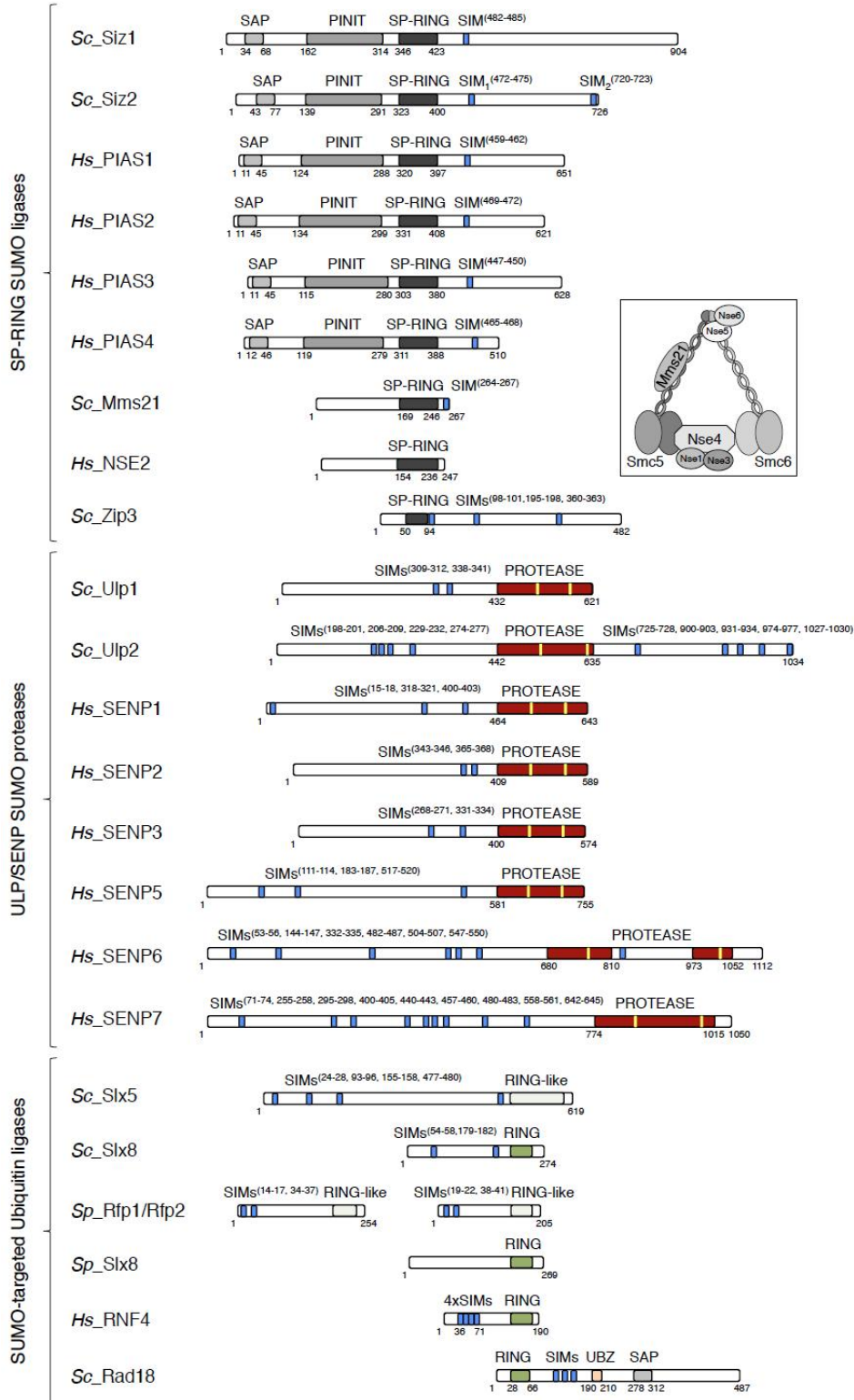


Figure 3. Scheme of SP-RING SUMO Ligases, SUMO-specific Proteases and SUMO-targeted Ubiquitin ligases

Shown are enzymes from *S. cerevisiae* (Sc), *S. pombe* (Sp) and humans (Hs) with their sizes and functional domains. The indicated domains are: sequence non-specific DNA-binding domain (SAP); substrate-binding PINIT domain; Ubc9-binding Siz/PIAS-RING finger (SP-RING); predicted SUMO-interaction motifs, SIMs (blue); protease domain (maroon) with catalytic His and Cys residues (yellow); RING and RING-like domains of STUBs; ubiquitin-binding UBZ domain. The presence of multiple SIMs ensures efficient recognition of SUMOylated substrates. The insert depicts schematically Mms21 (Nse2) ligase integrated into the yeast Smc5/6 complex.

INTRODUCTION

SUMO modification of certain DNA repair proteins as well as components of the Smc5/6 complex itself (Potts, 2009).

The importance of subcellular localization for the function and substrate selectivity of the canonical Siz/PIAS SUMO ligases can be exemplified in the case of the yeast Siz1. As was mentioned earlier, Siz1 is normally localized to chromatin via its sequence nonspecific DNA-binding SAP domain and mediates SUMOylation of the chromatin-bound substrates, for instance, replication processivity clamp PCNA at K164 specifically during the S-phase (Hoege et al., 2002; Papouli et al., 2005; Pfander et al., 2005). However, later during mitosis, a fraction of Siz1 relocates from the nucleus to the filamentous ring structure formed at the bud neck of dividing yeast cells (Takahashi et al., 2008). This scaffolding ring, composed of proteins called septins, provides a structural support for cell division and recruits other proteins involved in bud site selection, cell polarity, cytokinesis and spore formation. As a consequence of Siz1 recruitment, three out of five septins (Cdc3, Cdc11, Shs1) become collectively SUMOylated (Johnson and Blobel, 1999; Johnson and Gupta, 2001; Takahashi et al., 2001). Truncation analysis revealed that the C-terminus of Siz1 is required for its bud neck localization and septin SUMOylation, but not for its ligase activity *in vitro*. Notably, another SP-RING family member Siz2 is also capable of modifying septins *in vitro*, however *in vivo* it localizes to the nucleus and is therefore not involved in the modification of septin network (Takahashi and Kikuchi, 2005; Takahashi et al., 2003).

In addition to the SP-RING SUMO ligases several other proteins including Pc2, MUL1, TOPORS, HDAC4, HDAC7, TRAF7, FUS, RSUME were characterized as SUMO E3s in humans, as they can stimulate SUMO modification of certain substrates, yet, they do not harbor SP-RING domain for Ubc9 recruitment and their mode of action is largely not clear (Ulrich, 2009). However, humans additionally utilize a composite multisubunit SUMO ligase RanBP2/RanGAP1-SUMO1/Ubc9 complex (Werner et al., 2012), in which RanBP2/Nup358 is a component of the nuclear pore complex (NPC). During the interphase it serves essential functions in the nucleocytoplasmic transport, while the E3 ligase activity was shown to be important for chromosome segregation in mitosis. There, the ligase complex relocates to the mitotic spindle and mediates the SUMO modification of Borealin, a component of the chromosomal passenger complex that acts as a key regulator of mitosis (Klein et al., 2009).

INTRODUCTION

Subcellular localization is not only important for the substrate specificity of SUMO conjugation machinery, but also strongly influences substrate choice of the SUMO-specific proteases – yeast ULPs and mammalian SENPs (Hickey et al., 2012). In *S. cerevisiae* the two deconjugating enzymes Ulp1 and Ulp2 have restricted cellular localization; Ulp2 resides in the nucleoplasm, while Ulp1 is mainly associated with the inner surface of the NPC (Li and Hochstrasser, 2000, 2003). However, a fraction of Ulp1 relocates to the nucleolus under stress conditions, while during the last stages of cell division a portion is also exported to the cytoplasm and targets SUMOylated septin network mentioned earlier (Makhnevych et al., 2007; Sydorsky et al., 2010). Similarly, mammalian SENPs are mainly concentrated in the nucleus and additionally have distinct subnuclear localization pattern (Kolli et al., 2010). For example, SENP3 and SENP5 are found in the nucleolus, while SENP1 is associated with the NPC and also concentrates in nuclear foci. The localization of ULPs/SENPs is governed by their variable N-terminal tails, which typically harbor multiple SIMs (**Fig. 3**). Indeed, the deletion of the N-terminus of Ulp1 results in its localization throughout the cell.

SUMOylated substrates may not only be recognized and processed by differentially localized dedicated SUMO proteases, but can also be handled by so-called STUbLs (SUMO-Targeted Ubiquitin Ligases, **Fig. 3**). These are RING-type ubiquitin ligases that harbor multiple SIMs, which mediate the recognition of SUMO-conjugates (Perry et al., 2008; Praefcke et al., 2012). Initially two STUbLs have been characterized in budding yeast, both of which seem to be specifically localized in the nucleus. Ris1 is a member of the SWI/SNF family of DNA-dependent ATPases that plays a role in antagonizing silencing during mating-type switching (Zhang and Buchman, 1997). It was shown to bind Ubc4 and SUMO-conjugates, determining their half-lives (Uzunova et al., 2007). The second *S. cerevisiae* STUbL is a heterodimer consisting of Slx5 and Slx8, both of which are SIM-containing RING-finger proteins, that localizes to nuclear DNA repair foci and was also shown to be associated with the NPC (Nagai et al., 2008; Prudden et al., 2007). Interestingly, in fission yeast *S. pombe*, the known STUbL is related to Slx5/Slx8 and is also involved in genome stability and DNA damage repair. This composite ligase consists of the Slx8 protein (homologous to the one of budding yeast) and either of two related proteins Rfp1 or Rfp2. In mammals, the nuclear RING-finger ubiquitin ligase RNF4 binds SUMO-conjugates via four putative SIMs in its N-terminus, displays homology to Rfp1/Rfp2 and can complement deletions of STUbL genes in yeast (Sun

INTRODUCTION

et al., 2007). A proteomic analysis with the SIM-containing N-terminal domain of RNF4 identified multiple SUMOylated proteins as potential substrates of this homodimeric vertebrate STUbL (Bruderer et al., 2011). Notably, many other RING-type ubiquitin ligases harbor predicted SIMs, suggesting that they may also act as STUbLs (e.g., yeast Rad18, human RNF111/Arkadia). Moreover, depending on the ubiquitin E2 enzyme associated with the STUbL and the ubiquitin signal generated by their concerted action, different outcomes for the SUMO substrates are possible. They can either be targeted for selective proteasomal degradation via the UPS, or become endowed with novel functions. For example, RNF4 binds to and polyubiquitylates the SUMOylated PML protein, targeting it for degradation, which in turn results in the disassembly of PML nuclear bodies (Lallemand-Breitenbach et al., 2008; Tatham et al., 2008). However, upon DNA damage, RNF4 gets recruited to the SUMO-modified repair factors in so-called repair foci and induces the assembly of nonproteolytic K63-linked polyubiquitin chains (Yin et al., 2012). Similarly, in budding yeast, SUMOylated PCNA stimulates the recruitment of the Rad18 ubiquitin ligase via its SIM, thereby enhancing mono- or K63-linked poly-ubiquitylation at K164 of a different subunit within PCNA homotrimeric complex and thus promoting DNA damage tolerance (Parker and Ulrich, 2012).

II.2 DNA Damage Repair

The integrity of the genetic information is essential for all biological processes in cells, however it is constantly being threatened by numerous endogenous as well as exogenous DNA-damaging assaults. To counter these threats and protect the genome is therefore of critical importance, and life has evolved several lines of defense against DNA damage – collectively termed the DNA damage response (DDR) – in order to detect various DNA lesions, signal and tolerate their presence, and finally mediate their repair (Jackson and Bartek, 2009; Zhou and Elledge, 2000).

Cells constantly receive thousands of DNA lesions that can affect DNA transcription or block genome replication. Moreover, if the lesions are not correctly repaired, they may result in mutations or gross chromosomal rearrangements (GCRs) that can eventually lead to the development of diverse genetic diseases, including cancer syndromes (Hoeijmakers, 2001). Depending on the type of DNA damage inflicted, different dedicated repair pathways step into play, e.g., base-excision repair (BER), nucleotide-excision repair (NER), mismatch repair (MMR). Many DNA lesions arise during normal physiological processes, like DNA

INTRODUCTION

mismatches erroneously introduced during replication, or DNA strand breaks occurring as a consequence of faulty topoisomerase activity. Reactive oxygen species, hydrolytic and alkylating reactions produce numerous DNA-base lesions continuously. Chemical adducts, UV-light and ionizing radiation generate various forms of DNA damage leading to base loss, DNA single-strand breaks (SSBs) or stalling of progressing replication forks, that can eventually lead to fork collapse and formation of the DNA double-strand breaks (DSBs) (Pfeiffer et al., 2000). Despite being relatively rare compared to other types of DNA lesions, DSBs are difficult to repair and are extremely toxic to the cell (Haber, 1999; van Gent et al., 2001). Even a single DSB, if left unrepaired, may result in the cell death or lead to the formation of GCRs and ultimately in vertebrates to cancerogenesis. However, in certain cases the generation of the DSBs is programmed by cells. Meiotic recombination relies on error-free DSB repair and is required for correct chromosome segregation during the first meiotic division (Keeney et al., 1997). The V(D)J recombination of immunoglobulin genes in lymphocytes (Gellert, 1992) as well as the process of mating-type switching in budding yeast (Schiestl and Wintersberger, 1992) also depend on the controlled induction and repair of the DSBs. Not surprisingly, cells have evolved efficient mechanisms to sense, signal and repair this DNA lesion.

Two major pathways exist in cells to deal with the DSBs that are called non-homologous end-joining (NHEJ) and homologous recombination (HR). As can be judged from the pathway names, the NHEJ involves, in principal, the ligation of broken DNA ends, while HR uses homologous DNA sequences to guide DSB repair. The main differences as well as the pathway choice between the NHEJ and HR are dictated by the events that take place at broken DSB ends (Symington and Gautier, 2011). In NHEJ, the double-stranded DNA (dsDNA) ends become bound and are held together by the heterodimeric Ku70/Ku80 protein complex, which prevents the 5' DNA-end resection and promotes their direct ligation. This is a fast and effective way to re-join broken ends, but NHEJ often results in small deletions, insertions, mismatches at the DSB site, as well as GCRs, when different breaks are incorrectly ligated, and is therefore considered error-prone (Daley et al., 2005). In contrast to the NHEJ, the HR pathway relies on the resection of the DSB ends by nucleases together with helicases and exposure of 3' ssDNA overhangs, which are being eventually covered by the Rad51 recombinase forming a so-called nucleoprotein filament. In the process of genome-wide homology search, this filament is capable of finding and invading the homologous dsDNA sequence, one of the strands of which

INTRODUCTION

is then used as a template for DNA synthesis (Filippo et al., 2008). Therefore, HR is considered largely error-free. Moreover, the joint DNA molecule intermediates produced after strand invasion are differentially handled to generate noncrossover and crossover products, depending on the favored outcome appropriate in different contexts. Whereas NHEJ is favored in G1-phase but is also active throughout the cell cycle, the HR is preferentially utilized after DNA replication, when sister chromatid becomes available as a template for error-free repair.

II.2.1 Homologous Recombination-mediated DNA Double-strand Break Repair

The key reaction in HR is the pairing and exchange of strands between two homologous DNA sequences. This step is mediated by the action of the conserved RecA/Rad51 protein family of recombinases (Chen et al., 2008). To initiate homologous pairing Rad51 has to first bind to ssDNA, for which the complementary sequence is then being found during the genome-wide homology search (Renkawitz et al., 2013). Therefore, the HR-mediated DSB repair requires the resection of the broken DNA ends, which is achieved through coordinated action of multiple repair factors (**Fig. 4**). It is important to note that all DNA transactions take place in the context of chromatin and are tightly regulated by the cell cycle control as well as DNA damage checkpoint signaling (Branzei and Foiani, 2008; Chapman et al., 2012; Lukas et al., 2011; Symington and Gautier, 2011).

The first step in HR is the recognition of the DSB and initiation of resection by the conserved heterotrimeric MRX complex (Stracker and Petrini, 2011), which in *S. cerevisiae*, is composed of Mre11, Rad50 and Xrs2 (Nbs1 in humans). This DSB sensor binds to the broken chromosome ends and using extended coiled-coils of Rad50 that are crowned with the Zn-hook for dimerization (Hopfner et al., 2002) physically tethers the ends together (**Fig. 4**). The Mre11 subunit of the MRX complex is the bifunctional endo/exonuclease, which together with Sae2 (CtIP) endonuclease initiates short-range 5' strand degradation proximal to the DSB, resulting in limited end processing. Endonuclease activity is crucial when the DSB-ends are not clean, e.g., blocked by bound proteins, such as trapped topoisomerases or meiosis-specific endonuclease Spo11. However, resection of free DNA ends can also occur in the absence of Mre11 and Sae2 activity (Symington and Gautier, 2011). The Xrs2 subunit of MRX serves as a scaffold to recruit other proteins like checkpoint kinase Tel1 (ATM), which phosphorylates substrates in the vicinity of the break. In general, the MRX complex not only senses the DSBs and initiates short-track resection, but

INTRODUCTION

also recruits downstream repair factors and stimulates their activity (Stracker and Petrini, 2011).

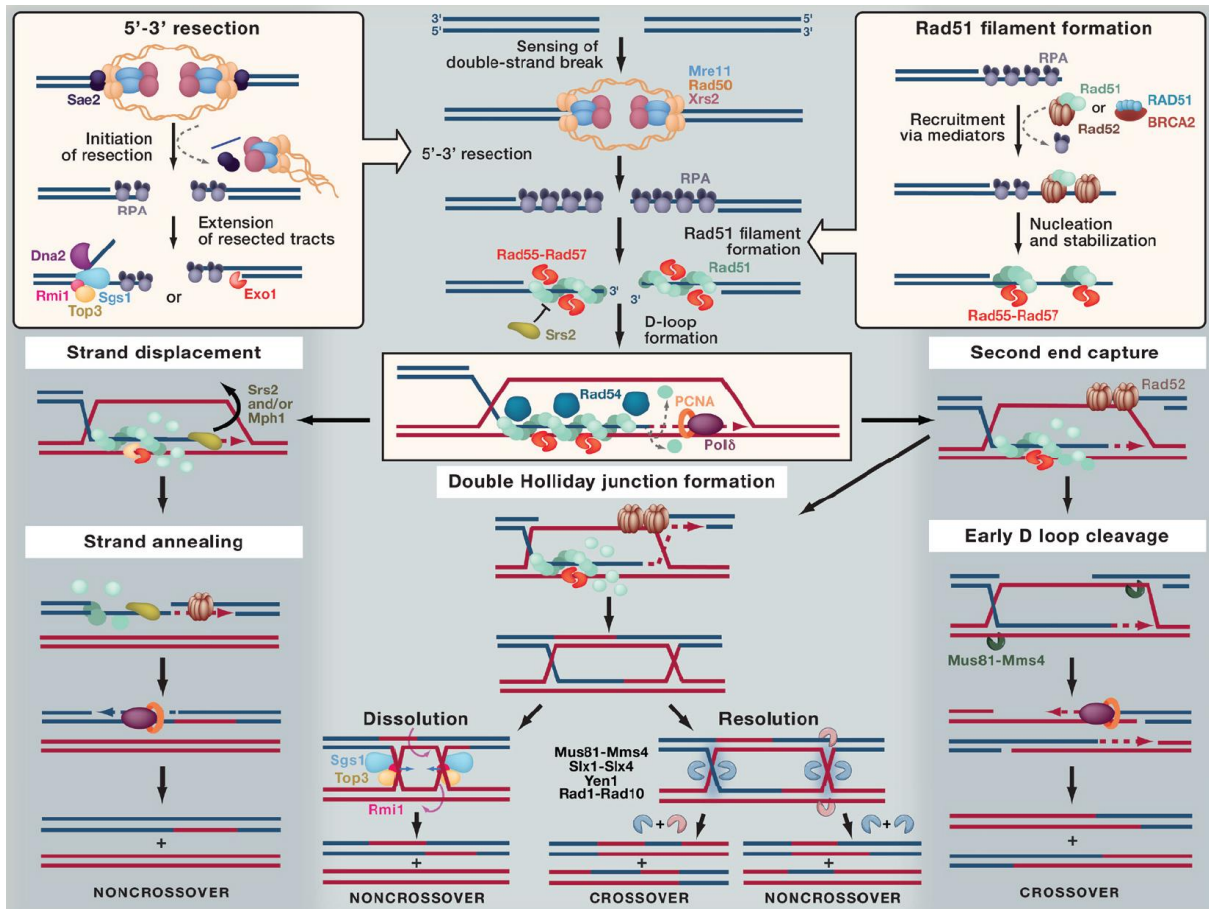


Figure 4. The Homologous Recombination in DNA Double-strand Break Repair

The DSB is sensed and broken ends are tethered by the heterotrimeric MRX complex, which together with Sae2 endonuclease initiates 5'-3' DNA resection and recruits downstream repair and checkpoint factors. Long track resection is mediated by the Exo1 exonuclease and in parallel by Sgs1-Top3-Rmi1 helicase working together with Dna2 endonuclease. Exposed ssDNA overhangs are immediately coated by RPA, which is then replaced by the Rad51 recombinase with the help of mediators (Rad52-Rad59 in yeast, BRCA2 in mammals). Rad51 forms nucleoprotein filaments stabilized by its paralogs (Rad55-Rad57 heterodimer) that counteract the action of the anti-recombinogenic helicase Srs2. These filaments search for homology genome-wide and catalyze the invasion of the homologous dsDNA resulting in the formation of D-loop. Homologous pairing is stimulated by the chromatin remodeling protein Rad54. DNA Pol δ then extends the 3' end of broken chromosome using the donor strand as a template. In the SDSA scenario (left), the extended strand is displaced from the D-loop with the help of Srs2 and anneals to complementary sequences exposed by resection allowing the gaps to be filled by DNA synthesis, thus forming noncrossover products. If the other DSB-end is captured (right), annealed to the displaced strand of the D-loop and extended, the repair proceeds via double Holliday junctions (center), resulting in noncrossover or crossover formation depending on the dis- or resolution of the junctions. Alternatively, early D-loop can be cleaved by resolvases (right), promoting the formation of crossovers (adapted from (Mazon et al., 2010)).

Short-range resection mediated by MRX-Sae2 alone can only generate 3' ssDNA overhangs of around 100-700 nt that can be used for Rad51-dependent recombination, however the presence of heterology adjacent to the DSB greatly

INTRODUCTION

reduces the efficiency of repair (Mimitou and Symington, 2008). Moreover, long-range resection is required to activate the DNA damage checkpoint and also needed to prevent incorrect repair between short repeats. To achieve long-range resection, two parallel independent pathways operate in the cell (Mimitou and Symington, 2008; Zhu et al., 2008). One relies on the action of the Exo1 exonuclease, while the second utilizes the STR complex composed of RecQ-family helicase Sgs1 (BLM), the type I topoisomerase Top3 and OB-fold containing protein Rmi1. Sgs1 helicase in STR complex unwinds dsDNA from broken ends, while the formed ssDNA is degraded by the endonuclease activity of bifunctional helicase/endonuclease Dna2 (Mimitou and Symington, 2011). Importantly, the MRX-Sae2 complex stimulates the recruitment and activation of both branches of long-track resection at the DSB (Nicolette et al., 2010; Symington and Gautier, 2011).

Exposed in the process of DSB resection ssDNA becomes rapidly coated by the ssDNA-binding heterotrimeric replication protein A (RPA), composed of Rfa1, Rfa2, and Rfa3 subunits in yeast. Coating of ssDNA by RPA dissolves secondary DNA structures, protects broken ends from cleavage (Chen et al., 2013) and serves as a platform for recruitment of the downstream repair and DNA damage checkpoint factors. Importantly, crucial checkpoint kinase Mec1 (ATR) via its recruiting factor Ddc2 (ATRIP) binds to RPA-covered ssDNA and initiates DNA damage checkpoint signaling (Zou and Elledge, 2003). Subsequently, in order for HR to proceed, RPA has to be displaced from resected ssDNA and exchanged by the Rad51 recombinase. This crucial step in *S. cerevisiae* is mediated by the action of the conserved homo-oligomeric ring-shaped protein Rad52 with the help of its paralog Rad59, while in humans BRCA2 promotes the RPA-Rad51 exchange (Filippo et al., 2008). Rad51 then forms a dynamic nucleoprotein filament on ssDNA stabilized by the heterodimer of its paralogs Rad55-Rad57, which balance the anti-recombinase activity of Srs2 helicase (Liu et al., 2011). Once formed, the Rad51 filament in the process of intricate genome-wide homology search scans the chromatin, invades the homologous dsDNA displacing one strand and subsequently forming a joint heteroduplex structure known as the displacement D-loop (**Fig. 4**). Homology search and homologous pairing by Rad51 are additionally stimulated by the member of the Swi2/Snf2 family of chromatin remodeling proteins Rad54 (Bugreev et al., 2006; Mazin et al., 2010; Petukhova et al., 1998). After invasion of ssDNA into donor dsDNA and base pairing the DNA polymerase δ gets access to and extends the

INTRODUCTION

3' ssDNA end of the broken chromosome using the donor strand as a template (Li et al., 2009).

The subsequent steps and the outcomes of HR depend on the events that take place at the D-loop following DNA repair synthesis. In the simplest case, the joint DNA molecule intermediate is resolved by displacing the extended strand via action of the Srs2 and Mph1 DNA helicases that can disrupt D-loops (Ira et al., 2003; Prakash et al., 2009; Veaute et al., 2003). The displaced strand then anneals to complementary sequences formed by the resection of the other side of the DSB. This in turn initiates another round of gap filling DNA synthesis followed by ligation and results in noncrossovers exclusively (**Fig. 4, left**). Notably, this mechanism of HR, known as synthesis-dependent strand annealing (SDSA), leads to gene conversion; the duplicate copy of the donor allele is transferred to the recipient locus, while the recipient allele is lost. In the canonical DSB repair model (Szostak et al., 1983), initially proposed in meiosis, the other end of the break is annealed with the help of Rad52 to the displaced strand in D-loop (second end capture). This event primes DNA synthesis and extension of the second broken end, forming a stable double Holliday junction (dHJ) intermediate (**Fig. 4, center**). The dHJ can be subsequently either dissolved by the STR complex forming noncrossovers (Cejka et al., 2010; Wu and Hickson, 2003) or resolved by a number of resolvases (Svendsen and Harper, 2010) giving rise to both crossovers and noncrossovers. Alternatively, the extended D-loop could be cleaved prematurely prior to dHJ formation (**Fig. 4, right**), promoting crossovers. After cleavage of HJs, the ends are ligated to complete the reaction.

II.2.2 DNA Damage Checkpoint

The DNA damage checkpoints are multifaceted signal transduction pathways that coordinate sensing of different DNA lesions with the signaling of their presence, repair and cell cycle progression (Bartek and Lukas, 2007; Harper and Elledge, 2007). Ultimately, checkpoint signaling stalls cell division providing sufficient time for efficient repair to take place. The signaling cascade is mediated by the DNA damage checkpoint kinases that phosphorylate numerous effectors involved in the regulation of diverse physiological functions (Matsuoka et al., 2007). The key factors implicated in sensing and transducing the checkpoint signals are highly conserved in eukaryotes and can be grouped according to their function into the DNA damage sensors, apical kinases, signal transducers and effector kinases.

INTRODUCTION

At the heart of the DNA damage checkpoint signaling are the apical phosphoinositide 3-kinase (PI3K)-like Mec1 (ATR) and Tel1 (ATM) kinases, mentioned earlier. Whereas, Tel1 is activated by direct binding to the MRX DSB sensor (Lee and Paull, 2005), the Mec1 activation involves its recruitment to the ssDNA-bound RPA complexes via the interacting protein Ddc2 (ATRIP) (Rouse and Jackson, 2002; Zou and Elledge, 2003). Therefore, the activation of these DNA damage checkpoint kinases is directly coupled to the sensing and resection of DSBs. Moreover, the apical kinases can regulate the DNA resection itself by targeting the key players of the resection machinery. For instance, in budding yeast the long-range resection factor Exo1 is phosphorylated at several sites following extensive formation of ssDNA, and these modifications are suggested to inhibit its activity in order to prevent aberrant hyper-resection (Morin et al., 2008). Another important early factor involved in full activation of the checkpoint signaling at resected DSB-ends and stalled replication forks is the 9-1-1 checkpoint clamp (Rad9/Rad1/Hus1 complex in mammals; Rad17/Mec3/Ddc1 in *S. cerevisiae*), which is structurally highly similar to PCNA, forming a heterotrimeric ring around DNA. After DNA resection and coating of ssDNA by RPA, the 9-1-1 complex is loaded to 5' ssDNA/dsDNA junctions (in contrast to PCNA, which localizes at 3' junctions) by an alternative form of the replication factor C (RFC) complex, in which Rad24 replaces the Rfc1 subunit (Majka et al., 2006; Sancar et al., 2004). The 9-1-1 loading is independent of Mec1 recruitment and is highly stimulated by RPA. The checkpoint clamp is subsequently phosphorylated by Mec1 and serves as a platform for the recruitment of downstream checkpoint factors thus strengthening the checkpoint signaling (Parrilla-Castellar et al., 2004).

After the activation of the apical checkpoint kinases at the sites of DNA damage, the next step of the signaling cascade involves the recruitment of the mediator proteins that transduce the checkpoint signal further to the effector kinases Chk1, Rad53 (Chk2) and Dun1. One of such signal transducers in budding yeast is the checkpoint adaptor protein Rad9 (53BP1 in mammals). Upon DNA damage it becomes hyperphosphorylated by Mec1 at multiple sites in a 9-1-1 complex-dependent manner, which in turn stimulates its oligomerization and strengthens localization to DNA lesions (Emili, 1998; Naiki et al., 2004). Following its hyperphosphorylation, Rad9 serves as a binding platform for the recruitment and activation of the downstream effector kinase Rad53. Multiple Rad53 molecules bind to patches of Rad9, which triggers rapid activation of the kinase through trans-

INTRODUCTION

autophosphorylation (Gilbert et al., 2001). The activated Rad53 kinase is subsequently released from Rad9 and targets multiple factors leading to cellular arrest, upregulation of dNTP levels, stabilization of stalled replication forks, and transcriptional repression of cyclins along with upregulation of DNA damage repair genes.

In general, the extent of resection and consequently the local concentration of early DNA damage checkpoint factors seem to be important for efficient checkpoint activation. A single RPA complex stably binds 30 nt of ssDNA, while at least 2 RPA complexes are required to recruit ATRIP-ATR heterodimer *in vitro* (Zou and Elledge, 2003). However, activation of ATR requires at least 200 nt of ssDNA and is greatly induced with ssDNA length above 1000 nt (Choi et al., 2010), suggesting that Mec1 (ATR) activation should be proportional to the length of DNA resection. Supporting this model, mutants lacking both branches of long-track resection ($\Delta exo1 \Delta sgs1$) in budding yeast are defective in Mec1/Ddc2 recruitment to DNA lesions and therefore fail to efficiently activate Rad53 kinase (Gravel et al., 2008; Zhu et al., 2008). Moreover, since the resected ssDNA in principle serves as a recruiting platform for checkpoint and other DDR factors, the artificial colocalization of Mec1/Ddc2 with the checkpoint 9-1-1 complex on DNA by fusing these factors to the LacI repressor and expressing in cells harboring Lac operator arrays is in fact sufficient to trigger DNA damage checkpoint signaling in the absence of any ssDNA (Bonilla et al., 2008).

II.2.3 SUMO Modification in DNA Repair

SUMO pathway is strongly implicated in the DDR (Bergink and Jentsch, 2009; Jackson and Durocher, 2013; Lukas et al., 2011) and several DNA repair factors were shown to be SUMO-modified in the last decade. One of the first potential SUMO substrates involved in HR-mediated DSB repair identified was the fission yeast protein Rad22 (Ho et al., 2001), homolog of the recombination protein Rad52, which was subsequently shown to be SUMOylated in response to DNA damage in budding yeast and human cells (Sacher et al., 2006). Despite the fact that SUMO pathway mutants are very sensitive to various DNA damaging agents (MMS, UV, ionizing radiation) and exhibit strong defects in damage-induced HR (Maeda et al., 2004), a SUMOylation-defective Rad52 mutant is largely recombination proficient and demonstrated only partial defect in MMS-induced interchromosomal HR (Ohuchi et al., 2008; Sacher et al., 2006). In addition, Rad52 SUMOylation was shown to sustain Rad52 activity and shelter the molecules engaged in repair from accelerated

INTRODUCTION

proteasomal degradation. Following studies in budding yeast revealed that Rad52 SUMOylation-defective mutant does not support nucleolar exclusion of Rad52 recombination foci (Torres-Rosell et al., 2007), while in general the duration of these repair foci is reduced (Altmannova et al., 2010).

In human cells, SUMO isoforms and SUMOylation machinery were also shown to rapidly co-localize with sites of DNA damage in repair foci and several DDR proteins were shown to be SUMO modified, including BRCA1, 53BP1 and MDC1 (Galanty et al., 2009; Luo et al., 2012; Morris et al., 2009). Moreover, responsible SUMO ligases PIAS1 and PIAS4 were shown to be required for complete accumulation and prolonged residence time of the DDR proteins downstream of RNF8 at DNA damage sites, for effective formation of ubiquitin conjugates mediated by RNF8, RNF168 and BRCA1, and for efficient DSB repair via both NHEJ and HR.

The next SUMOylation target involved in efficient DNA repair via HR to be identified was the ssDNA-binding protein RPA. Dou and coworkers found that upon camptothecin (CPT)-induced replication stress and after ionizing radiation SENP6 deSUMOylating enzyme dissociates from RPA allowing its modification by SUMO, which in turn facilitates the recruitment of Rad51 recombinase to the DNA damage foci and promotes repair via HR (Dou et al., 2010; Dou et al., 2011). SUMOylation-defective RPA mutant fails to efficiently recruit Rad51 to repair foci and shows partially reduced sister chromatid exchange (SCE) rates in response to CPT as well as reduced repair of Scel-induced DSBs.

Another piece of evidence demonstrating importance of SUMOylation machinery this time targeting multiple NER proteins for efficient repair of UV-induced lesions came from the study of Silver and coworkers in budding yeast. They demonstrated that cells lacking both canonical Siz/PIAS SUMO ligases Siz1 and Siz2 are sensitive to UV-light and show delayed cyclobutane pyrimidine dimer (CPD) repair. Moreover, many NER factors (Rad4, Rad16, Rad7, Rad1, Rad10, Ssl2, Rad3, and Rpb4) are SUMO targets, modification of which is increased by DNA damage (Silver et al., 2011). Importantly, blocking downstream steps of the repair pathway results in the accumulation of SUMOylated species of repair proteins acting upstream, analogous to increase of Rad52 SUMOylation in the absence of Rad51 (Ohuchi et al., 2009; Sacher et al., 2006), which indicates that modified molecules are engaged in repair process. However, despite strong modification of Rad16 after UV-treatment, SUMOylation-defective Rad16 mutant alone had no detectable abnormalities in NER, which suggested the possibility that Siz1/Siz2-dependent SUMO modification of

INTRODUCTION

multiple repair proteins collectively promotes efficient NER. Similarly, recent study showed that SUMOylation machinery mutants are sensitive to MMS, and by using a directed biochemical screen, confirmed SUMOylation of multiple proteins involved in replication, HR, NHEJ, BER, NER and MMR in response to genotoxic stress (Cremona et al., 2012).

These observations strongly implicate SUMO modification in the regulation of DNA damage repair and DDR in general. However, mechanistic details and basic principles clarifying how simply organized SUMO machinery precisely recognizes its substrates upon DNA damage and what are the consequences of multiple SUMOylation events at numerous DDR factors frequently organized into repair foci are largely missing.

II.3 Aim of This Study

The principles of substrate specificity and the mechanistic consequences of the ubiquitin modification are extensively studied and well understood. The highly diversified and elaborate ubiquitin conjugation machinery ensures precise recognition of individual substrates, whereas numerous ubiquitin-binding domains specifically recognize various types of ubiquitin signals. On the contrary, much less is known about the principles of substrate selectivity and mechanisms of action of the ubiquitin-related modifier SUMO.

The SUMO pathway targets hundreds of substrates with high specificity, yet surprisingly only a handful of enzymes mediate the entire modification spectrum. Moreover, the recognition of the SUMOylated substrates is extremely simple, as it in principle relies on a single short hydrophobic SUMO-interacting motif (SIM). SUMO modification is essential for viability, and therefore, SUMO pathway mutants have strong pleiotropic phenotypes. However, for the most substrates the biological significance of the modification is not known, and in many cases the respective specific SUMOylation-defective mutants barely exhibit any phenotypes.

Here, instead of studying the phenotypes of SUMO pathway mutants, we aimed to address the principles of substrate specificity and mechanistic consequences of SUMO modification at the substrate level, using the DNA double-strand break repair pathway via homologous recombination as a case study. This pathway has strong ties to the SUMO system, and several repair factors are known to be SUMOylated. We show that DNA damage triggers a SUMOylation wave collectively targeting multiple repair proteins of the same pathway. This suggests that perhaps

INTRODUCTION

SUMOylated proteins act in concert. Indeed, we find that SUMO machinery targets functionally engaged protein group rather than individual repair factors, and show that multiple modifications act synergistically by fostering SUMO-SIM mediated interactions between proteins. We propose and provide evidence for the model, in which regulated and highly spatially confined protein group SUMOylation provides glue-like properties to the substrates at reach of localized conjugation machinery in order to promote physical interactions, stabilize protein complexes and concentrate enzymatic activities.

III. RESULTS

III.1 Protein Group SUMOylation upon DNA Damage

III.1.1 Identification of SUMO Substrates Induced by Specific DNA Damage Types

To address the question of substrate specificity in the SUMO system we focused on the HR-mediated DNA DSB repair pathway as a model for our study. This pathway is well characterized, and many of the HR proteins are modified by SUMO after DNA damage, while SUMO pathway mutants show strong sensitivities towards DSB-inducing agents (Cremona et al., 2012; Dou et al., 2010; Sacher et al., 2006).

To screen for novel SUMO substrates and confirm previously identified targets that accumulate after specific DNA damage, we used a SILAC-based mass spectrometry approach (Mann, 2006; Ong et al., 2002). It allows the quantitative comparison of the protein abundance in differentially treated cell cultures on a proteome-wide level. For our purpose, we treated yeast cycling cells with a high dose of methyl methanesulfonate (MMS), the DNA-alkylating agent that induces replication fork stalling with subsequent fork collapse and DSB formation, and compared the isolated SUMO-conjugates from MMS-treated and untreated cells (**Fig. 5**). The mass spectrometry screen identified 844 potential SUMO substrates, the abundance of the majority of which did not change after MMS-induced damage. However, among those few SUMO-conjugates that were strongly enriched in response to DSB induction were specifically proteins involved in the HR and the DNA damage checkpoint response to replication stress (**Fig. 5, right**). This suggests that proteins acting in the same DNA damage repair pathway become collectively SUMOylated upon a specific stimulus, and that perhaps the modifications may serve a common purpose. The observed behavior of the SUMO machinery to simultaneously modify a number of repair factors that act together functionally and also form protein complexes is unusual, since most canonical PTMs typically target individual substrates with high selectivity to affect their properties. However, in case of the SUMO system this mode of action might be rather typical, as in a number of previous studies multiple factors involved in the ribosome biogenesis (Finkbeiner et al., 2011a; Panse et al., 2006), proteins of the septin network (Johnson and Blobel, 1999; Johnson and Gupta, 2001; Takahashi et al., 2001), and many nucleotide excision repair (NER) factors (Silver et al., 2011) were identified as SUMO substrates.

RESULTS

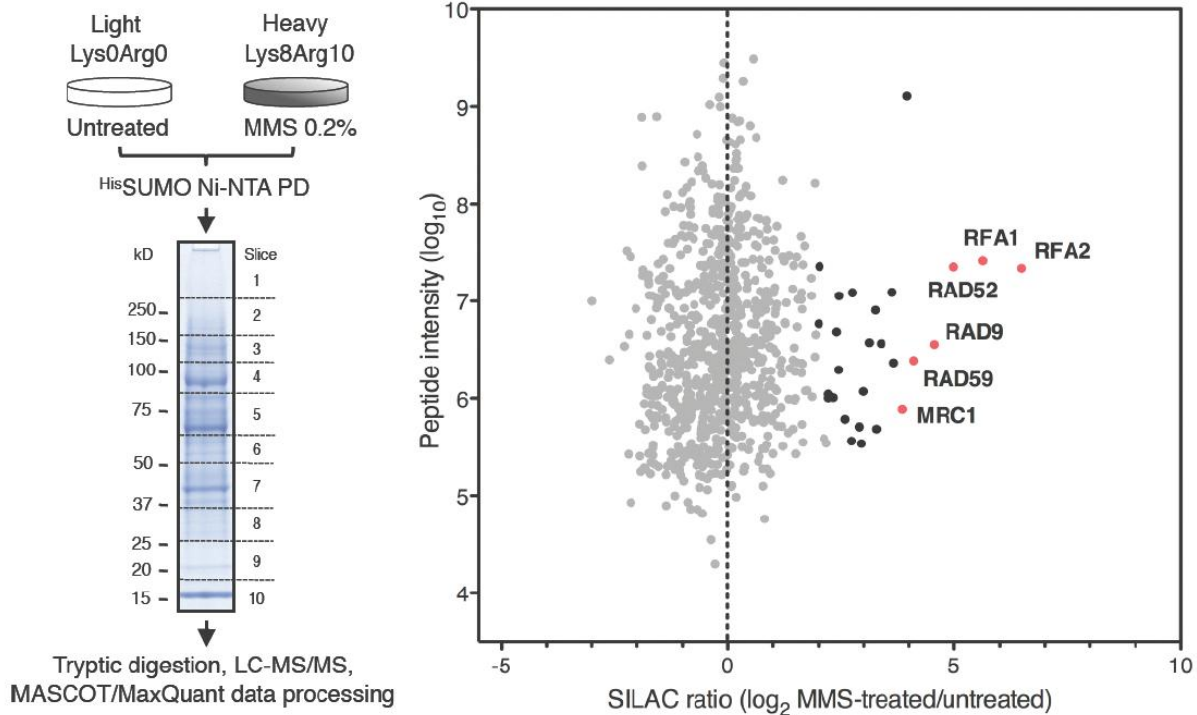


Figure 5. Proteins Acting in the HR-mediated DSB Repair Pathway are Collectively SUMOylated after MMS Treatment

Outline of SILAC experiment performed to detect SUMOylated substrates enriched after MMS-induced DNA damage (Left). SILAC ratios (MMS-treated versus untreated) for 844 quantified proteins plotted against the sum of the relevant peptide intensities (Right). Proteins are colored according to values of MaxQuant Significance(B): gray, Significance(B) > 10^{-2} ; black, SUMOylated proteins enriched after DNA damage with Significance(B) $\leq 10^{-2}$; red, proteins with Significance(B) < 10^{-4} that are involved in HR and checkpoint activation.

To further confirm the observed behavior of the SUMO system to collectively target a whole set of proteins acting in the same DNA repair pathway following specific DNA damage stimulus, we repeated the mass spectrometry screen described earlier with the only difference that this time cells were treated with UV-light instead of MMS. Exposure to UV-light creates crosslinking between adjacent cytosine and thymine bases resulting in pyrimidine dimers, bulky DNA lesions that require NER factors for recognition, excision and repair. The NER pathway can be further divided into global genomic NER and transcription-coupled NER subpathways, which differ in the mechanisms of DNA lesion recognition but share the same steps needed for the repair of bulky adducts (de Laat et al., 1999). In our quantitative proteomic screen for SUMO-conjugates that increasingly accumulate after UV-irradiation we specifically identified repair proteins playing roles in both branches of the NER (**Fig. 6**), whereas SUMOylation of the HR factors was not induced significantly. Thus, this strongly suggests that multiple proteins functionally

RESULTS

engaged in specific repair pathway in response to certain type of DNA damage become collectively modified by SUMO conjugation machinery.

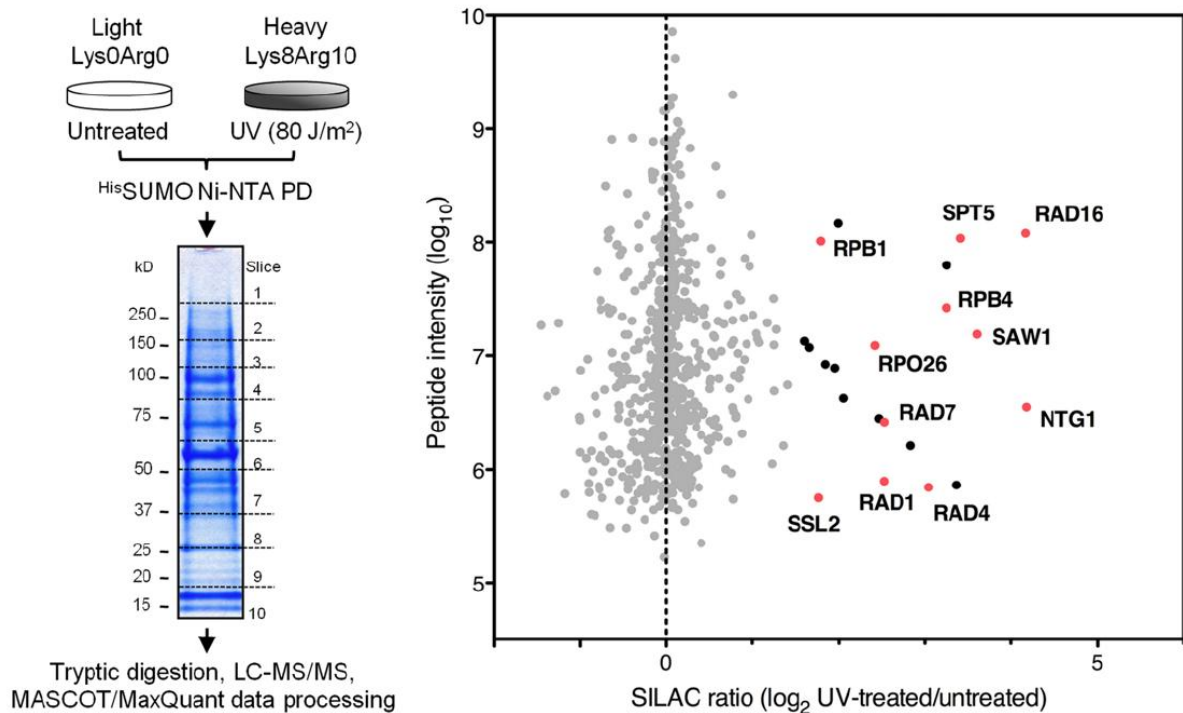


Figure 6. Proteins Acting in the Nucleotide Excision Repair Pathway are Collectively SUMOylated after UV-light Treatment

Following UV-light treatment specifically factors implicated in nucleotide excision repair (NER) become increasingly SUMOylated. Cells grown in heavy media were UV-irradiated (80 J/m^2) instead of MMS-treatment. SILAC ratios (UV-treated versus untreated) for 717 quantified proteins plotted against the sum of the relevant peptide intensities. Proteins are colored according to values of MaxQuant Significance(B): gray, Significance(B) $> 10^{-7}$; black, SUMOylated proteins enriched after UV-irradiation with Significance(B) $\leq 10^{-7}$; red, proteins with Significance(B) $\leq 10^{-8}$ that are involved in NER (both transcription-coupled and global genomic repair) and base-excision repair.

III.1.2 Synchronous Collective SUMOylation of a Whole Set of HR Proteins

After establishing that the SUMO system collectively modifies multiple HR and checkpoint factors following MMS-treatment, we then studied these proteins individually in order to estimate the extent of SUMOylation, to evaluate the timing of its induction, and characterize the requirements for the modification in greater detail. To this end, we C-terminally tagged yeast repair factors of interest with HA (human influenza hemagglutinin) or Myc (human c-Myc) epitopes at their endogenous genomic loci, treated the cells with MMS and isolated SUMO-conjugates using denaturing $^{\text{His}}$ SUMO Ni-NTA pull-down assays (Ni PD; as described in (Sacher et al., 2005)), subsequently probing with HA/Myc and substrate-specific antibodies. The SUMOylation of the 3-phosphoglycerate kinase Pgc1 is largely not affected by DNA

RESULTS

damage and was therefore used to control the pull-down efficiency, whereas hyperphosphorylation of the Rad53 checkpoint kinase served as a read-out for the DNA damage checkpoint activation.

First, we analyzed SUMOylation of the HR factors involved in the DSB repair directly and found that basically all early repair proteins (Lisby et al., 2004) participating in break sensing, DNA resection initiation and Rad51 recombinase loading onto resected ssDNA (**Fig. 7**) become massively SUMOylated specifically after MMS treatment.

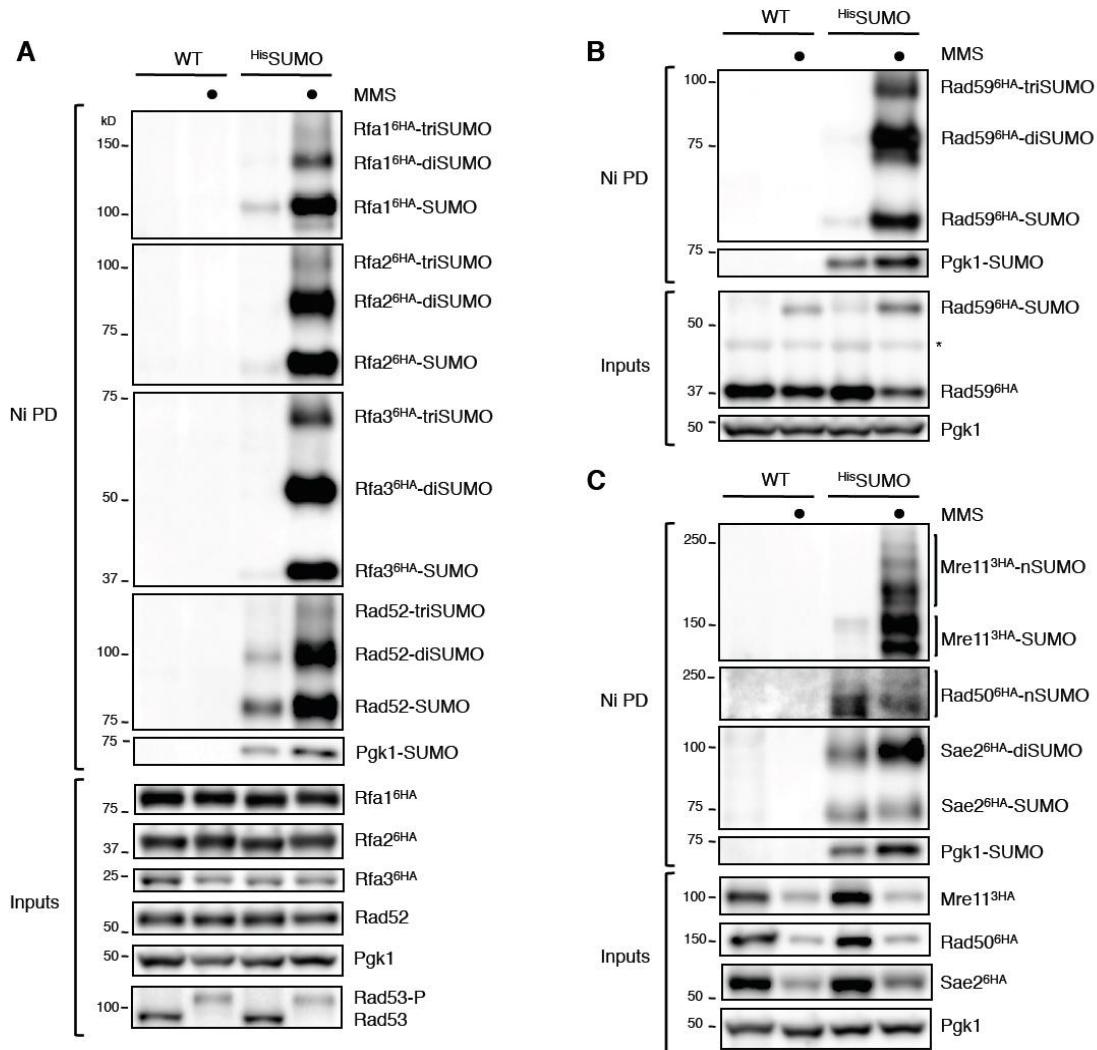


Figure 7. SUMOylation of Proteins Involved in HR-mediated DSB Repair

(A) SUMOylation of all three subunits of yeast RPA is triggered after exposure to MMS (indicated by dots). Ni-NTA pull-down (Ni PD) under denaturing conditions was performed from untreated or MMS-treated WT cells, or cells overexpressing His-tagged SUMO (^{His}SUMO), in which RPA subunits (Rfa1, Rfa2, Rfa3) were C-terminally tagged with an HA epitope. Slower migrating bands corresponding to RPA subunits modified by several SUMO moieties are indicated. SUMOylation of the RPA complex and of Rad52 is synchronously triggered by DNA damage. Pgk1 SUMOylation was followed to control pull-down efficiency. (B) Rad59 is SUMOylated upon DNA damage. Experiment was conducted similar to (A); the asterisk denotes a cross-reactive band. (C) Two subunits of the DSB-sensing MRX complex, Mre11 and Rad50, as well as Sae2 are SUMOylated upon DNA damage. Experiment was conducted similar to (A).

RESULTS

Moreover, in all cases, several slower-migrating SUMO-modified species of repair proteins were detected, indicating that modification targets multiple acceptor lysines or SUMO-chain formation takes place on the substrates. SUMOylation synchronously targeted repair factors acting upstream of the Rad51 nucleoprotein filament formation, however without affecting Rad51 itself, which suggested that perhaps modifications play a role earlier in the HR pathway.

Next, we focused on SUMOylation of the DNA damage checkpoint mediator proteins found in our SILAC screen (Rad9 and Mrc1) as well as apical checkpoint kinases (Mec1 and Tel1) that become recruited to the DSB sites (**Fig. 8**). We could to some extent detect MMS-induced SUMOylation of these factors by Western blot despite their hyperphosphorylation and broad distribution of the signal in gel. However, their SUMOylation was already significant in the absence of MMS, indicating that probably endogenous DNA lesions are sufficient to induce the modification.

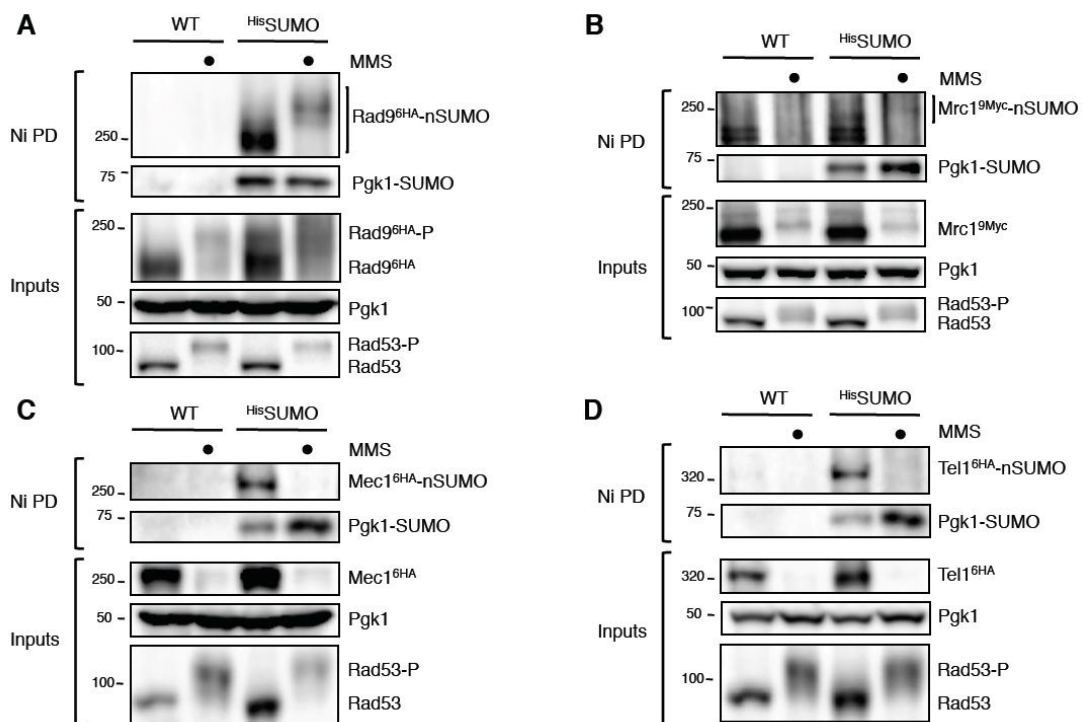


Figure 8. SUMOylation of the DNA Damage Checkpoint Proteins after MMS Treatment
 (A-D) To confirm enrichment of SUMOylated proteins involved in checkpoint activation following exposure to MMS, DNA damage checkpoint mediator protein Rad9 (A), S-phase checkpoint protein Mrc1 (B) (identified by the SILAC approach), and the apical checkpoint kinases Mec1 (C) and Tel1 (D) were C-terminally tagged with either HA or Myc epitopes in WT cells, or cells overexpressing ^{His}SUMO. SUMOylated species of the checkpoint proteins were detected by Ni PD already in untreated cells. Upon DNA damage, checkpoint proteins become hyperphosphorylated, causing mobility shifts (smears) and a weakening of Western blot signals; nevertheless SUMOylation of Rad9 and Mrc1 is detected by Ni PD from ^{His}SUMO cells after exposure to MMS. Pgk1 SUMOylation was followed to control pull-down efficiency.

RESULTS

We next aimed to characterize the kinetics of HR protein SUMOylation following DNA damage and found that not only the MMS dose-dependent induction of SUMO modification was very similar for all analyzed core repair proteins (**Fig. 9A**), but also the timing of their SUMOylation after exposure to MMS was almost identical. In addition, SUMOylation perfectly coincided with the activation of the DNA damage checkpoint as can be judged from the Rad53 hyperphosphorylation profile (**Fig. 9B**). This suggests that the synchronous SUMOylation wave is rapidly triggered after DNA damage, in parallel to the checkpoint-signaling cascade, and collectively targets multiple repair proteins. Supporting the latter, in mutant yeast strains lacking individual HR factors ($\Delta rad51$ or $\Delta rad52$), the SUMO modification of other repair proteins still took place (**Fig. 9C**). Moreover, the SUMOylation levels of the early-acting ssDNA-binding protein RPA were even higher in the absence of Rad51 or Rad52, which mediate the removal of RPA from resected DNA. This further indicates that SUMOylation targets proteins functionally engaged in repair reaction, because preventing the pathway completion most likely traps early SUMO-modified factors at the sites of DNA damage and causes their accumulation.

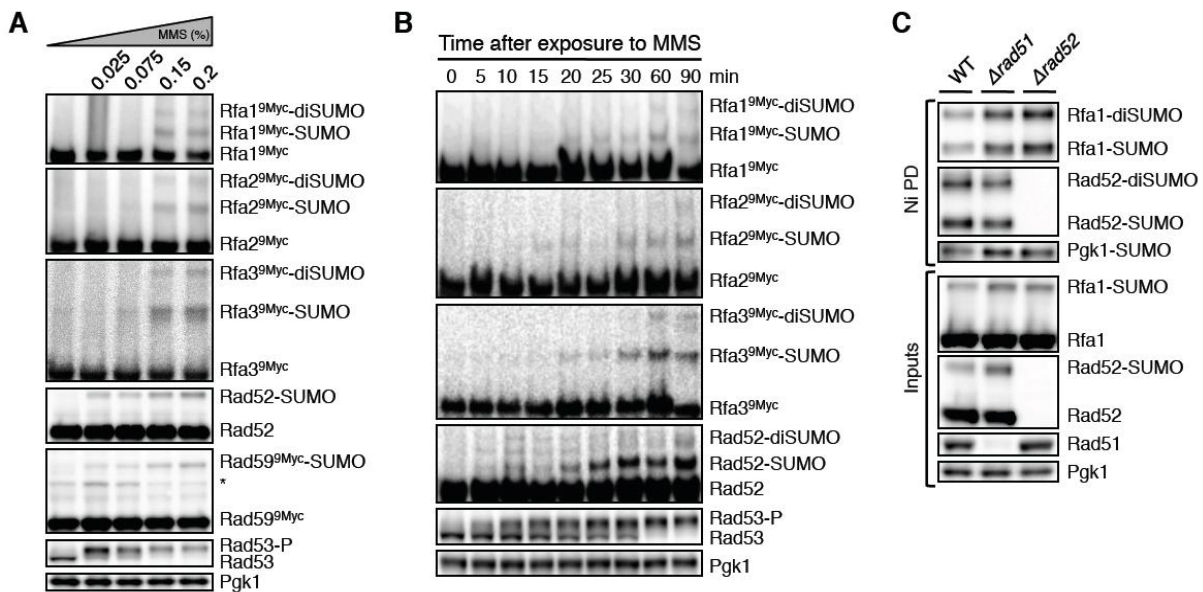


Figure 9. Synchronous SUMOylation Wave Collectively Targets HR Proteins

(A) SUMOylation of the HR proteins in response to DNA damage is triggered in a dose-dependent manner. Hyperphosphorylated Rad53 was followed to assay for checkpoint activation. (B) SUMOylation of repair proteins is triggered upon DNA damage and can be detected by Western blot already 15-20 min after induction with 0.2% MMS. The SUMOylation wave occurs parallel to checkpoint activation as judged from the Rad53 hyperphosphorylation profile. (C) Absence of the downstream-acting HR proteins Rad51 and Rad52 results in increased SUMOylation of RPA (Rfa1). ^{His}SUMO Ni PD from WT or mutant cells ($\Delta rad51$, $\Delta rad52$) after treatment with MMS.

RESULTS

III.2 Resection and Exposure of ssDNA Triggers SUMOylation Wave in HR

III.2.1 Long-range DNA Resection is Required for SUMOylation of HR Proteins

We next addressed what the requirements for the DNA-damage induced protein group SUMO modification in the HR pathway are. As expected, HR protein SUMOylation was heavily induced not only by MMS, but also by a member of the bleomycin family Zeocin that causes DSBs by cleaving DNA. By contrast, exposure to UV-light (assayed by SILAC approach earlier) or 4-nitroquinoline 1-oxide (4NQO), which act similarly by creating bulky DNA lesions that are repaired by NER, induced SUMOylation only to some extent (**Fig. 10**). The same was also true when cells were treated with hydroxyurea (HU), a ribonucleotide reductase (RNR) inhibitor that depletes dNTP pools and causes replication arrest (Bianchi et al., 1986). The HU-induced replication fork stalling in *S. cerevisiae* is, however, reversible, and the fork collapse and DSB formation occur only in strains defective in the DNA replication checkpoint response, e.g., *mec1* or *rad53* mutants (Lopes et al., 2001), in which the HR pathway is activated for repair (Meister et al., 2005). Together, these observations suggest that in wild-type (WT) yeast cells primarily the DSBs are robust inducers of the HR protein group SUMOylation.

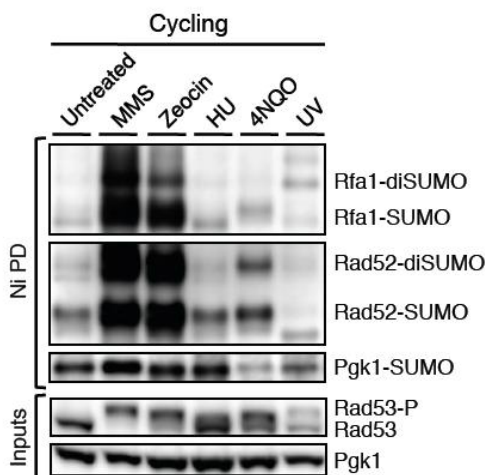


Figure 10. DSB Induction Leads to Massive SUMOylation of HR Proteins

In cycling yeast cells, SUMOylation of HR proteins is strongly induced following treatment with MMS (0.2%) or the DSB-inducing agent Zeocin (0.2 mg/ml), but to a much lesser extent following DNA damage either with replication inhibitor HU (100 mM), or UV-light (80 J/m²) and exposure to 4NQO (1 µg/ml), both of which generate bulky DNA lesions repaired by NER.

The finding that protein group SUMOylation of the HR factors is rapidly triggered primarily after DSB induction (**Fig. 9B** and **Fig. 10**) suggested that perhaps the

RESULTS

DSB-sensing MRX complex recruits the SUMO conjugation machinery to the break sites. In fact, previous work (Sacher et al., 2006) already established that the presence of the MRX complex is required for efficient DNA damage-induced SUMOylation of Rad52. Consistent with this finding, yeast mutants lacking individual MRX complex subunits ($\Delta mre11$, $\Delta rad50$, $\Delta xrs2$) exhibited strongly reduced SUMOylation levels of other HR factors upon DNA damage as well (**Fig. 11A**). However, the SUMO modification was not completely absent, indicating that the MRX complex facilitates the induction, but is not absolutely required to trigger the SUMOylation wave in HR.

The MRX complex is not only involved in sensing the DSBs and tethering the broken ends together, but is also strongly implicated in initiating DNA-end resection and, importantly, recruiting long-range resection factors to the DSB (Mimitou and Symington, 2011; Symington and Gautier, 2011). These factors then generate extensive ssDNA tracts at the break sites, which in turn serve as a recruiting platform for repair proteins. We therefore investigated whether DNA resection is the crucial trigger for protein group SUMOylation in HR.

Resection starts with short-range trimming of DSB-ends mediated by the nucleolytic activities of the Mre11 subunit of MRX complex and its associated endonuclease Sae2. This step is in many cases not required, but may stimulate the long-range resection executed by the 5'→3' exonuclease Exo1 and also in parallel by another pathway involving Sgs1 helicase operating together with the endonuclease Dna2 (Symington and Gautier, 2011). When we hindered the initial short-range resection by deleting Sae2 endonuclease alone ($\Delta sae2$), or in a mutant strain additionally defective in the nuclease activity of Mre11 (*mre11-H125N*), the SUMOylation of HR proteins was hardly affected (**Fig. 11B** and **11C**). However, interfering with long-range resection by deleting Exo1 ($\Delta exo1$), or by abolishing its nuclease activity (*exo1-D173A*, *ND*), resulted in strong reduction of HR protein SUMOylation (**Fig. 11B** and **11D**). The same was true when we abrogated the other branch of the long-range resection by deleting Sgs1 helicase ($\Delta sgs1$; **Fig. 11B**). Finally, elimination of both long-range resection pathways ($\Delta exo1 \Delta sgs1$) resulted in barely detectable SUMOylation of HR proteins (**Fig. 11B**) following MMS treatment. Therefore, we conclude that the long-range DSB-end resection is required for the efficient induction of the SUMOylation wave in HR.

RESULTS

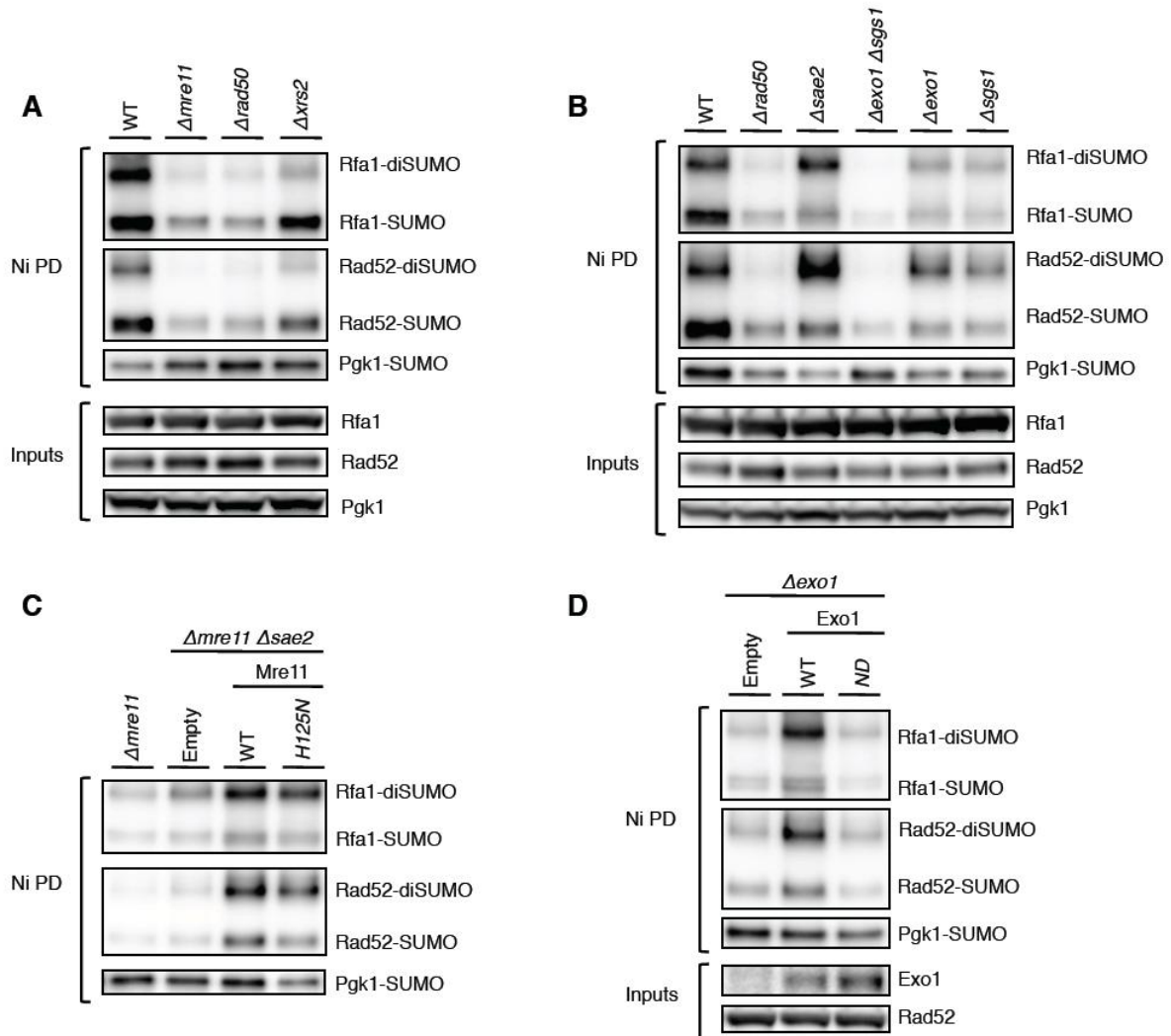


Figure 11. Long-range DNA-end Resection is Required for Efficient SUMOylation in HR
 (A) Disruption of MRX complex by deleting individual subunits results in pronounced decrease of SUMOylation of HR proteins following DNA damage. Denaturing Ni-NTA pull-down (Ni PD) was performed to isolate ³⁵S-SUMO-conjugates from MMS (0.2%)-treated cells lacking Rad50, Mre11 or Xrs2. (B) Long-range resection by the action of Exo1 and Sgs1/Dna2, but not short-range processing of DNA ends by Sae2 endonuclease, triggers SUMOylation of DNA repair proteins. Similar to (A), but with MMS-treated cells lacking Sae2, Exo1, Sgs1, or both Exo1 and Sgs1. Both branches of long-range resection contribute to induction of SUMOylation wave in DNA repair pathway. (C) Short-range processing of DNA DSB-ends by Sae2 and Mre11 is not required for the induction of SUMOylation wave following DNA damage. Similar to (A), but with MMS-treated $\Delta mre11 \Delta sae2$ cells expressing either WT or nuclease-dead (*mre11-H125N*) Mre11. (D) Nuclease activity of Exo1 is required for SUMOylation induction in response to DNA damage. Similar to (A), but with MMS-treated cells expressing either WT or nuclease-dead (*exo1-D173A*, ND) Exo1.

III.2.2 Exposure of ssDNA is the Trigger for HR Protein Group SUMOylation

As mentioned earlier, the DSB-end resection generates long ssDNA tracts that are needed to recruit a large number of HR and checkpoint factors to the sites of DNA damage in order to efficiently signal and repair the DNA breaks. We therefore asked

RESULTS

whether it is the exposure of ssDNA, rather than the process of resection during DSB processing, that is the primary trigger for SUMOylation of HR proteins. To address this issue, we induced the accumulation of ssDNA in cells independently of DSB formation by three different means. First, we used the property of noncycling G1-arrested cells that were treated with UV-light to convert NER intermediates into long ssDNA gaps through the action of Exo1 (**Fig. 12A**) and thereby promote checkpoint activation (Giannattasio et al., 2010). Second, we induced the accumulation of ssDNA gaps behind replication forks by shifting the mutant strain lacking the nonessential DNA polymerase δ subunit Pol32 to low temperature (**Fig. 12B**), at which it undergoes faulty replication (Karras and Jentsch, 2010). Third, we took advantage of the telomere-capping protein Cdc13 mutant (*cdc13ts*) that releases telomeric ssDNA when shifted to higher temperatures (Garvik et al., 1995) (**Fig. 12C**). Under all tested conditions we detected SUMOylation of HR proteins coinciding with checkpoint activation. Thus, the exposure of ssDNA stretches of sufficient length, and not DSB processing as such, is the crucial trigger for protein group SUMOylation in HR.

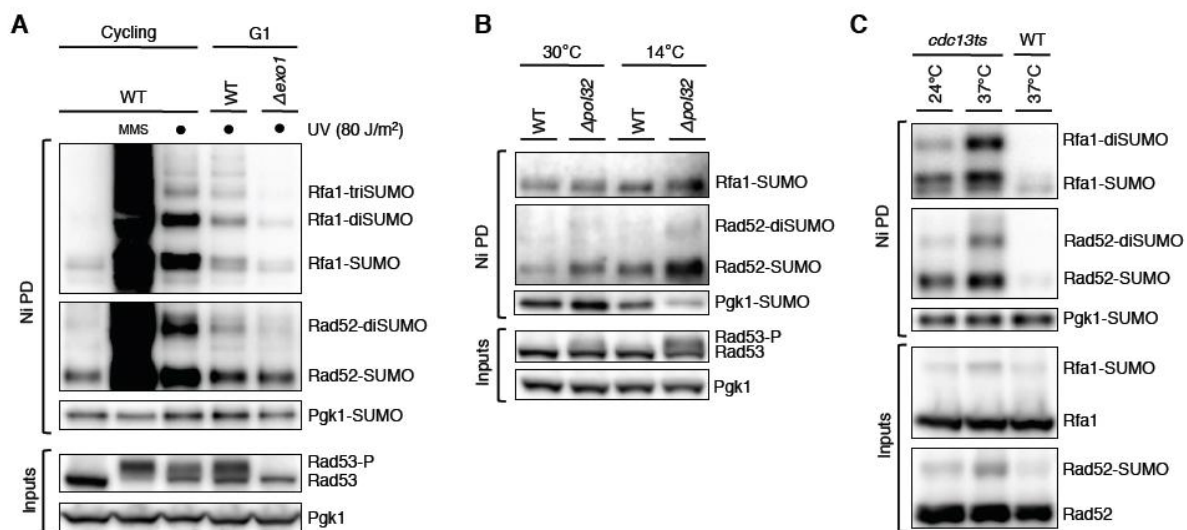


Figure 12. Exposure of ssDNA Triggers SUMOylation of HR Proteins

(A) ssDNA gaps generated after UV-light treatment by Exo1 in G1-arrested cells are sufficient to trigger SUMOylation of repair proteins. Denaturing Ni-NTA pull-down (Ni PD) was performed to isolate ^{His}SUMO-conjugates from cycling or G1-arrested WT or Exo1-deficient (Δ exo1) cells, which were treated either with MMS (0.2%) or UV-light (80 J/m²). Hyperphosphorylated Rad53 indicates checkpoint activation triggered by resection following DNA damage. (B) ssDNA gaps that accumulate due to faulty replication in cells lacking the polymerase δ subunit Pol32 (Δ pol32) grown at 14°C are sufficient to trigger Rad53 phosphorylation and HR protein SUMOylation, detectable by Ni PD of ^{His}SUMO conjugates. (C) Uncapping of telomeres and exposure of ssDNA in temperature-sensitive *cdc13ts* mutants triggers HR protein SUMOylation. ^{His}SUMO Ni PD from WT and *cdc13ts* cells, grown to an OD₆₀₀ of 0.7 at 24°C and then shifted to 37°C.

RESULTS

III.2.3 Crosstalk between SUMOylation in HR and DNA Damage Checkpoint

The HR pathway is largely limited to the S and G2 phases of the cell cycle when following DNA replication sister chromatid becomes available as a template for repair. In part, this can also be explained by the reduced DSB resection efficiency in G1 phase, which is negatively regulated by DSB binding of the NHEJ Ku70/Ku80 complex that competes with MRX and Exo1. However, DSB resection in G1 is not abolished (Barlow et al., 2008) and is in fact sufficient to trigger SUMOylation of HR proteins (**Fig. 13A**), which is largely dependent on Exo1. In parallel, generation of ssDNA tracts activates checkpoint kinases that target numerous substrates including resection machinery. Multisite phosphorylation of Exo1 was shown to inhibit its activity, preventing excessive ssDNA formation and thus limiting the checkpoint activation (Morin et al., 2008). We therefore analyzed how phosphorylation-defective *exo1-SA* mutant, which is no longer negatively regulated by checkpoint control, would affect HR protein SUMOylation, and found that it was indeed significantly increased compared to WT cells (**Fig. 13B**).

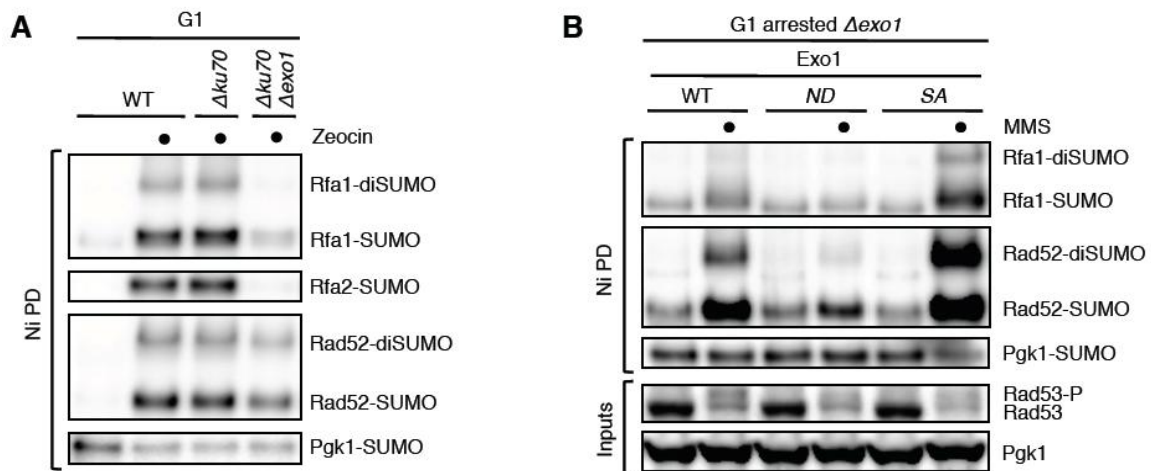


Figure 13. Exo1 Resection-induced SUMOylation in HR Is under Checkpoint Control

(A) SUMOylation of repair proteins can be efficiently triggered by Exo1-resected DNA DSB-ends in cells arrested in G1. Denaturing Ni-NTA pull-down (Ni PD) was performed to isolate ^{His}SUMO-conjugates from G1-arrested and Zeocin-treated WT cells, cells lacking nonhomologous end-joining factor Yku70 ($\Delta ku70$), or both Yku70 and Exo1 ($\Delta ku70 \Delta exo1$). (B) Exonuclease activity of Exo1 is required for efficient DNA resection and SUMOylation of HR proteins following MMS treatment in G1-arrested cells. α -factor arrested cells expressing nuclease-dead Exo1 ($\Delta exo1$ cells expressing *exo1-D173A*; ND) do not show efficient SUMOylation of RPA and Rad52 compared to cells expressing WT Exo1. In contrast, cells expressing Exo1 mutant (*exo1-S372A,S567A,S586A,S692A*; SA) that is not negatively regulated by DNA damage checkpoint kinases, show elevated levels of SUMOylated repair proteins due to uncontrolled resection.

The increased levels of Rad52 SUMOylation were observed previously in DNA damage checkpoint mutants, e.g., in *rad53* cells, and were proposed to correlate with

RESULTS

elevated levels of ssDNA formation during replication (Ohuchi et al., 2009). Our findings provide explanation for these observations and suggest that inactivation of the checkpoint signaling leads to the accumulation of HR protein SUMOylation not only because DNA damage levels are elevated, but also because excessive DNA resection is no longer repressed.

When we analyzed SUMOylation of HR proteins in mutant cells lacking apical checkpoint kinase Mec1, or its adaptor protein Ddc2, which recruits the kinase to the ssDNA-RPA bound complexes (Rouse and Jackson, 2002; Zou and Elledge, 2003), strong enrichment of SUMOylated HR proteins was observed even in the absence of exogenous DNA damage (**Fig. 14A**). Deletion of Mec1/Ddc2 is lethal to the cells, but can be suppressed by removal of Sml1, an inhibitor of ribonucleotide reductase that catalyzes the rate-limiting step in dNTP synthesis (Zhao et al., 1998). Sml1 deletion increases the dNTP levels otherwise downregulated in checkpoint kinase mutants.

Similar to the absence of Mec1/Ddc2, deletion of the checkpoint mediator Rad9, which is crucial for the DNA damage checkpoint but is not required for normal growth, resulted in strong accumulation of SUMOylated HR factors (**Fig. 14B**). Mutants lacking the components of the 9-1-1 checkpoint clamp ($\Delta rad17$, $\Delta mec3$) or its loader ($\Delta rad24$) also showed elevated SUMOylation levels of HR proteins (**Fig. 14C**) following MMS treatment.

Elimination of the DNA damage checkpoint signaling resulted in pronounced enrichment of HR protein SUMOylation in cycling cells even when both long-range resection pathways were absent ($\Delta exo1 \Delta sgs1$; **Fig. 14D**), in contrast to the scenario when the checkpoint is intact. This is indicative of a high DNA damage load leading to accumulation of ssDNA in checkpoint mutants most probably arising from the stalling and subsequent collapse of multiple replication forks. Interestingly, disruption of the DSB-sensing MRX complex ($\Delta rad50$; **Fig. 14D**) did not reduce SUMOylation of HR proteins to the same level as in resection-defective mutants, further suggesting that ssDNA in checkpoint mutants arises largely in the form of extensive single-stranded gaps and faulty replication intermediates. Moreover, exposure of checkpoint mutants to HU or 4NQO, which in WT cells barely induce SUMOylation in HR, resulted in strong accumulation of SUMO-modified repair factors (**Fig. 14E**). Thus, the HR protein SUMOylation wave and checkpoint signaling are initiated in parallel; however, checkpoint kinases restrict excessive ssDNA formation and therefore regulate the extent of SUMOylation in HR.

RESULTS

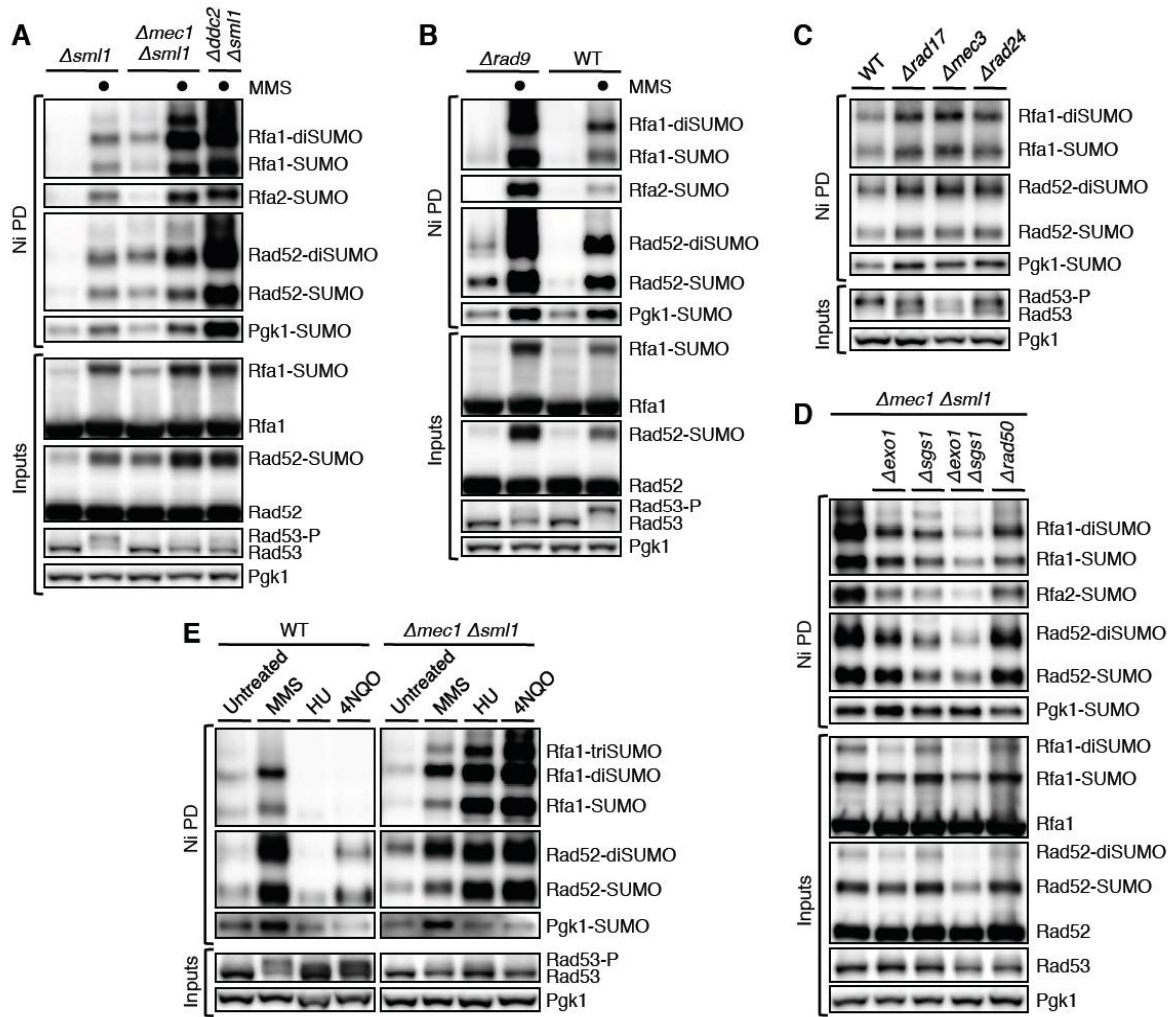


Figure 14. HR Protein SUMOylation Accumulates Heavily in the Absence of Checkpoint

(A) Inactivation of the DNA damage checkpoint in mutants lacking the apical checkpoint kinase Mec1 ($\Delta mec1 \Delta sml1$), or its adaptor protein Ddc2 ($\Delta ddc2 \Delta sml1$), results in strong SUMOylation of HR proteins, even in the absence of exogenous DNA damage. (B) Absence of the checkpoint mediator Rad9 ($\Delta rad9$) results in increased SUMOylation of HR proteins, similar to $\Delta mec1 \Delta sml1$ cells. (C) Absence of subunits of the 9-1-1 checkpoint clamp ($\Delta rad17$, $\Delta mec3$), or of its loader ($\Delta rad24$), results in a partial increase of SUMOylation of HR proteins upon MMS treatment. (D) Strong accumulation of SUMOylated HR proteins in DNA-damage checkpoint mutants can be attributed to increased DNA resection by Exo1- and Sgs1/Dna2-dependent resection pathways. ^{His}SUMO Ni PD from checkpoint-deficient ($\Delta mec1 \Delta sml1$) cells lacking additionally DNA resection pathways, following MMS treatment. HR protein SUMOylation is reduced in mutants lacking resection pathways ($\Delta exo1$, $\Delta sgs1$, $\Delta exo1 \Delta sgs1$). SUMOylation is still substantial even in resection-defective cells because DNA damage is significant in the absence of checkpoint signaling. Disruption of the MRX complex ($\Delta rad50$) does not reduce SUMOylation of repair proteins to the same extent as in mutants defective in long-range resection ($\Delta exo1 \Delta sgs1$). (E) In the absence of normal checkpoint activation ($\Delta mec1 \Delta sml1$), SUMOylation of HR proteins can be efficiently triggered even by DNA-damaging agents (HU, 4NQO) that do not normally trigger the SUMOylation wave in unperturbed cycling cells. ^{His}SUMO Ni PD from WT and checkpoint deficient $\Delta mec1 \Delta sml1$ cells following treatment with indicated DNA-damaging agents.

RESULTS

III.3 DNA-bound SUMO Ligase Siz2 Induces a SUMOylation Wave in HR

III.3.1 SUMOylation in HR is Mediated by Sequence-nonspecific DNA-bound Siz2

After establishing that exposure of ssDNA triggers protein group SUMOylation in HR, we next asked how this is being achieved mechanistically. Substrate selectivity in the SUMO pathway is mediated largely by the localization of conjugation machinery, therefore we initially hypothesized that the responsible SUMO ligase is specifically recruited by ssDNA. There are currently three SUMO ligases known to operate in the mitotic cells of *S. cerevisiae* (Geiss-Friedlander and Melchior, 2007). Consequently, we individually analyzed DNA-damage induced SUMOylation of HR proteins in mutants lacking canonical Siz/PIAS SUMO ligases Siz1 or Siz2, as well as in mutant *mms21-11* cells, harboring Mms21 defective in its ligase activity (**Fig. 15**). The SUMOylation of HR proteins was virtually absent in cells lacking Siz2, whereas it was largely not affected in other SUMO E3 mutants. Therefore, Siz2 is the key SUMO ligase that mediates protein group SUMO modification in HR.

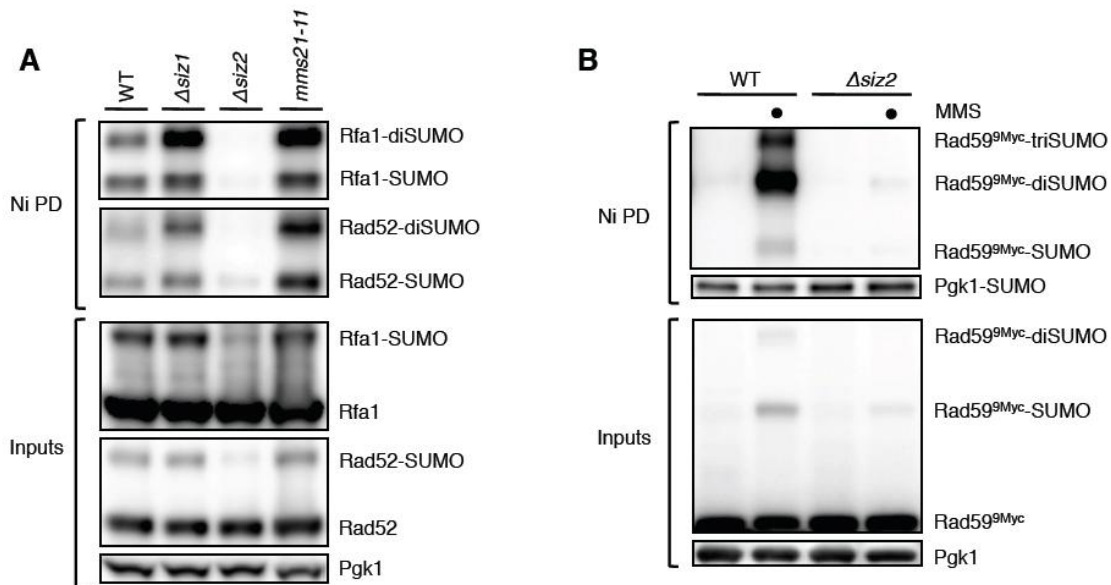


Figure 15. SUMO Ligase Siz2 Mediates Protein Group SUMOylation in HR

(A) SUMO ligase Siz2 stimulates SUMOylation of RPA and Rad52 after DNA damage. Denaturing Ni-NTA pull-down (Ni PD) was performed to isolate ^{His}SUMO conjugates from MMS-treated WT cells, mutants lacking SUMO ligases Siz1 ($\Delta siz1$) or Siz2 ($\Delta siz2$), or mutant *mms21-11* cells, lacking ligase activity of Mms21. (B) SUMO ligase Siz2 stimulates modification of the HR protein Rad59 in response to DNA damage. ^{His}SUMO Ni PD from WT cells or cells lacking Siz2 ($\Delta siz2$) before and after MMS treatment. SUMO modified species of C-terminally Myc-epitope-tagged Rad59 are almost absent in cells lacking Siz2.

We next determined whether Siz2 binds to DNA *in vitro*. To this end, we purified N-terminally His-tagged recombinant Siz2 protein expressed in *E. coli* and analyzed

RESULTS

its ability to bind DNA using chemiluminescent-based electrophoretic mobility shift assay (EMSA). Indeed, Siz2 could bind to both random dsDNA and ssDNA, however, very weakly to the latter (**Fig. 16A**). Moreover, we did not detect any binding preference of Siz2 toward preassembled DNA structures that represent resected DSB-ends or replication forks (**Fig. 16B**). Thus, in the absence of accessory proteins, recombinant Siz2 *in vitro* preferentially binds to dsDNA in a sequence-nonspecific manner.

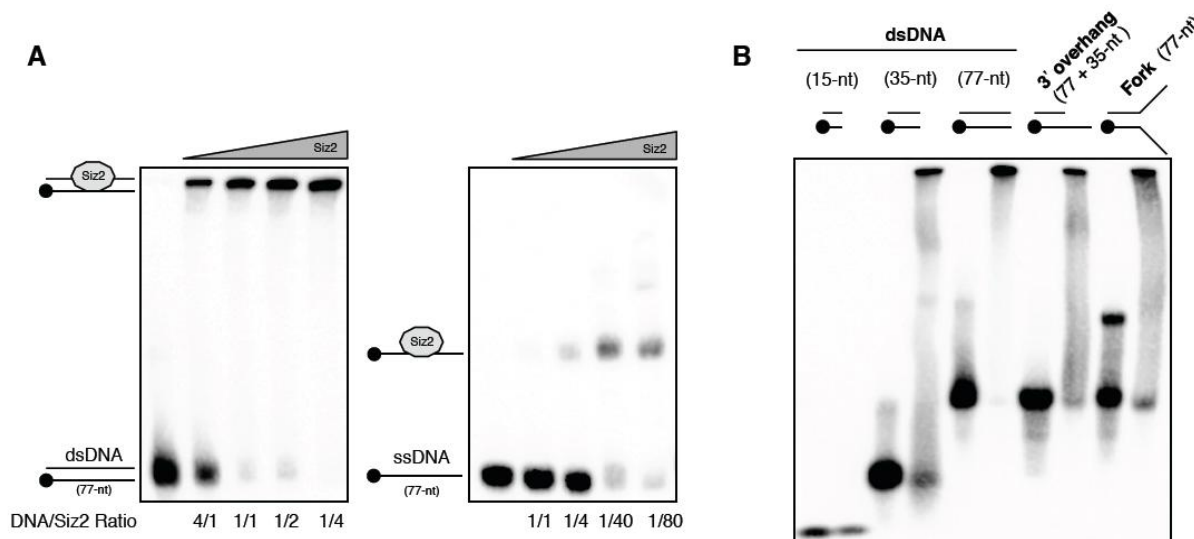


Figure 16. Recombinant SUMO Ligase Siz2 Preferentially Binds to dsDNA *in vitro*

(A) Recombinant ^{His}Siz2 protein binds dsDNA and weaker ssDNA. Increasing amounts of ^{His}Siz2 were added to 5'-end biotin-labeled 77-nucleotide long dsDNA and ssDNA (20 fmol), and the binding was detected using chemiluminescent-based electrophoretic mobility shift assay (EMSA). (B) Recombinant, purified ^{His}Siz2 protein has no binding preference *in vitro* to assembled DNA structures, representing replication forks or 3'-end ssDNA overhangs.

The canonical Siz/PIAS SUMO ligase Siz2 contains an unstructured C-terminal tail harboring a SIM close to an SP-RING domain that is required for binding to SUMO-charged Ubc9, a PINIT domain associated with substrate binding, and an N-terminal SAP domain, which mediates DNA binding in many other proteins (**Fig. 17A**). We next verified whether sequence-nonspecific interaction of Siz2 with DNA is achieved through this short conserved module. Indeed, Siz2 binds to DNA via the SAP domain, because purified recombinant Siz2 variants with either deleted SAP (Δ SAP) or carrying substitutions of the three conserved residues to alanines within this domain (G64A, K66A and L69A; SAP*) are no longer able to bind DNA *in vitro* (**Fig. 17B**).

RESULTS

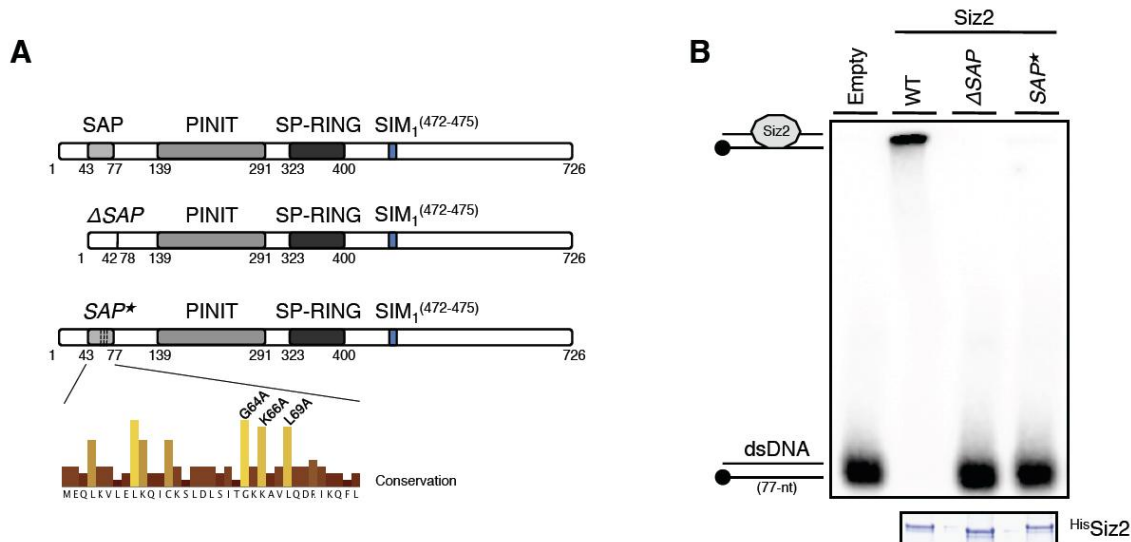


Figure 17. DNA Binding of Siz2 is Mediated via the Conserved SAP Domain

(A) Schematic representation of the domain architecture of Siz2 and its mutant variants constructed to study the role of the SAP domain in the DNA binding and SUMOylation of HR proteins. Δ SAP denotes a Siz2 variant, in which conserved residues (aa 43-77) of the DNA-binding domain (DBD) were deleted. SAP^* denotes a ligase variant, in which three conserved residues (G64, K66 and L69) of the SAP domain were changed to alanines. (B) Recombinant His Siz2 variants either lacking the DNA-binding SAP domain (Δ SAP) or having three highly conserved residues replaced by alanine residues (SAP^*) are unable to bind DNA. EMSA with random 5'-end biotin-labeled 77-nucleotide long dsDNA (20 fmol).

We then examined the role of SAP-mediated DNA binding of Siz2 in the SUMOylation of HR proteins after DNA damage *in vivo*. Interestingly, expression of the DNA-binding-deficient Siz2- SAP^* from its endogenous promoter resulted in the loss of HR protein group SUMOylation, however, the ligase mutant variant was barely detectable in the cell lysates compared to WT Siz2 (**Fig. 18A**). Expression of the mutant protein via a strong copper-inducible promoter (pCUP- SAP^*) restored its intracellular levels (**Fig. 18B**) and to some extent rescued the DNA-damage-induced SUMOylation of HR proteins (**Fig. 18C**). This suggests that the mutant is not enzymatically inactive, but that the SUMO ligase has to properly localize to DNA in order to efficiently mediate the modification of its substrates.

The SAP domain with a consensus sequence of just 35 residues is a putative DNA-binding domain found in diverse nuclear proteins implicated in chromosomal organization (Aravind and Koonin, 2000), which was previously shown to nonspecifically bind to A/T-rich DNA sequences. In our *in vitro* DNA-binding experiments (EMSA) we also used random DNA oligos and observed strong sequence-nonspecific SAP-mediated interaction of Siz2 preferentially with dsDNA, suggesting that the SAP domain localizes the SUMO ligase to chromatin broadly and not specifically to certain DNA sequences or ssDNA. To further test if Siz2 has to

RESULTS

bind DNA in a sequence-nonspecific manner in order to support DNA-damage-induced SUMOylation of HR proteins, we decided to exchange the SAP domain of Siz2 with the short sequence-specific DBD of the well-known transcription factor Gal4 (Fig. 19A).

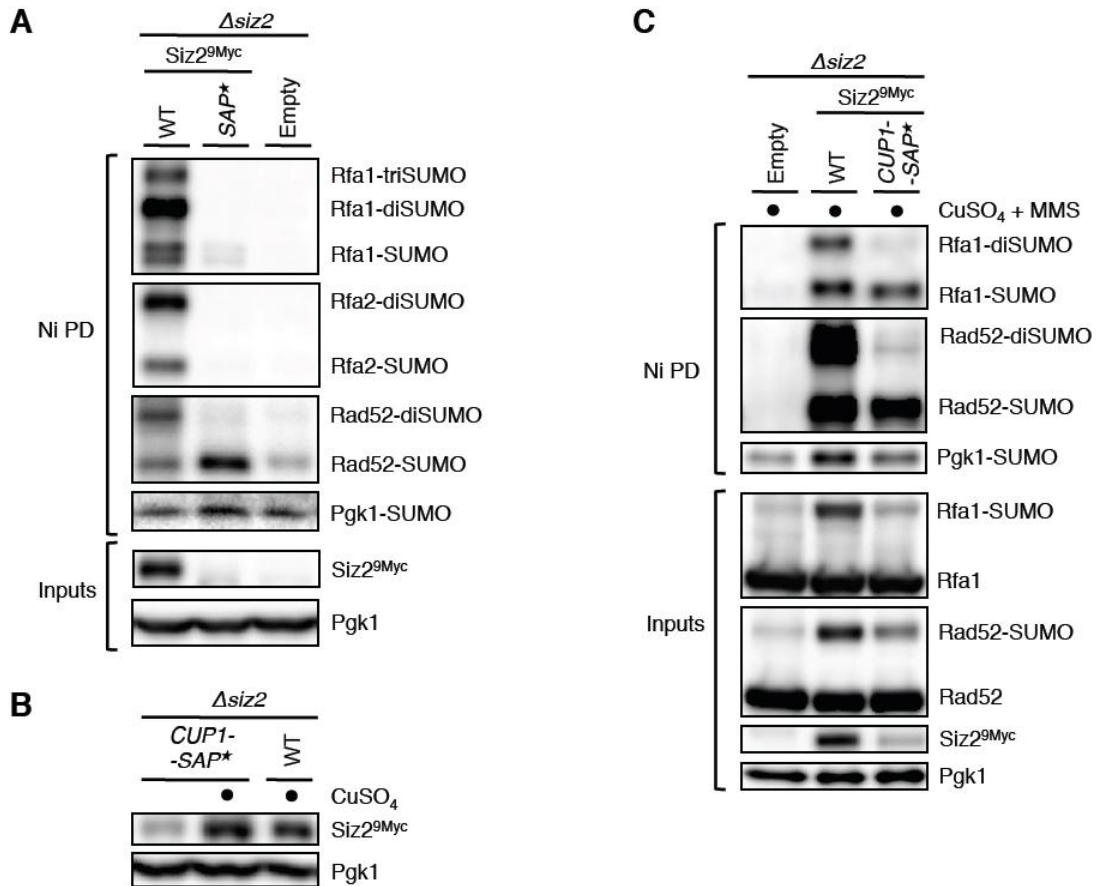


Figure 18. SAP-mediated DNA Binding Stabilizes Siz2 and Ensures SUMOylation in HR (A) DNA-binding-deficient Siz2 is destabilized in vivo and does not stimulate SUMOylation of HR proteins after DNA damage. HisSUMO Ni PD from $\Delta siz2$ cells expressing either Myc-tagged WT Siz2 or DNA-binding-deficient Siz2 (SAP*) following MMS treatment. (B) Intracellular protein level of Siz2 SAP* expressed under CUP1-promoter control (100 μ M CuSO₄) is similar to the protein level of WT Siz2. (C) Expression of DNA-binding-deficient Siz2 via the strong CUP1 promoter (CUP1-SAP*) partially restores its protein level and HR protein SUMOylation after MMS treatment.

Remarkably, localization of Siz2 to specific DNA sequences by the DBD of Gal4 (*siz2*^{-Gal4DBD}) restored the protein level of the SUMO ligase compared to its DNA-binding-deficient variant, however, without supporting HR protein group SUMOylation (Fig. 19B). By contrast, when we replaced the N-terminus of Siz2 harboring SAP domain with the N-terminus of related canonical Siz/PIAS ligase Siz1 carrying its SAP domain (Siz1 SAP; Fig. 19A), not only the protein levels of chimeric protein were identical to WT Siz2, but also the SUMOylation wave in HR was fully supported (Fig. 19C). Thus, together these findings strongly suggest that SAP-mediated

RESULTS

localization of Siz2 to DNA is required for efficient DNA damage-induced protein group SUMOylation in HR. Moreover, and importantly, Siz2 binds DNA widely in a sequence-nonspecific manner and is not explicitly recruited by ssDNA, which nevertheless serves as a key trigger for HR protein SUMOylation.

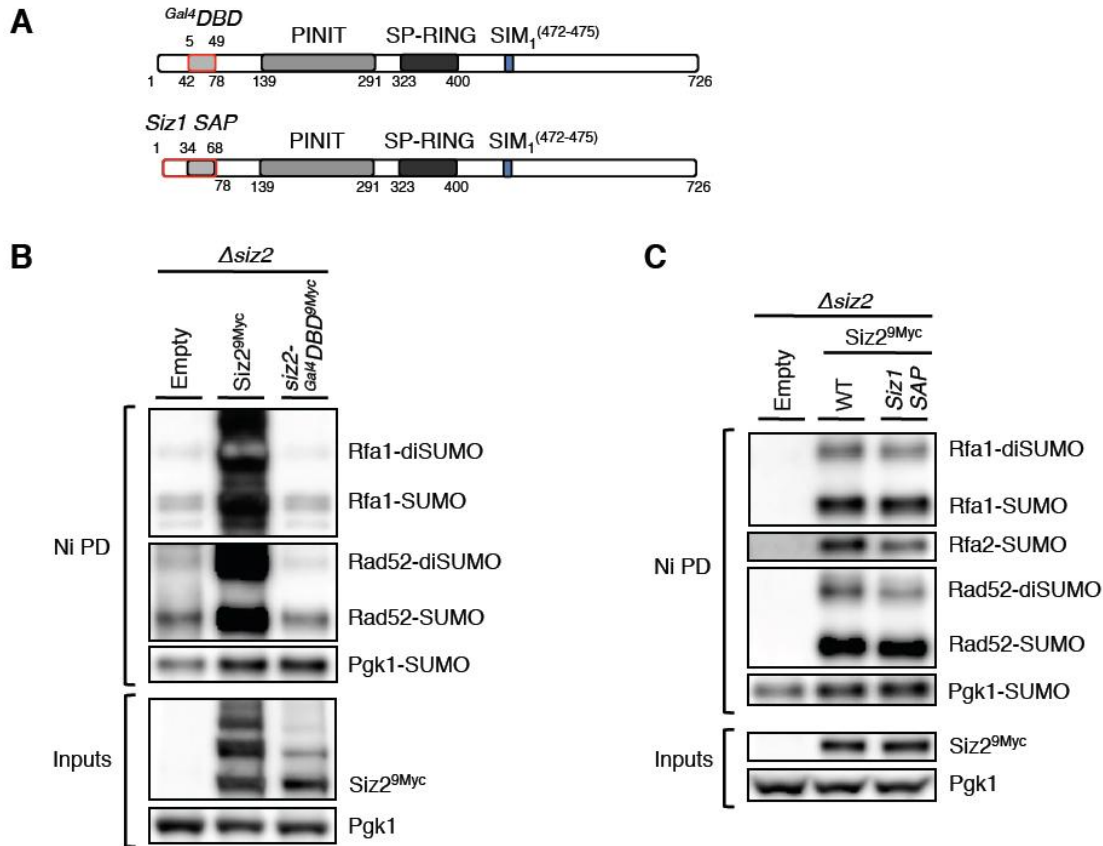


Figure 19. Sequence-nonspecific DNA Binding of Siz2 via the Conserved SAP Domain is Required for Efficient SUMOylation in HR

(A) Schematic representation of mutant variants constructed to study the role of the DNA-binding SAP domain of Siz2 in the modification of HR proteins. *Gal4DBD* denotes a Siz2 variant in which its SAP domain (aa 43-77) was replaced by the sequence-specific DBD of the Gal4 transcription factor (aa 5-49). *Siz1 SAP* denotes a chimeric Siz2 variant, in which the N-terminal region (aa 1-77) of Siz2 (harboring its SAP domain) was replaced by the N-terminal region (residues 1-68) of Siz1 (harboring its SAP domain). (B) A Siz2 variant harboring the sequence-specific DNA-binding domain of Gal4 (*siz2-Gal4DBD*) instead of Siz2's SAP domain does not support efficient SUMOylation of HR proteins after DNA damage even though its intracellular protein level is similar to WT Siz2. (C) Chimeric Siz2 carrying the N-terminus of Siz1 harboring Siz1's SAP domain (*Siz1 SAP*) is expressed to a similar level as WT Siz2 and is fully functional in stimulating HR protein SUMOylation.

III.3.2 Features of Siz2 Required for Efficient Protein Group SUMOylation in HR

After establishing an important role of the conserved SAP domain in broad sequence-nonspecific localization of Siz2 to DNA and efficient SUMOylation of HR proteins upon DNA damage, we next addressed what other features of Siz2 are required for full-scale SUMOylation response in HR.

RESULTS

The conserved PINIT domain of the related canonical Siz/PIAS SUMO ligase Siz1 was previously shown to be important for correct positioning of the ligase substrate (PCNA) and its efficient SUMO modification at the non-consensus SUMO-acceptor site (K164) (Yunus and Lima, 2009). To test whether also the PINIT domain of Siz2 contributes to the SUMOylation of HR proteins, we again constructed a chimeric protein this time carrying the PINIT domain of Siz1 in place of the Siz2's PINIT (Siz1 PINIT; **Fig. 20A**).

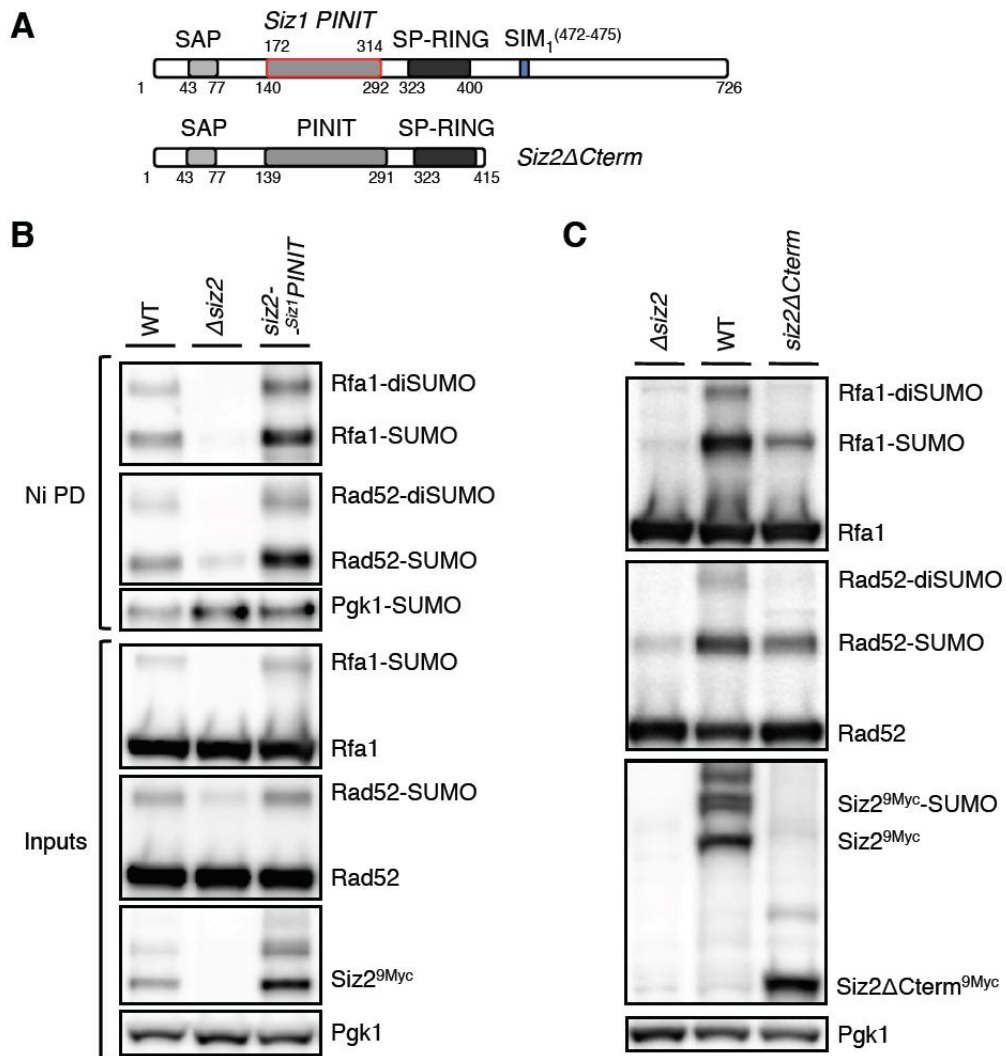


Figure 20. C-terminal Tail of Siz2 is Required for Full-scale SUMOylation Wave in HR

(A) Schematic representation of Siz2 mutant variants constructed to study the role of its PINIT domain and the C-terminal tail in the modification of HR proteins. *Siz1* PINIT denotes a Siz2 variant, in which its conserved PINIT domain (aa 141-291) was replaced by the PINIT domain of Siz1 (aa 172-314). *Siz2* Δ Cterm denotes a C-terminal truncation (aa 416-726) of Siz2. (B) A Siz2 variant *Siz2*^{-Siz1PINIT} harboring the PINIT domain of Siz1 fully supports SUMOylation of HR proteins. (C) A Siz2 variant *Siz2* Δ Cterm with a deleted C-terminal tail (aa 416-726) supports SUMOylation of HR proteins, however, with reduced activity.

RESULTS

The chimeric Siz2 protein harboring Siz1's PINIT was stably expressed *in vivo* and fully supported HR protein group SUMOylation after DNA damage (**Fig. 20B**). This indicates that the features of Siz2 required for efficient SUMOylation in HR are located elsewhere in the ligase, most likely in its C-terminal tail, which differs significantly from the C-terminal domain of the related canonical Siz/PIAS SUMO ligase Siz1. Indeed, a Siz2 variant lacking its C-terminal tail (Siz2 Δ Cterm, **Fig. 20A**) failed to induce a full-scale SUMOylation wave in HR (**Fig. 20C**) compared to the full-length ligase, even though it was expressed at similar levels. Importantly, however, truncated Siz2 was still able to weakly catalyze SUMO modification of HR proteins, suggesting that C-terminal elements of the ligase further facilitate, but are not absolutely necessary for protein group SUMOylation in HR.

We next investigated how C-terminal tail of Siz2 contributes to the full-scale SUMOylation wave induction in HR, hypothesizing that specific motifs located in this domain target or restrict the ligase, which is sequence-nonspecifically distributed on DNA, to the DSB repair sites. Interestingly, using yeast two-hybrid assays, we found that the C-terminal domain of Siz2 interacts specifically with the Mre11 subunit of the DSB-sensing MRX complex (**Fig. 21A**). Mapping of the Mre11 interaction site in the tail of Siz2 revealed that deletion of the last 25 residues readily abolishes ligase binding to Mre11 (**Fig. 21B**). Interestingly, this C-terminal stretch of Siz2 contains a potential SIM (aa 720-723). Destroying this motif by the replacement of two hydrophobic residues to alanines (V720A, V721A; **Fig. 21C**) resulted not only in the loss of interaction with Mre11 (**Fig. 21B**), but also strongly reduced SUMOylation of HR proteins after DNA damage (**Fig. 21D**). Since Mre11 can directly bind to Ubc9 in two-hybrid assays (**Fig. 21A**), Ubc9-mediated SUMOylation of Mre11 likely further stimulates Siz2 binding to the MRX complexes loaded at DSB sites. This is reminiscent of Srs2 binding to SUMOylated PCNA via tandem SIM and PIP-box (Armstrong et al., 2012; Pfander et al., 2005). Therefore, the C-terminal tail of Siz2 most likely contains additionally a specific motif necessary for interaction with Mre11, which alone without its C-terminal SIM is not sufficient to bind Mre11. We next asked whether replacement of the C-terminal domain of the related Siz/PIAS ligase Siz1 with the C-terminal tail of Siz2 (**Fig. 21C**) would be sufficient to stimulate SUMOylation in HR. However, the chimeric protein failed to support SUMOylation of HR proteins (**Fig. 21E**), but was expressed at very low levels, suggesting that either two proteins additionally differ in other aspects, or the expression levels of the ligases play an important role.

RESULTS

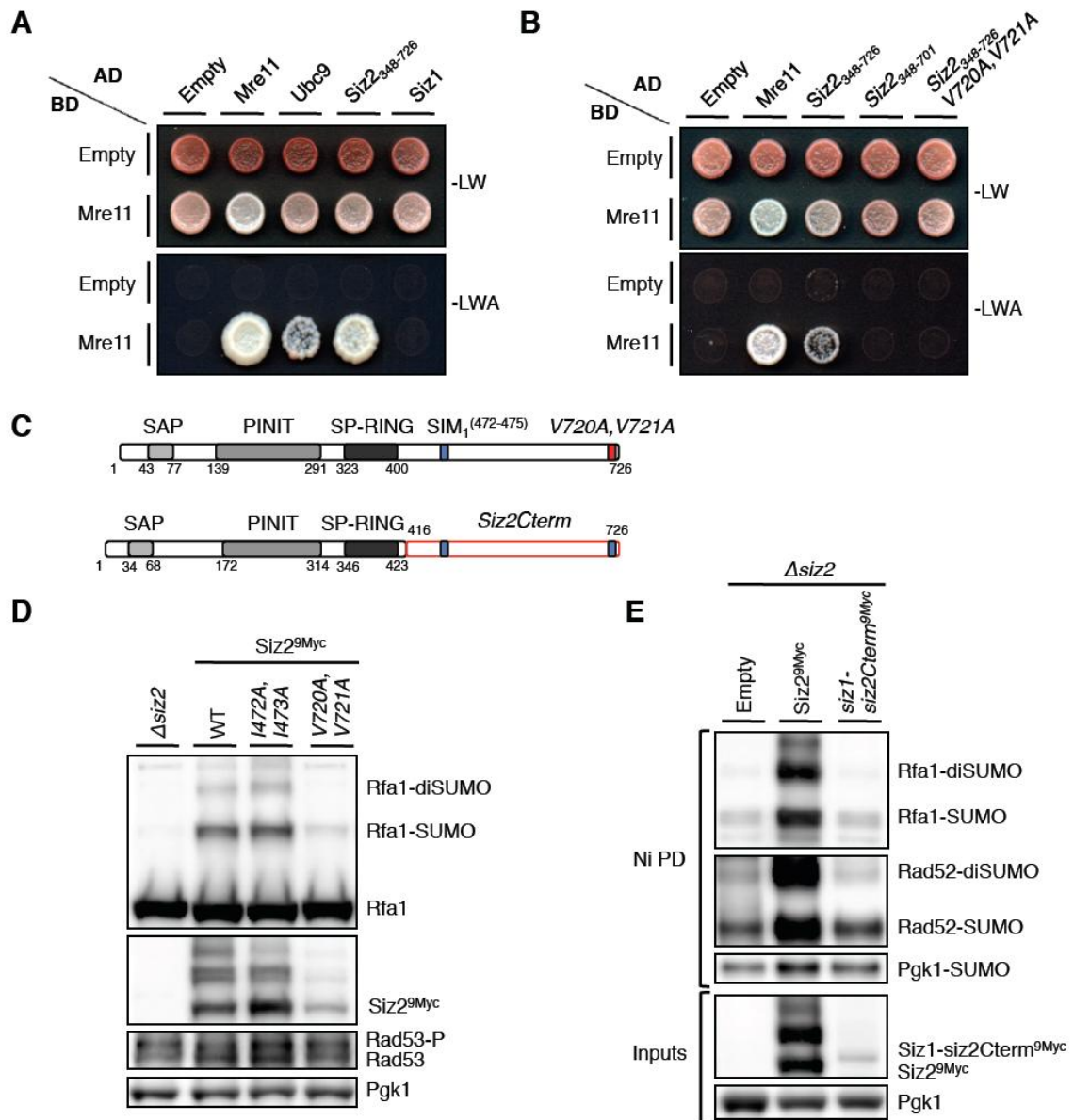


Figure 21. Binding to the Mre11 Subunit of MRX via SIM-containing Tail of Siz2 is Required for Efficient SUMOylation in HR

(A) SUMO-conjugating enzyme Ubc9 and SUMO ligase Siz2, but not Siz1 interact with Mre11 in the two-hybrid system. C-terminal tail of Siz2 (aa 348-726) is sufficient for Mre11 interaction. (B) The C-terminal SUMO-interacting motif of Siz2 (SIM₂, aa 720-723) mediates its binding to the Mre11 subunit of MRX in a two-hybrid assay. (C) Schematic representation of mutant variants constructed to study the role of Siz2's C-terminal tail in the modification of HR proteins. *Siz2-V720A, V721A* denotes a Siz2 variant with mutated C-terminal SUMO-interacting motif. *Siz1-siz2Cterm* denotes a Siz1 variant, in which its C-terminal tail (aa 424-904) was replaced by the C-terminal tail of Siz2 (aa 416-726). (D) Siz2 with mutated C-terminal SUMO-interacting motif (*Siz2-V720A, V721A*), which no longer binds to Mre11 in the two-hybrid system, does not fully support HR protein SUMOylation. (E) A Siz1 chimeric protein harboring the C-terminal domain of Siz2 (*Siz1-siz2Cterm*) does not support SUMOylation of HR proteins after DNA damage.

Taken together, these findings indicate that Siz2 is localized to DNA broadly in a sequence-nonspecific manner via its SAP domain, where it can potentially encounter and mediate collective modification of HR proteins loaded onto resected ssDNA in its

RESULTS

vicinity. At the same time, the C-terminal tail unique to Siz2 harbors a dedicated SIM and probably additional motifs that restrict the ligase on DNA to SUMO-modified Mre11 at DSB sites recognized by the MRX complexes in order to stimulate full-scale SUMOylation in HR.

III.3.3 Artificial Targeting of HR Proteins to DNA Triggers Their SUMOylation

After we verified that the dedicated SUMO ligase Siz2 responsible for DNA-damage induced SUMOylation in HR is not specifically recruited to exposed ssDNA, which serves as a key trigger for protein group modification, we then scrutinized another plausible model briefly outlined earlier. Specifically, since ssDNA acts as a recruiting platform for HR proteins engaged in DSB repair, we speculated that perhaps simple localization of repair factors to chromatin in the vicinity of the broadly DNA-bound SUMO ligase Siz2 is sufficient for their modification.

To test this hypothesis, we decided to artificially target the HR proteins to DNA by directly fusing them to the sequence-specific DBD of the Gal4 transcription factor (residues 1-147, termed BD). As anticipated, the ectopically expressed BD-Rad52 fusion protein became efficiently SUMOylated in the absence of any exogenous DNA damage in a Siz2-dependent manner (**Fig. 22A**), bypassing the requirement of ssDNA as a crucial trigger. Notably, artificial DNA targeting of Rad52 did not induce the SUMOylation of its interacting partner RPA, which acts earlier in the HR pathway and is recruited to ssDNA prior to Rad52. By contrast, expression of the BD-Rfa1 fusion protein resulted not only in its robust SUMO modification in the absence of DNA damage, but also induced the SUMOylation of Rad52, which apparently was recruited to chromatin by the chromatin-bound RPA (**Fig. 22B**). Thus, these findings strongly suggest that the localization of HR proteins to DNA in the vicinity of DNA-bound SUMO ligase Siz2 is essential for their modification and that only DNA-bound HR factors engaged in DSB repair become collectively SUMOylated upon DNA damage. We therefore conclude that DNA resection and exposure of ssDNA serves as a trigger of protein group SUMOylation in HR by recruiting and assembling the substrates at reach of the dedicated chromatin-bound SUMO ligase.

RESULTS

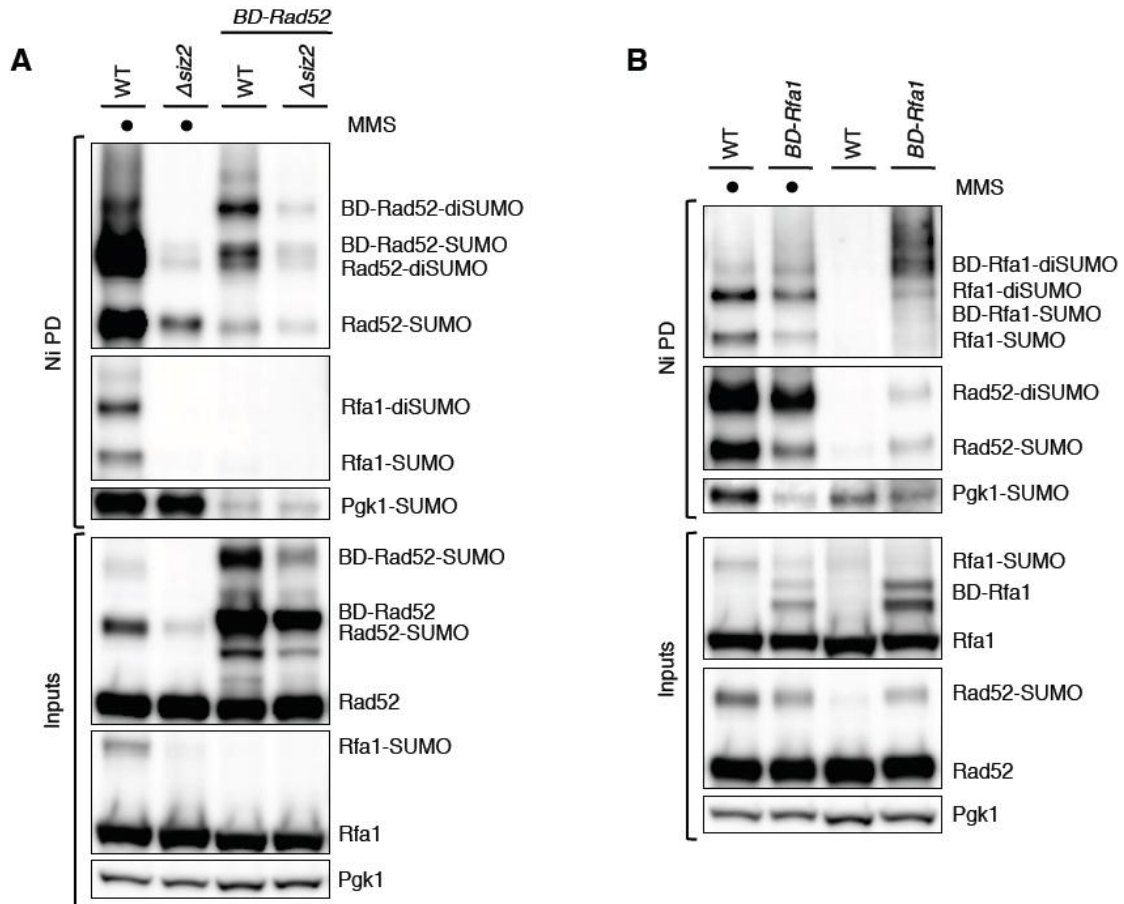


Figure 22. Artificial Tethering of HR Proteins to DNA Triggers Their SUMOylation

(A) N-terminal Gal4 DNA-binding domain (aa 1-147, BD) fusion protein BD-Rad52 ectopically expressed from high-copy pGBD vector becomes strongly SUMOylated in a *Siz2*-dependent manner in the absence of DNA damage. (B) Expression of BD-Rfa1 with its subsequent SUMOylation stimulates SUMO modification of both endogenous RPA (Rfa1) and Rad52 in the absence of DNA damage.

Importantly, *Siz2*-dependent SUMO modification of the DNA-targeted BD-Rad52 fusion took place at the correct SUMO-acceptor lysine residues of Rad52 mapped previously, because no SUMOylation was observed when SUMOylation-defective Rad52 BD-fusion with *in vivo* targeted lysines replaced by arginines (BD-rad52-KR, **Fig. 23A**) was expressed. Notably, SUMOylation of BD-Rad52 was not further stimulated by additional expression of *Siz2* variant *Siz2*^{Gal4}DBD (**Fig. 23A**), which should be specifically targeted to Gal4-binding sites where BD-fusions reside. Moreover, in the absence of endogenous *Siz2* ligase the *Siz2*^{Gal4}DBD variant failed to support SUMOylation of BD-Rad52 fusion (**Fig. 23B**), emphasizing that intact SAP domain is required for proper localization of the ligase to DNA to fulfill its functions.

RESULTS

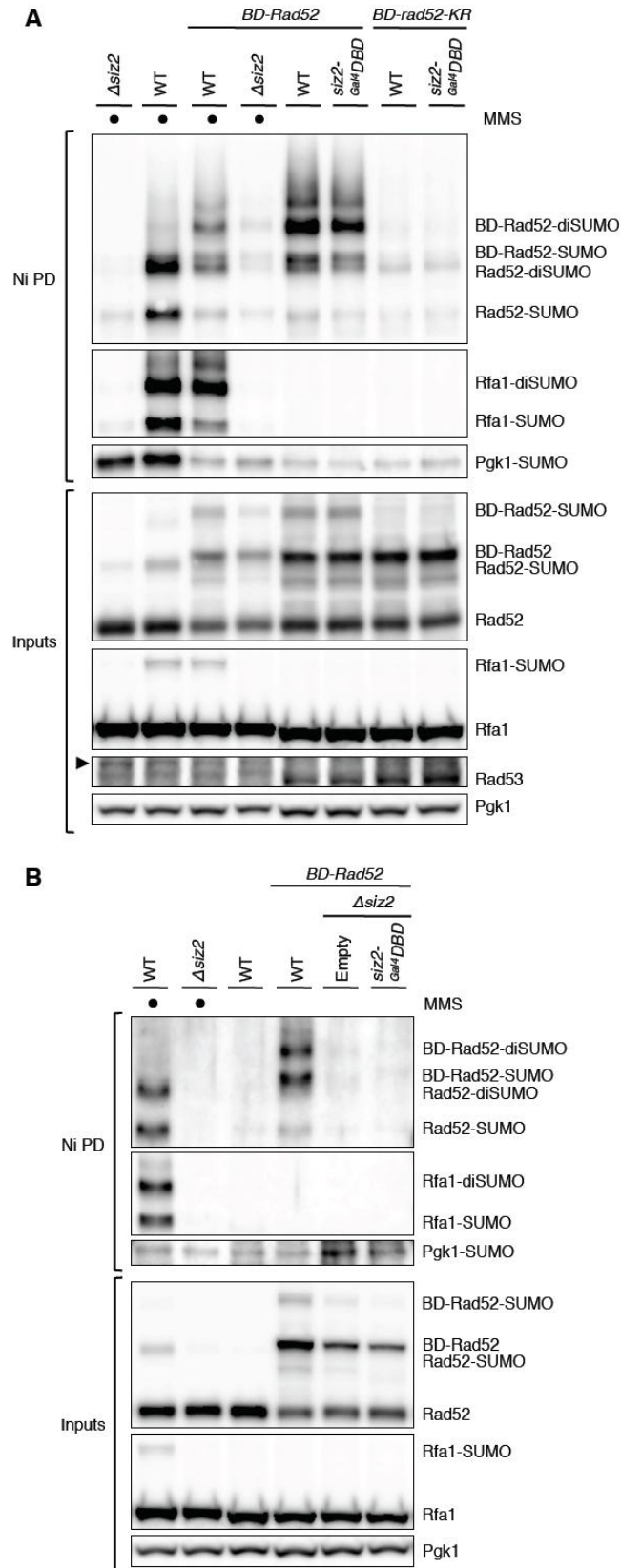


Figure 23. Siz2-dependent SUMOylation of Artificially DNA-bound HR Proteins Occurs at Correct SUMO-Acceptor Lysine Residues and Requires Intact SAP-domain

(A) Siz2-dependent SUMOylation of BD-Rad52 takes place specifically at previously confirmed SUMO-acceptor lysines on Rad52 and cannot be further stimulated by additionally targeting Siz2 variant Siz2^{Gal4}DBD to Gal4-binding sites where BD-Rad52 resides. (B) SUMOylation of BD-Rad52 cannot be supported by Siz2^{Gal4}DBD in the absence of endogenous Siz2 ligase.

RESULTS

III.4 SUMOylation Promotes Physical Interactions between HR Proteins

III.4.1 SUMOylation of HR Proteins on Chromatin Promotes Complex Formation

After concluding that ssDNA serves as a key trigger for SUMOylation in HR by recruiting substrates to chromatin in close vicinity to the dedicated DNA-bound SUMO ligase Siz2, which catalyzes HR protein group modification, we then verified whether SUMOylated HR proteins are indeed located on chromatin. To this end, we performed subcellular fractionation of MMS-treated cells followed by denaturing Ni-NTA pull-down of ^{His}SUMO conjugates. As expected, we observed that the SUMO-modified HR proteins are enriched in the chromatin fraction (**Fig. 24**), further strengthening that specifically DNA-bound pools of HR proteins engaged in DSB repair after DNA damage become collectively targeted by SUMO modification.

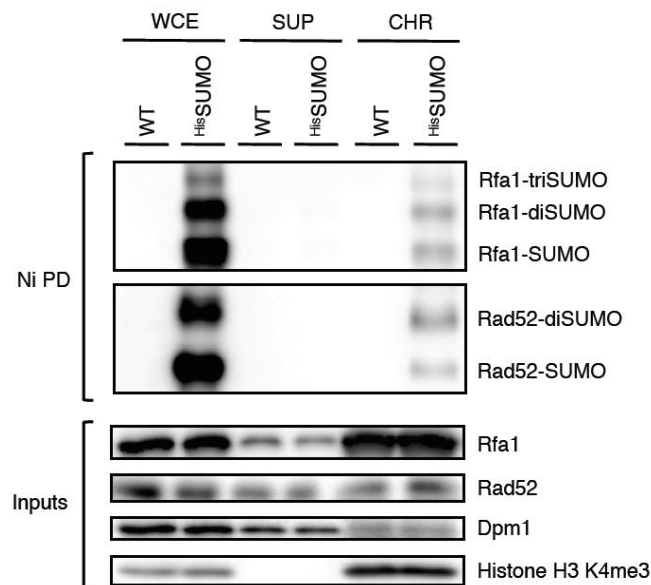


Figure 24. SUMOylated HR Proteins are Enriched in Chromatin after DNA Damage

Following subcellular fractionation of MMS-treated WT cells, or cells overexpressing ^{His}SUMO into soluble (SOL) and chromatin-enriched (CHR) fractions, the denaturing Ni-NTA pull-down (Ni PD) of ^{His}SUMO conjugates was performed. SUMOylated forms of Rfa1 and Rad52 were specifically enriched in the chromatin fraction. To control chromatin fractionation efficiency, the levels of histone H3 lysine-4 tri-methylation (H3 K4me3) and the ER-membrane protein Dpm1 were detected in fractions prior to Ni PD.

Since the SUMOylation wave specifically targets the whole set of HR proteins that not only act together in one DSB repair pathway, but also physically interact and form functional protein complexes at sites of DNA damage, we therefore asked how protein group SUMOylation might affect physical interactions between HR factors. For that purpose, we co-immunoprecipitated (co-IP) DSB repair protein complexes after DNA damage by pulling down the individual HR factors and quantified the ratios

RESULTS

of SUMO-modified/unmodified HR protein fractions in co-IPs versus inputs. Importantly, interacting repair proteins formed complexes precisely after DNA damage with marked preference towards SUMO-modified species. Specifically, immunoprecipitation of Rad59, which forms a complex with RPA and Rad52 (Davis and Symington, 2003) that is required for efficient exchange of RPA to Rad51 recombinase on ssDNA, brought down proportionally higher amounts of SUMO-modified RPA (Rfa1) and Rad52 compared to their unmodified pools (**Fig. 25**).

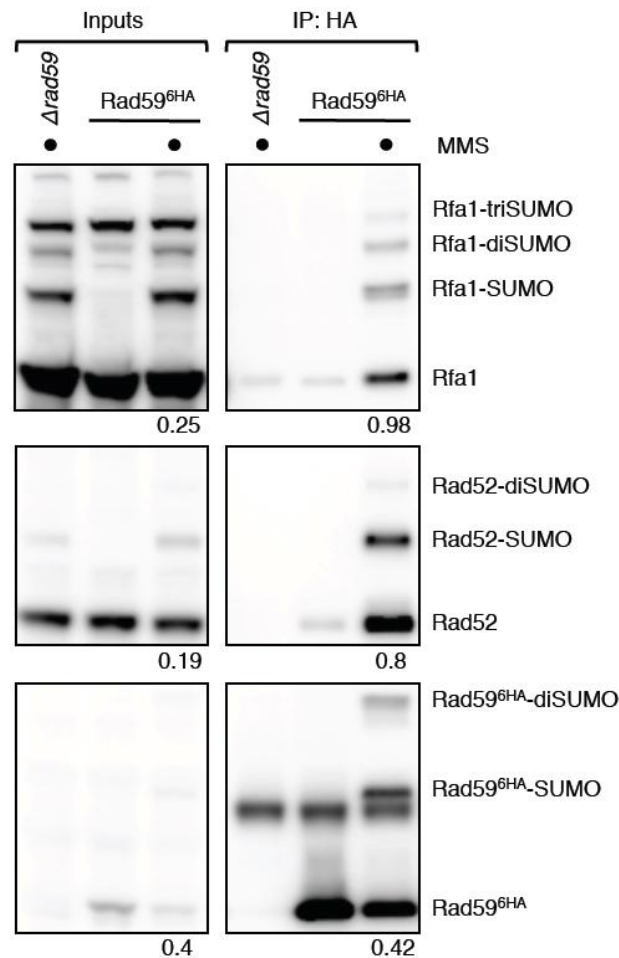


Figure 25. SUMOylation of HR Proteins after DNA Damage Fosters Physical Interactions

The RPA-Rad52-Rad59 repair complexes, which assemble following MMS-induced DNA damage, were co-immunoprecipitated (co-IP) from yeast cell extracts by immunoprecipitation of C-terminally HA-tagged Rad59. The preference for SUMOylated species is reflected by the ratios of SUMOylated/unmodified HR protein fractions in co-IPs versus inputs (quantified by ImageJ software).

Likewise, pulling down RPA (Rfa1^{9Myc}) from yeast cell extracts following DNA damage preferentially co-immunoprecipitated the SUMOylated Rad52 species compared to the unmodified Rad52 (**Fig. 26A**). Moreover, absence of Rad51 ($\Delta rad51$), HR protein that acts downstream in the pathway and is exchanged for RPA

RESULTS

on ssDNA by Rad52, further increased the binding preference of RPA towards SUMOylated partner protein (**Fig. 26A**). Notably, in the absence of checkpoint signaling ($\Delta mec1 \Delta sml1$), which leads to increased DNA damage and hyper-resection, the preferential binding of RPA to SUMOylated Rad52 was observed already without any exogenous DNA damage, but was further increased by MMS-induced DNA lesions (**Fig. 26B**). Strikingly, the binding of RPA to Rad52 in our experimental co-IP setup was dramatically reduced in the absence of the SUMO ligase Siz2 (**Fig. 26B**).

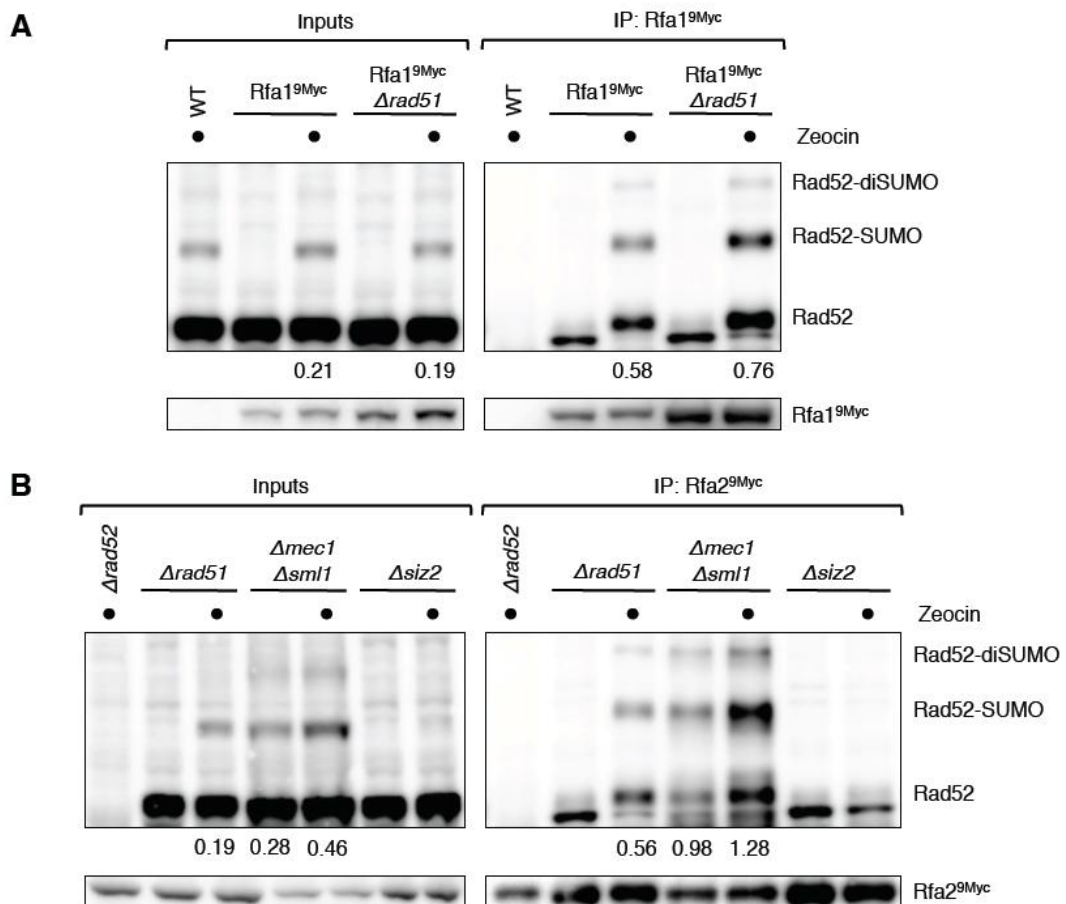


Figure 26. SUMOylation of HR Proteins Promotes DSB Repair Complex Formation

(A and B) RPA-Rad52 protein complexes, which assemble on resected ssDNA following treatment with DSB-inducing agent Zeocin, were co-immunoprecipitated (co-IP) from yeast extracts by immunoprecipitation of either Myc-tagged RPA subunit Rfa1 (A) or Rfa2 (B). RPA (Rfa1, Rfa2) interacts with unmodified Rad52, but with preference towards the SUMOylated Rad52 species. This preference is indicated by the difference in the ratios of SUMO-modified/unmodified Rad52 fractions in co-IPs compared to inputs. In the absence of Rad51 ($\Delta rad51$), RPA-Rad52 association is enhanced, especially with the SUMOylated form of Rad52. In the absence of the checkpoint kinase Mec1 ($\Delta mec1 \Delta sml1$), RPA-Rad52 association is strong even in the absence of exogenous DNA damage and binding exhibits preference towards the SUMOylated form of Rad52 (B). Notably, in cells lacking the SUMO ligase Siz2 ($\Delta siz2$), RPA-Rad52 complex formation is strongly affected (B).

RESULTS

After determining that SUMOylation of HR factors strengthens physical interactions between them and promotes protein complex formation, we next asked what mediates the stronger binding of SUMOylated repair proteins to each other. Because SUMO modification is typically recognized by a short hydrophobic linear SUMO-interacting motif (SIM), we first performed a bioinformatic prediction and found that in principle all DNA DSB repair proteins potentially harbor multiple SIMs (**Tab. 1**).

Table 1. SUMO-interacting Motif Prediction in DNA DSB Repair Proteins

Protein	Description	Predicted SIMs	Position
Mre11	Subunit of a complex with Rad50 and Xrs2 (MRX DSB sensing complex), exhibits nuclease activity	IESDK IKVV PLLFQ AQPKY VFIL DIKYG EISNE VGIL STNEE IDEND IIMV STDEE	158 – 161 280 – 283 495 – 498 633 – 636
Rad50	Subunit of a complex with Mre11 and Xrs2 (MRX DSB sensing complex)	SNSID ILD L SKPDL KSKEK VIQL LSENL LLEKH IITL NSINE	294 – 297 629 – 632 740 – 743
Xrs2	Subunit of a complex with Mre11 and Rad50 (MRX DSB sensing complex)	VLKST IIEL GTTPI LNRRR VLPL DSLDF RVKST IVEL KDEEL ENNRN LFVV KEMNL	102 – 105 363 – 366 578 – 581 795 – 798
Sae2	Endonuclease that processes hairpin DNA structures with the MRX complex at DSBs	LSLDE LLNV QYDVT NKTRK LLGI ELENP HRSLs VVIE SQNSD	25 – 28 167 – 170 245 – 248
Rfa1	Largest subunit of heterotrimeric Replication Protein A	SNRKN LIMI SDGIY ERKKY VLLV DDFEL NSNVD VLGI IQTIN FDRRD ITIV DDSGF DQAKQ LLGV DANTL	47 – 50 97 – 100 319 – 322 345 – 348 544 – 547
Rfa2	Subunit of heterotrimeric Replication Protein A	VLTHH LEVI KCHSI	168 – 171
Rfa3	Smallest subunit of heterotrimeric Replication Protein A	PTESQ LILQ SPTIS LSLNG VVAL QRLCK	36 – 39 108 – 111
Rad52	Protein that stimulates strand exchange by facilitating Rad51 binding to ssDNA	IEGWR VINL ANQIF DSTKN LVKI ENTVS	53 – 56 218 – 221
Rad59	Protein involved in the repair of DSBs via recombination and single-strand annealing	WSVQR IGLL QSKIE GWRMD VIDV EAREC LSFEK IILD YETKI	48 – 51 99 – 102 183 – 186
Rad51	Strand exchange protein, forms a helical filament with DNA that searches for homology	APRKD LLEI KGISE MRRSE LICL TTGSK NADHQ LRL L DAAAG ESRFS LIVV DSVMA	118 – 121 157 – 160 259 – 262 276 – 279
Mec1	Genome integrity checkpoint protein required for cell cycle arrest prompted by damaged or unreplicated DNA	YLDEL ILAI KDLNS YSSKT ILDI FQRYI EMVFN VVTL RSILS IQTGK VLHV DFDCL	12 – 15 720 – 723 2135 – 2138 2239 – 2242
Tel1	Protein kinase that together with Mec1 contributes to cell cycle checkpoint control in response to DNA damage	ISERL VAIL EFSDC LDSSN IINI MNSIS QIHDE VITI FSSLL CGVDD VVLV SLLFS	839 – 842 993 – 996 1348 – 1351 1442 – 1445
Rad9	DNA damage-dependent checkpoint protein; transmits checkpoint signal by activating Rad53 and Chk1	ELETQ IIVS SLSQG ATRDD IIIA GSDDF TSPKK LVVE EETLM AKRAK IILE DNEKN	429 – 432 545 – 548 622 – 625 906 – 909

RESULTS

We then wanted to check if the predicted SIMs could indeed interact with SUMO. To validate the SUMO-binding properties of these multiple linear motifs, we synthesized peptides of a length of 12 aa containing previously verified SIMs, as well as potential SIMs in repair proteins flanked by their native sequences on a single membrane, and probed the resulting peptide array for binding to poly-SUMO chains *in vitro*. Indeed, a large number of the predicted SIMs in DSB repair proteins as well as previously known SIMs could efficiently interact with SUMO, but lost this ability when two core hydrophobic residues of a SIM were replaced with alanines (**Fig. 27**). This suggests that the HR proteins engaged in DNA repair are not only collectively SUMOylated, but are also covered with multiple SIMs that mediate stronger physical interactions between modified proteins and foster complex formation.

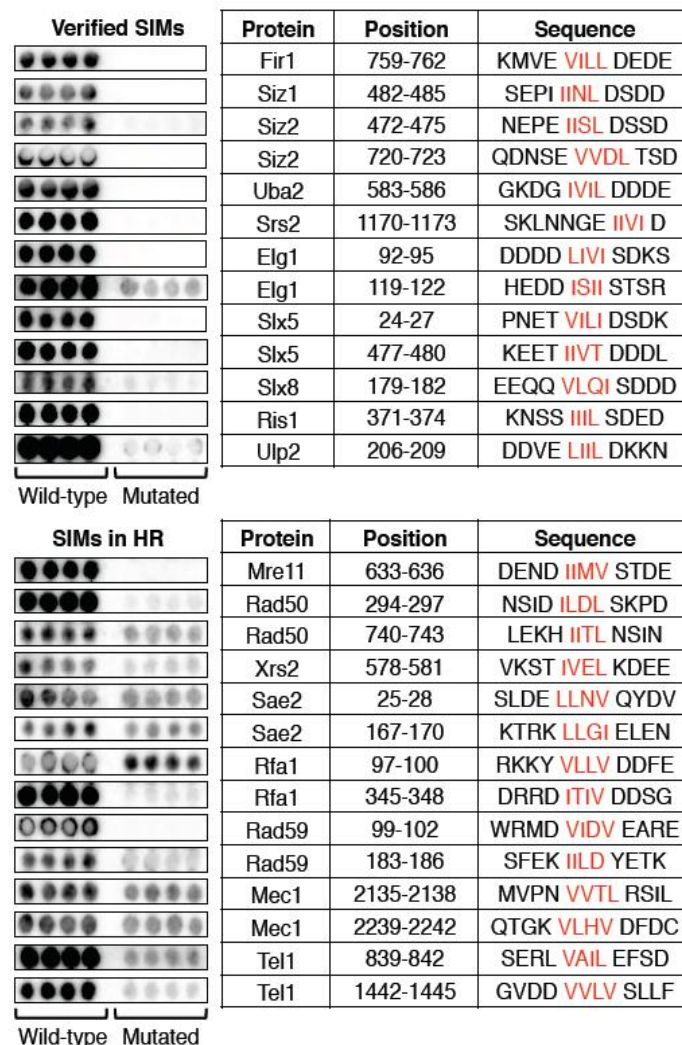


Figure 27. HR Proteins are Decorated with Multiple SUMO-interacting Motifs

In vitro binding of poly-SUMO chains to membrane-bound peptides harboring known and verified SIMs (top panel) and predicted SIMs (bottom panel) of HR pathway proteins and their mutant versions (two core hydrophobic residues replaced by alanine residues). Detection by anti-SUMO antibodies.

RESULTS

III.4.2 Identification of SUMO-Acceptor Lysine Residues in the Core HR Proteins

Protein group SUMOylation in HR fosters physical interactions between modified factors engaged in DNA repair and promotes SUMO-SIM-mediated protein complex formation, indicating that multiple SUMO modifications might act in concert and have synergistic effect on the efficiency of DSB repair. To address the functional importance of the SUMOylation wave in HR, we aimed to map and specifically eliminate the SUMO-acceptor sites in the core DSB repair proteins. Because HR proteins contain multiple lysine residues that could be targeted by SUMO conjugation machinery, we decided to apply a mass spectrometry based approach to directly map the SUMOylation sites used *in vivo*.

The identification of the SUMO-targeted lysines relied on the proteomic analysis of peptide pools generated after digestion of purified SUMO conjugates by trypsin or thermolysin. The proteinases cleave SUMO (yeast Smt3) close to its C-terminal tail, generating “branched” peptides in the cases when the modifier was conjugated to the substrate. These peptides correspond to the substrate-derived sequences carrying additional mass of the SUMO-derived fragment at acceptor lysine (EQIGG in case of trypsin and IGG in case of thermolysin digestion), which can be detected by LC-MS/MS analysis.

Using this approach we successfully mapped two SUMOylation sites in the largest subunit of RPA (Rfa1) and detected individual modifications in its other subunits (Rfa2, Rfa3), as well as in Rad59 and Rad52 (**Fig. 28A**), confirming previously verified SUMO-acceptor lysine of Rad52 (K220) (Sacher et al., 2006). To validate the mapped SUMOylation sites, we constructed mutant strains carrying substitutions of the acceptor lysine residues to arginines that were introduced at the endogenous genomic loci of HR proteins using pop-in/pop-out allele replacement method (Scherer and Davis, 1979). Elimination of the mapped SUMO-acceptor sites resulted either in the almost complete loss (for Rfa2 and Rfa3), or strong reduction (for Rfa1 and Rad59) of SUMOylation after DNA damage (**Fig. 28B-28E**). This suggests that the mass spectrometry based approach indeed identified the major *in vivo* SUMOylation sites of the core HR proteins. However, Rfa1 and Rad59 carry additional acceptor lysines targeted to a lower extent by the SUMO conjugation machinery, because additional removal of predicted SUMOylation consensus sites further reduced the DNA damage-induced modification of these HR proteins (**Fig. 28D and 28E**).

RESULTS

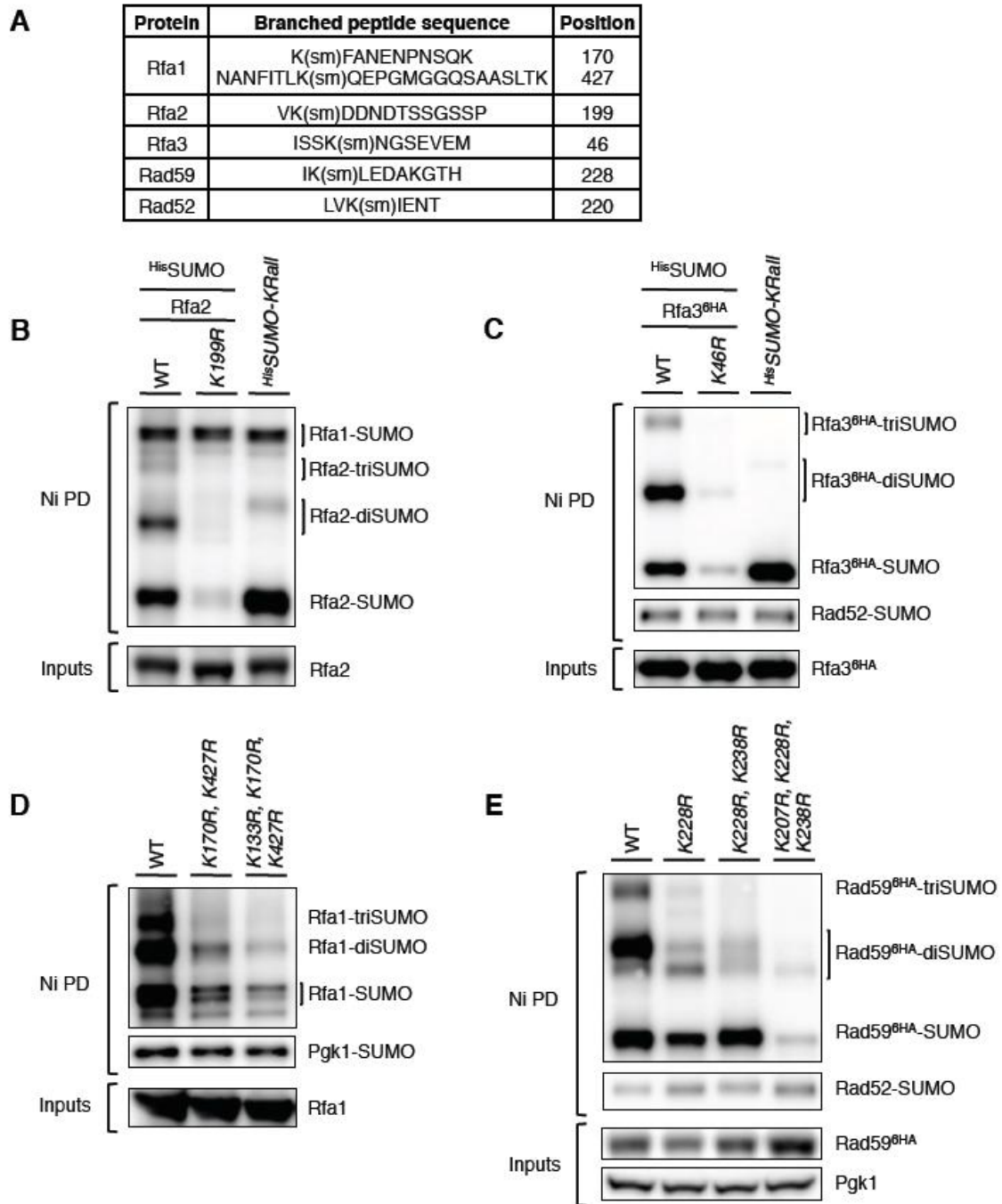


Figure 28. Mapping and Verification of SUMO-Acceptor Lysine Residues in HR Proteins

(A) Identification of SUMO-attachment sites in HR proteins using proteomic mass spectrometry. Following Ni-NTA pull-down (Ni PD) after MMS-induced DNA damage, ^{His}SUMO-conjugates were digested either with trypsin or thermolysin, and branched peptides with characteristic SUMO remnants attached to target lysines were detected by LC-MS/MS. (B-E) HR proteins are SUMOylated independently at multiple sites following DNA damage. ^{His}SUMO Ni PD from MMS-treated cells expressing either WT Rfa2 (B), C-terminally HA-tagged Rfa3 (C), Rfa1 (D), C-terminally HA-tagged Rad59 (E) or their various KR mutant variants. In addition, cells expressing a ^{His}SUMO variant in which all lysine residues were replaced by arginines (^{His}SUMO-KRall) as the only source of SUMO were used for pull-down to distinguish poly-SUMOylation from multisite SUMOylation (B and C).

RESULTS

Interestingly, when we analyzed SUMOylation of HR proteins in a mutant strain expressing a SUMO variant with all lysine residues replaced by arginines (*SUMO-KRall*) as the only source of the modifier, the disappearance of the slower-migrating di- and tri-SUMOylated species of Rfa2 and Rfa3 was observed (**Fig. 28B** and **28C**). This suggests that the HR proteins are also partially modified by poly-SUMO chains, because the lysine-less SUMO variant does not support polySUMOylation. Taken together, these findings indicate that protein group SUMO modification in HR is robust and excessive by not only targeting a whole set of HR proteins at multiple sites, but also by generating poly-SUMO chains at acceptor lysine residues. Importantly, elimination of individual SUMOylation sites did not impair the modifications at other acceptor lysines or HR factors, strengthening that SUMOylation targets members of the protein group independently and simultaneously.

III.5 HR Protein SUMOylation Accelerates DNA Repair

III.5.1 Protein Group SUMOylation Facilitates HR

After we mapped and validated the *in vivo* SUMOylation sites of the core HR proteins, we then addressed the functional significance of the SUMO modifications in DNA repair. Because HR protein group SUMOylation fosters physical interactions between modified repair factors promoting complex formation, we previously speculated that multiple modifications might act synergistically or have redundant roles. Indeed, SUMOylation-defective mutants of individual HR proteins did not exhibit reduced resistance to DNA-damaging treatment ((Sacher et al., 2006) and data not shown). We thus wondered whether elimination of the complete set of SUMOylation sites in the core HR proteins would affect the efficiency of recombination-mediated DNA repair.

For that purpose, we constructed a mutant strain in which we combined SUMOylation-defective variants of the core repair proteins RPA, Rad52 and Rad59 (*rfa1-K133R,K170R,K427R rfa2-K199R rfa3-K46R rad52-K10R,K111R,K220R rad59-K207R,K228R,K238R*) that were generated by pop-in/pop-out allele replacement method. The resulting strain (termed *KR* mutant) carried 11 substitutions of the SUMO-acceptor lysines to arginines in the HR proteins that form SUMO-SIM-assisted repair complexes after DNA damage required for efficient loading of the Rad51 recombinase onto resected DSB ends.

RESULTS

The generated *KR* strain grew at WT rates in the absence of DNA damage, however a substantial growth delay of roughly 4 hours was observed upon chronic exposure to MMS (**Fig. 29A**). Furthermore, both spontaneous and MMS-induced interchromosomal recombination rates measured between *his1* heteroalleles in *KR* mutant diploid cells were significantly reduced, similar to cells lacking SUMO ligase Siz2 (**Fig. 29B**). In general, the *KR* mutant and Siz2 deficient (Δ *siz2*) strains exhibit largely similar phenotypes and are epistatic (**Fig. 29**) under tested conditions, suggesting that in the recombination-mediated DNA repair Siz2 acts mainly through SUMO modification of HR factors. Thus, Siz2-dependent protein group SUMOylation facilitates HR and supports efficient repair of DNA lesions that rely on recombination.

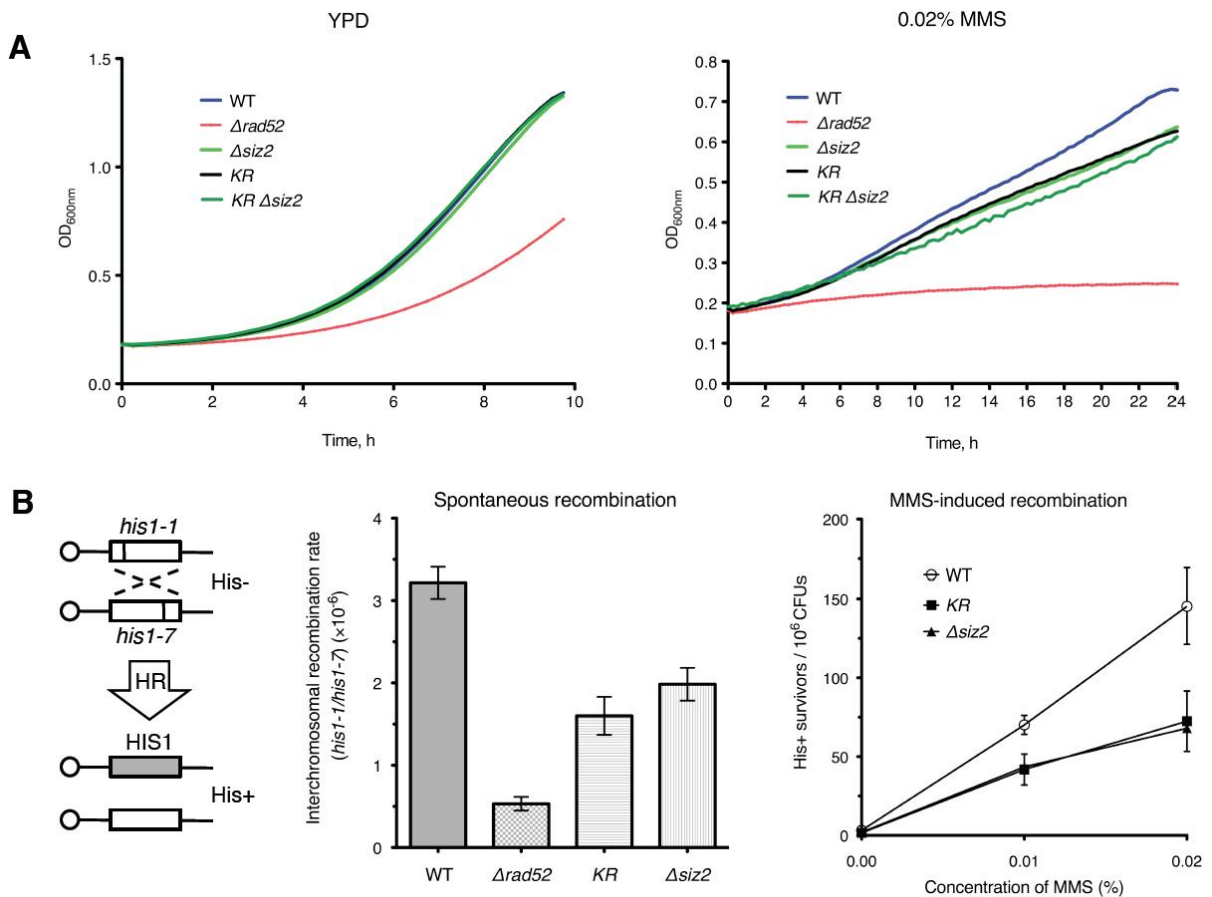


Figure 29. Protein Group SUMOylation is Required for Efficient HR

(A) Cells deficient in HR protein SUMOylation either due to the absence of Siz2 (Δ *siz2*) or the lack of 11 SUMO-acceptor sites in the core HR proteins RPA, Rad52 and Rad59 (*KR*) show delayed growth upon chronic exposure to DNA damage. Growth curves for WT cells, cells deficient in Rad52 (Δ *rad52*) or Siz2 (Δ *siz2*), and cells deficient in SUMOylation sites of HR proteins (*KR*) and also in combination with Δ *siz2* (*KR* Δ *siz2*), were measured in YPD medium or YPD containing 0.02% MMS. (B) Deficiency in HR protein SUMOylation results in reduction of spontaneous and MMS-induced recombination. The interchromosomal recombination rates between chromosomal *his1* heteroalleles were measured by fluctuation analysis in WT cells, cells lacking Siz2 (Δ *siz2*) and mutant cells deficient in SUMOylation sites of HR proteins (*KR*). The results are the average of at least three independent studies and error bars represent SD.

RESULTS

III.5.2 SUMOylation in HR Accelerates DSB Repair by Promoting Rad51 Loading

After determining that protein group SUMOylation facilitates HR, we next addressed how it might be mechanistically achieved using yeast mating-type switching mechanism as a case study (Connolly et al., 1988; Weiffenbach and Haber, 1981; White and Haber, 1990). During mating-type switching in *S. cerevisiae*, a single DSB is generated by the HO endonuclease specifically at the mating type (*MAT*) locus, which is subsequently repaired by HR using either of two homologous donor sequences (*HML α* or *HMR α* , located on the same chromosome III with *MAT*). We first confirmed that a single DSB is sufficient to trigger protein group SUMOylation in HR using donor deficient ($\Delta hml \Delta hmr$) strain defective in repair (**Fig. 30**). Indeed, SUMOylation wave was induced, however to a much lesser extent compared with MMS-treatment that generates many DNA lesions with long tracts of ssDNA.

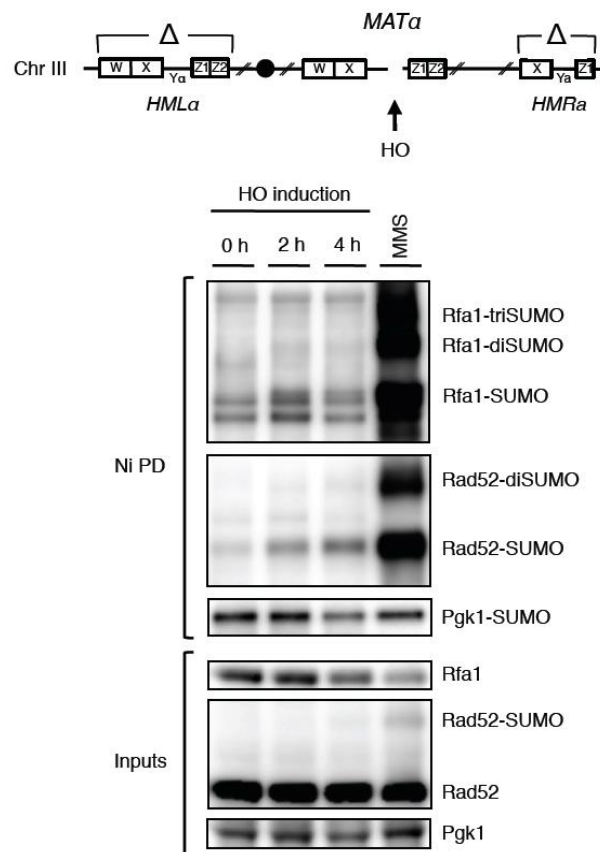


Figure 30. A Single DSB is Sufficient to Trigger SUMOylation of HR Proteins

A single DSB is generated by HO endonuclease at the *MAT* locus of the yeast mating-type switching system (top; map of chromosome III) to follow the induction of SUMOylation of HR proteins. HO is expressed from a galactose-inducible *GAL*-promoter, and repair is prevented by deletion of *HML* and *HMR* homologous donor sequences (donor deficient strain). Two hours after HO induction, mono- and di-SUMOylated species of RPA (Rfa1) and Rad52 appear. Detection by Western blotting following Ni-NTA pull-down of ^{His}SUMO conjugates. MMS-induced SUMOylation is shown for comparison.

RESULTS

Because Siz2-mediated protein group SUMOylation of the core HR factors fosters physical interactions within the RPA-Rad52-Rad59 complexes that are required for efficient loading of the Rad51 recombinase onto resected DSB ends, we next asked whether Rad51 nucleofilament formation in mating-type switching system is affected in the absence of Siz2. The DSB formation was rapidly induced at the *MAT* locus of donor deficient WT and Δ *siz2* cells by constant expression of HO endonuclease under the control of *GAL*-promoter (**Fig. 31A**). When we then monitored the recruitment of the HR factors at sites 0.2 kb and 5.7 kb distal to the persistent DSB by chromatin immunoprecipitation (ChIP), we observed that RPA (Rfa1^{9Myc}) was efficiently loaded to the resected ssDNA with similar kinetics in both WT and Δ *siz2* cells (**Fig. 31B**, top). However, recruitment of the Rad51 recombinase was substantially delayed when HR protein group SUMOylation was abolished (**Fig. 31B**, bottom).

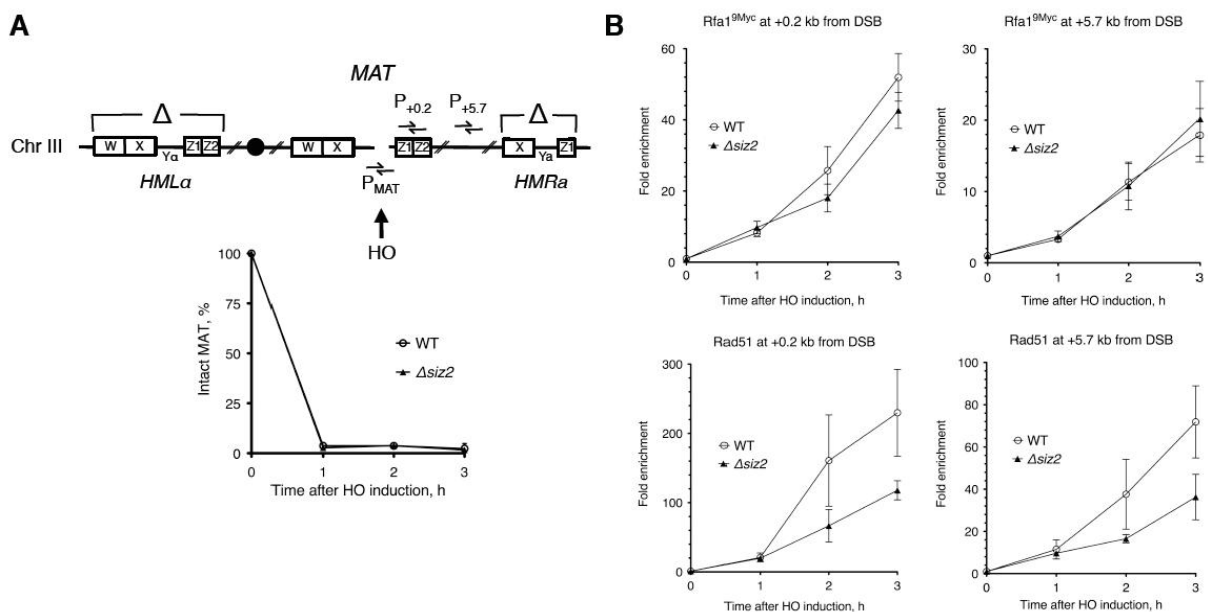


Figure 31. Rad51 Loading at the DSB is Affected in the Absence of SUMOylation in HR (A) A single unreparable DSB was induced by HO-endonuclease at *MAT* of cells lacking *HML* and *HMR* (donor-deficient strain). DSB-induction was monitored in WT and *Siz2*-deficient cells (Δ *siz2*) by real-time quantitative PCR with primers (P_{MAT}) spanning the HO-cut site. (B) ChIP directed against C-terminally Myc-tagged Rfa1 and Rad51 at 0.2 and 5.7 kb distal from DSB was performed 1, 2, and 3 hrs after HO-induction to compare loading of RPA (top) and Rad51 (bottom) in the absence of HR protein SUMOylation. The results are the average of at least three independent studies and error bars represent SEM.

Inefficient Rad51 nucleofilament formation in the absence of HR protein SUMOylation should result in a delay of DSB repair, similar to the delay observed when DSB-end resection is compromised in cells lacking MRX complex (Δ *rad50*) (Ivanov et al., 1994). We therefore transiently induced the DSB and directly

RESULTS

monitored the speed of its repair (mating type switching) in donor proficient cells that harbor homologous sequence (*HML α*) as well as efficiently induce SUMOylation wave in HR (**Fig. 32A**). Indeed, we found that the DSB repair was significantly delayed in the *KR* mutant strain (**Fig. 32B**) compared to WT. Thus, HR protein group SUMOylation accelerates DSB repair by fostering SUMO-SIM-assisted repair protein complex formation that is required for efficient Rad51 nucleofilament assembly at resected DSB ends.

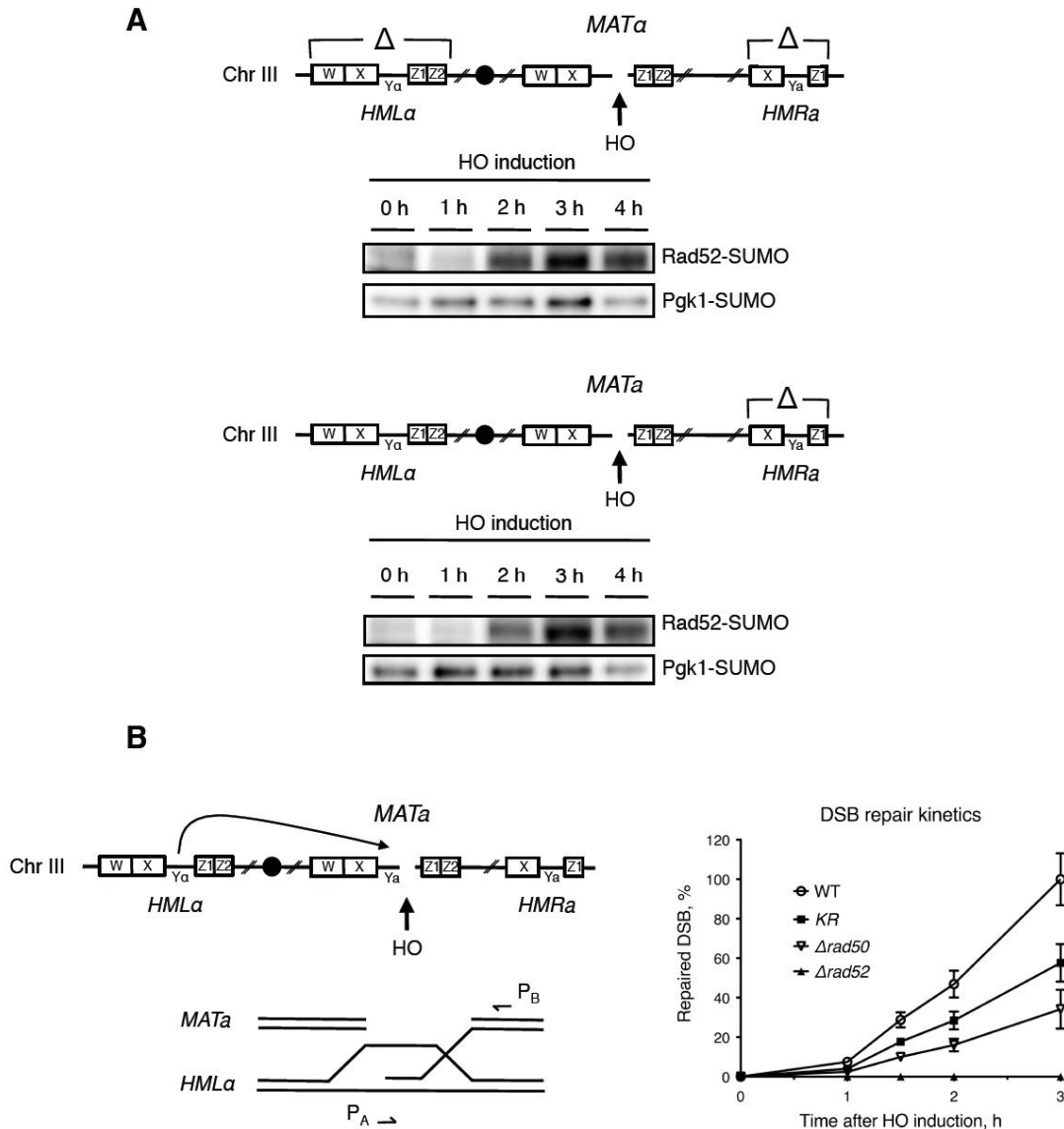


Figure 32. The Speed of DSB Repair is Reduced in the Absence of SUMOylation in HR
 (A) A single DSB can trigger SUMOylation of HR proteins independent of the absence (top panel) or presence (bottom panel) of homology required for repair. Experiment was conducted similar to (Fig. 30). (B) A single repairable DSB (arrow indicates repair reaction) was transiently induced by HO at *MAT α* in WT cells, cells lacking the MRX subunit Rad50 ($\Delta rad50$) defective in DSB-resection initiation, or the Rad52 protein ($\Delta rad52$), and the *KR* mutant. Repair kinetics was measured by real-time quantitative PCR (with primers P_A and P_B) following the appearance of repaired product Y_G at *MAT*, 1, 2, and 3 hrs after inactivation of HO (shift from galactose to glucose-containing media). The results are the average of at least three independent studies and error bars represent SEM.

IV. DISCUSSION

Despite extensive studies of the SUMO modification pathway during the last decade and identification of hundreds of proteins targeted by SUMOylation, little has been known about the principles that guide substrate specificity of this PTM (Gareau and Lima, 2010; Geiss-Friedlander and Melchior, 2007; Ulrich, 2009). Especially puzzling was how precise recognition of multiple SUMO targets upon specific stimuli is achieved by a modifier-conjugation apparatus comprised of just a handful of enzymes, in striking contrast to the elaborate ubiquitin system. Interestingly, the SUMOylation enzymes are additionally rather promiscuous *in vitro*, while SUMO substrates lack distinctive modification signals analogous to motifs that specifically recruit ubiquitin ligases. Moreover, the recognition of the SUMO modification is also surprisingly simple as it basically relies on a single SUMO-interacting motif, whereas multiple ubiquitin-binding domains operate in the ubiquitin pathway. These enigmatic features of the SUMO system together with the observations that SUMO modification typically affects only a small fraction of a given substrate, while specific SUMOylation-defective mutants often barely exhibit any phenotypes, suggested that other principles of substrate selectivity must apply and perhaps distinct mechanisms of PTM action exist in the SUMO pathway.

IV.1 Protein Group SUMOylation

By focusing on SUMOylation of HR proteins upon cell treatment with DSB-inducing agents, we discovered that the SUMO pathway functions remarkably distinct from typical PTM systems. In contrast to most protein modifications that are highly specific for individual substrates in order to selectively affect their properties, SUMOylation often collectively targets an entire physically and functionally engaged protein group rather than an individual protein. In case of the DSB repair, multiple HR and checkpoint proteins recruited to DNA lesions become synchronously modified at multiple sites by a SUMOylation wave. The modifications are catalyzed by the chromatin-associated conjugation machinery that independently and in parallel targets accessible SUMO-acceptor sites on a whole set of HR proteins engaged in DNA repair. Interestingly, these sites are not conserved in homologs of other species, SUMOylation of which still takes place (Dou et al., 2010; Sacher et al., 2006), but at other sites typically located outside of conserved globular domains. In fact, this might not be so surprising, because SUMOylation usually targets lysines located in context

DISCUSSION

of flexible loops or unstructured regions that could adopt an extended conformation and fit into catalytic site of Ubc9. Therefore, modified sites in most cases lie outside of conserved functional regions and are themselves less conserved.

The observed SUMOylation wave in HR is not a unique phenomenon, as a similar scenario is found for several other protein groups, like proteins involved in nucleotide excision repair (**Fig. 6** and (Silver et al., 2011)), yeast septins (Johnson and Blobel, 1999; Johnson and Gupta, 2001; Takahashi et al., 2001), ribosomal proteins (Finkbeiner et al., 2011a; Finkbeiner et al., 2011b; Panse et al., 2006), and proteins of snoRNPs (Westman and Lamond, 2011; Westman et al., 2010). In all these cases, the SUMOylation machinery seems to target several proteins of the respective complexes synchronously and often at multiple sites. Therefore, protein group modification appears to be a typical feature of the SUMO pathway. Importantly, protein group modification in the SUMO pathway differs significantly from other PTM waves like phosphorylation reactions, as most of the SUMO modifications do not proceed via reaction cascade and are functionally additive or redundant.

In addition to sites of DNA damage, several other SUMOylation hotspots appear to exist in the nucleus. Particular hubs for SUMOylation are telomeres, where the SUMOylation machinery targets multiple proteins involved in telomere length homeostasis and genomic stability. In *S. pombe* and *S. cerevisiae*, SUMOylation appears to limit telomere length, and multiple telomere-binding proteins (Cdc13, Yku70/80, Pif1, Rap1) have been identified as SUMO substrates. The SUMOylation of *S. cerevisiae* Cdc13 promotes its association with the Stn1-Ten1 telomerase inhibitory complex (likely through binding to multiple SIMs of Stn1) and thus restrains telomerase-mediated lengthening of telomeres directly (Hang et al., 2011). Telomere elongation is further inhibited by reversible telomere anchoring to the nuclear periphery, a process that is mediated by Siz2-catalyzed SUMOylation of Yku70/80 and Sir4 proteins (Ferreira et al., 2011). Conversely, telomere elongation in yeast requires the release of telomeres from the nuclear periphery, most likely by Ulp1-mediated deSUMOylation of several SUMOylated telomere-anchoring proteins (Nagai et al., 2011). Interestingly, in human ALT (alternative lengthening of telomeres) cancer cells, telomeres re-localize to specialized so-called ALT-associated PML bodies (APBs), where telomeres become elongated by an HR-dependent mechanism. This telomere movement is mediated by a re-localization of the SUMO ligase NSE2 to APBs and concomitant SUMOylation of four subunits of the hexameric telomere-protecting shelterin complex (TRF1, TRF2, TIN2, RAP1).

DISCUSSION

Indeed, SUMOylation-defective mutants of TRF1 and TRF2 fail to localize to PML bodies, suggesting that SUMOylation of multiple subunits of the shelterin complex is required for APB formation (Potts and Yu, 2007). Similarly, siRNA-mediated depletion of NSE2 in ALT cells inhibits APB formation and HR at telomeres, resulting in telomere shortening and cell senescence. Thus, both in yeast and human (ALT) cells, collective protein group SUMOylation of telomere-associated proteins leads to a re-localization of telomeres, yet to different nuclear compartments (periphery versus APBs), and with different outcomes for telomere length and stability.

PML nuclear bodies generally emerge as strong hubs for SUMOylation in mammalian cells. These dot-like nuclear territories are functionally associated with a variety of functions including DNA repair, transcriptional control and tumorigenesis, and are thought to function as a dynamic repository for nuclear factors (Bernardi and Pandolfi, 2007). The tumor suppressor protein PML, initially identified as an oncogenic protein fusion in promyelocytic leukemia patients, localizes to PML bodies and is also crucial for their formation. Because PML proteins are SUMOylated and possess multiple SIMs, it has been suggested that PML proteins trigger the formation of protein networks with themselves and other proteins through multiple SUMO-SIM interactions (Shen et al., 2006). Indeed, other proteins of PML bodies like SP100 and the transcriptional repressor Daxx are SUMO modified or contain SIMs, and may thus be incorporated into the PML network (Lin et al., 2006).

A particularly active SUMOylation hub is the nucleolus, largely because SUMOylation controls pre-ribosome assembly, as indicated by phenotypes of SUMO pathway mutants. Indeed, in *S. cerevisiae*, pre-ribosomal particles along the 60S and the 40S synthesis pathways are decorated with SUMO, and several proteins of these pathways are known SUMO substrates (Panse et al., 2006). Similarly, in human cells deSUMOylation of several substrates implicated in ribosome biogenesis mediated by the nucleolar deSUMOylation enzyme SENP3 is important for the maturation of the 28S rRNA and subsequent export of the 60S pre-ribosomal particle (Finkbeiner et al., 2011a; Haindl et al., 2008). Notably, a proteomic approach identified among potential nucleolar SUMO targets specifically snoRNP-related proteins (Nop58, Nhp2, Dkc1 and Nolc1). Indeed, the functional characterization of Nop58 SUMOylation revealed its importance for snoRNP biogenesis (Westman et al., 2010), once again strengthening the extensive role of SUMO system for ribosome biogenesis.

IV.2 Specificity of SUMO Modification

Protein group SUMO modification is based on different principles of substrate specificity. Whereas selective modification of an individual substrate involves a highly specific interaction between a modifying enzyme and its target, protein group modification may only require close proximity of a promiscuous E2 enzyme to its multiple substrates, plus accessible modification sites within flexible protein domains (scenario observed for SUMOylation of substrates *in vitro* by Ubc9 alone without the need for ligases). In other words, a simple organization and the promiscuous character of the SUMO conjugation machinery are key features of the SUMO system that underlie protein group modification. Specificity toward an entire protein group is in turn provided by two principles: a highly specific trigger and topological specificity. In case of HR-mediated DSB repair pathway, the crucial trigger for damage-induced SUMOylation is the resection of the DSB ends and exposure of ssDNA, which serves as a platform for the loading of repair factors in the vicinity of the responsible chromatin-bound SUMO ligase Siz2 (**Fig. 33**). Interestingly, the requirement for resection as the trigger for Siz2-mediated SUMOylation in HR can be bypassed by artificially targeting repair proteins to DNA (e.g., by fusing them to the DBD of the Gal4 transcription factor). These experiments support the conclusion that the SUMO ligase is not being specifically recruited to resected ssDNA at damage sites, but is pre-bound to chromatin in a sequence nonspecific manner and collides with the substrates that become loaded onto DNA in its proximity. Therefore, the topological specificity for protein group modification is provided by the precise localization of the SUMO ligases, which play the role of adaptors for recruiting SUMO-conjugating enzyme Ubc9 in the vicinity of its substrates.

While protein group modification of septin network involves Siz1 localized to the yeast bud neck via its C-terminal tail (Takahashi et al., 2008), the HR protein group SUMOylation requires chromatin localization of related canonical Siz/PIAS ligase Siz2 via its sequence nonspecific SAP domain. Even though both Siz1 and Siz2 harbor SAP domains and have similar DNA-binding properties, they differ in other aspects (e.g., protein abundance, C-terminal tails) and in particularly in Siz2's ability (mediated in part by its C-terminal SIM) to bind selectively the Mre11 subunit of the DSB-sensing MRX complex, potentially restricting the localization of the ligase and concentrating SUMOylation activity at the sites of ongoing DNA repair. Moreover, the SIMs of the E3 ligases might in general facilitate their binding to the SUMOylated

DISCUSSION

substrates further promoting concentration of ligase activity and accelerating SUMOylation, perhaps with characteristics of a chain reaction. This could explain the rapid accumulation of mammalian SUMO ligases PIAS1 and PIAS4 in repair foci at sites of DNA damage (Galanty et al., 2009).

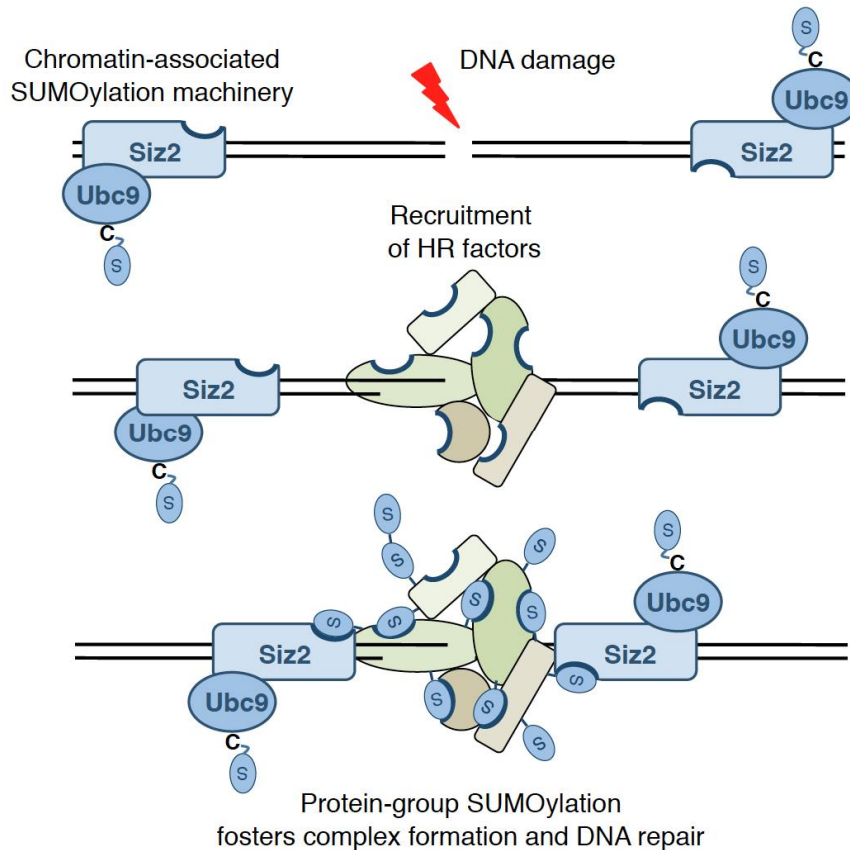


Figure 33. Events Leading to Collective Protein Group SUMOylation of Factors Involved in Homologous Recombination (HR)

The SUMOylation machinery (SUMO-charged Ubc9, Siz2) is pre-bound to chromatin via SAP domain of Siz2 that binds DNA in a sequence nonspecific manner. Upon DNA damage (DSB induction), HR factors assemble on resected DNA (ssDNA). Collision with Siz2 initiates protein group SUMOylation of HR proteins. Stable binding of Siz2 to the HR complex is fostered by a SUMO-interacting motif (SIM) in Siz2's C-terminal tail. Because the HR proteins are decorated with multiple SIMs (indicated by wedges), collective SUMOylation stabilizes the complex through multiple SUMO-SIM interactions and fosters DNA repair.

Taken together, these features of the SUMO system reveal, how upon certain stimuli rather simply organized promiscuous SUMOylation machinery mediates specific simultaneous modification of multiple substrates within dedicated pathways and collectively provides its targets with new properties. Moreover, protein group SUMOylation specifically marks functionally-engaged protein pools for the action by downstream factors, e.g., SUMO-targeted ubiquitin ligases, which in turn use their own SIMs in order to distinguish the right targets to bind and to act upon.

IV.3 Synergy in the SUMO Pathway

In contrast to typical substrate-selective posttranslational modifications that specifically endow individual targets with new properties, protein group SUMOylation affects collectively an entire set of physically and functionally engaged factors simultaneously providing all of them with new characteristics. In fact, systematic mutation analysis of SUMOylation sites in HR protein group revealed that individual SUMO modifications act in concert, explaining why single acceptor-site mutants often exhibit barely any deleterious phenotypes (Sacher et al., 2006; Silver et al., 2011). Because SUMOylation of HR proteins fosters protein-protein interactions, the most reasonable explanation for the observed functional synergy is that individual SUMO-SIM interactions add up affinities for complex formation. Several important features appear to be relevant for this activity. First, factors within functionally engaged protein group already possess low affinities towards each other on their own, even in the absence of SUMOylation, which allows them to interact. Second, upon the formation of protein assemblies interacting factors become collectively modified at numerous accessible SUMO-acceptor sites by a highly localized SUMOylation machinery. Finally, because recognition of SUMO modifications is mediated by simple hydrophobic linear SIMs, individual components of the modified group harbor these motifs, often in multiple copies. Indeed, we could show that basically all HR proteins possess *in vitro* functional SIMs (**Fig. 27**), providing many binding surfaces for potential SUMO interactions. Thus, SUMO functions comparable to a glue in order to foster physical interactions and stabilize protein assemblies.

In case of HR protein group SUMOylation, upon DNA damage and DSB resection, a chromatin-bound, concentrated SUMO ligase Siz2 mediates local modification of HR proteins loaded onto exposed ssDNA in its vicinity, thereby facilitating formation of functional repair protein complexes and in that way accelerating overall DSB repair (**Fig. 33**). However, because the SUMO conjugation machinery is highly promiscuous, it readily modifies all accessible acceptor sites in its proximity, even additional lysines introduced by epitope tagging of SUMO-targeted proteins (e.g., Myc-tag). Therefore, although SUMO modifications in the HR pathway act synergistically and add up for efficient repair, not all of them are expected to be equally important for complex formation. Nevertheless, because similar to DNA repair many biological pathways take place within so-called nuclear bodies or foci, it seems

plausible that the protein group SUMOylation stabilizes several of these large protein assemblies.

IV.4 Dynamics of SUMO-SIM-assisted Assemblies

If SUMOylation drives the stabilization or formation of protein complexes, networks or nuclear bodies, then the question arises: how do such interactions become eventually disentangled? The SUMO pathway seems to offer three possibilities (Fig. 34). The first option is disassembly catalyzed by recruited deSUMOylation enzymes ULPs/SENPs, which typically possess multiple SIMs (Hickey et al., 2012). In humans, this mechanism is employed at sites of DSB repair and pre-ribosome assembly (Dou et al., 2010; Finkbeiner et al., 2011a; Haindl et al., 2008). In *S. cerevisiae*, the deSUMOylation enzyme Ulp1 localizes primarily to the inner face of the nuclear pore, but redistributes to the nucleolus under stress conditions (Sydorsky et al., 2010), and a fraction also to the septin ring during final stages of cell division (Li and Hochstrasser, 2003; Makhnevych et al., 2007). The second deSUMOylation enzyme of yeast, Ulp2, appears to be more specific for chromatin-related functions like DNA repair and SUMO-regulated sister-chromatid cohesion at centromeres (Felberbaum and Hochstrasser, 2008; Kroetz et al., 2009; Lee et al., 2011).

A second way to disrupt SUMO-SIM-stabilized interactions is selective proteasomal degradation promoted by SUMO-targeted ubiquitin ligases. These enzymes are RING-type ubiquitin ligases, which, due to the presence of SIMs, possess affinities for SUMO conjugates (Geoffroy and Hay, 2009; Perry et al., 2008; Praefcke et al., 2012). One of the known *S. cerevisiae* STUbLs, Slx5/Slx8, is a heterodimer formed by two RING-finger proteins, of which Slx5 harbors two strong SIMs. Slx5/Slx8 is genetically linked to DNA repair and localizes to nuclear DNA repair foci (Cook et al., 2009; Prudden et al., 2007), but also at nuclear pores (Nagai et al., 2008). Monomeric RNF4, a vertebrate homolog of Slx5/Slx8, possesses four putative SIMs through which the RING-finger ligase is potentially targeted to multiple SUMOylated proteins including DDR factors (Galanty et al., 2012; Yin et al., 2012). Intriguingly, RNF4 localizes also to PML bodies, where it attaches a polyubiquitin chain specifically on PML proteins that are modified by poly-SUMO chains. Polyubiquitylation of PML causes its proteasomal degradation, which in turn leads to the destabilization of PML bodies (Lallemand-Breitenbach et al., 2008; Tatham et al., 2008). However, the finding that Slx5/Slx8 mediates ubiquitylation and degradation of

DISCUSSION

the yeast MAT α 2 transcription factor independent of SUMOylation (Xie et al., 2010) brings to attention that targeting to SUMO conjugates is just one option for substrate selection of enzymes originally classified as STUbLs. Moreover, STUbLs may play non-proteolytic roles as well. For example, *S. cerevisiae* Rad18 binds via its SIM to SUMO-modified PCNA, thereby stimulating non-proteolytic mono- or K63-linked polyubiquitylation of a different subunit of PCNA (Parker and Ulrich, 2012). Likewise, in human cells upon DNA damage, RNF4 is recruited to SUMOylated DNA-damage response factors where it promotes formation of non-proteolytic K63-linked polyubiquitin chains (Yin et al., 2012).

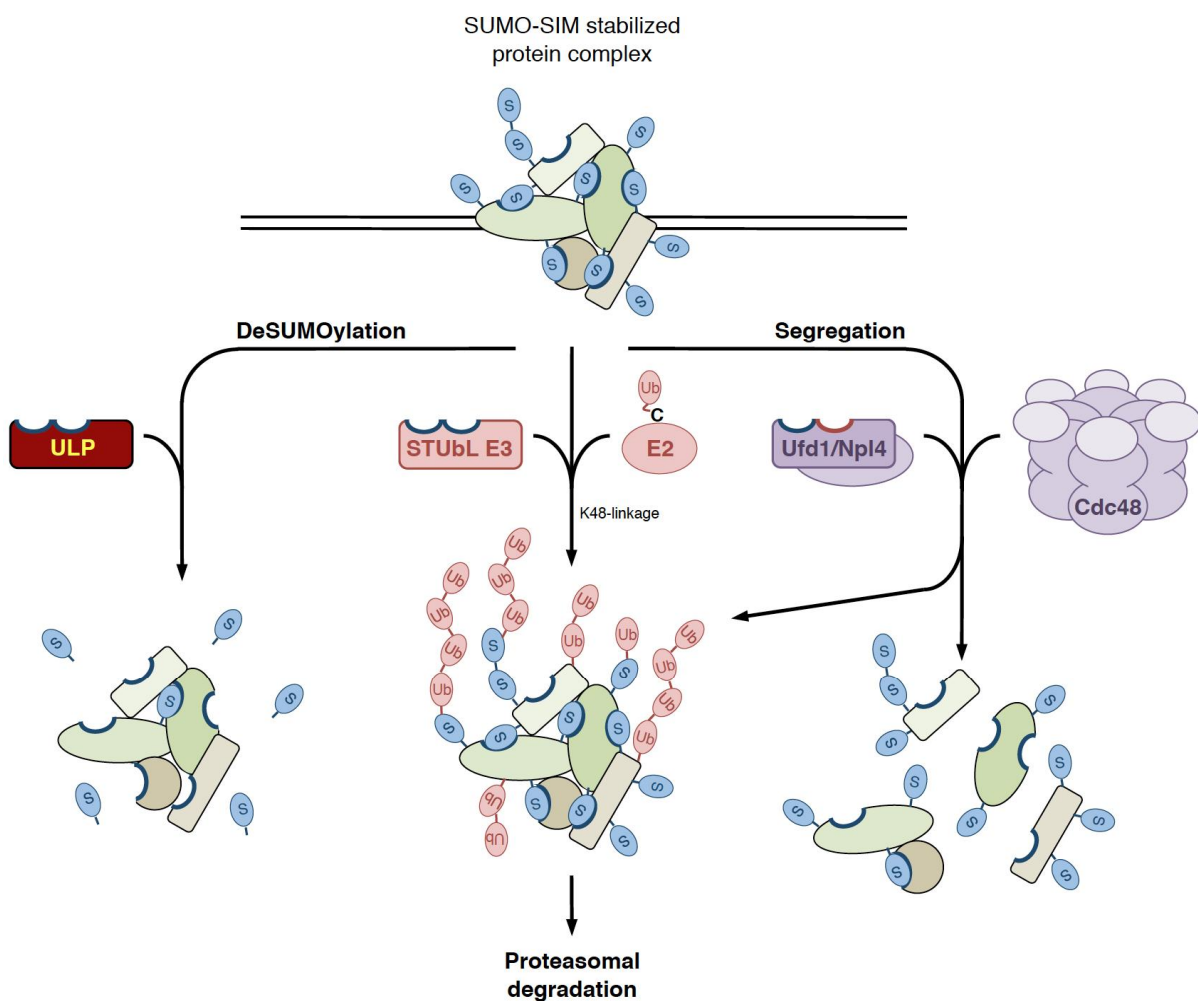


Figure 34. Pathways Used for Disentangling SUMO-SIM Stabilized Protein Assemblies First, deSUMOylation (left) weakens physical interactions. Second, recruitment of STUbLs (middle) mediates polyubiquitylation (K48-linked) of SUMOylated factors, typically leading to proteasomal degradation of the conjugate. Third, the chaperone-like enzyme Cdc48 (p97), in conjunction with its heterodimeric co-factor Ufd1-Npl4, recognizes SUMO conjugates and mediates their disassembly by an ATP-driven mechanism (right). Because the Cdc48 complex also associates with ubiquitin conjugates and ubiquitin ligases (not shown), it may integrate ubiquitin and SUMO signaling and may function as a STUbL as well. Notably, all three pathways employ SIM-harboring factors for SUMO conjugate recognition.

DISCUSSION

The third mechanism used to disrupt SUMO-SIM-mediated interactions involves Cdc48 (p97 in mammals), a conserved chaperone-like AAA-type ATPase. This homohexameric segregase was previously known to bind and dislodge specifically ubiquitylated proteins from their protein environment (Dantuma and Hoppe, 2012; Jentsch and Rumpf, 2007; Rape et al., 2001). For example, in endoplasmic reticulum-associated degradation (ERAD), Cdc48, assisted by substrate-recruiting ubiquitin-binding cofactors (Ufd1-Npl4), is thought to mobilize ubiquitylated ERAD substrates from the ER for cytosolic proteasomal degradation. However, it is now known that Cdc48 acts on SUMOylated substrates as well. Interestingly, both Cdc48 and Ufd1 not only bind ubiquitin via special domains, but also SUMO via SIMs (Bergink et al., 2013; Nie et al., 2012). In yeast, Cdc48 associates with SUMOylated Rad52 in complex with Rad51, which possesses a SIM but is not SUMO modified itself. By acting on this SUMO-SIM-stabilized complex, Cdc48 displaces the two proteins from chromatin. Notably, inactivation of Cdc48 leads to increased spontaneous recombination and causes aberrant Rad51 foci formation in yeast and mammalian cells (Bergink et al., 2013). Inferring from this finding, Cdc48 might be generally competent to break up SUMO-SIM-assisted protein complexes or networks. Moreover, because Cdc48 also associates with a number of ubiquitin ligases (Bohm et al., 2011; Koegl et al., 1999; Verma et al., 2011), the Cdc48 complex may not only function as a segregase but also as a multisubunit STUbL. Additionally, the presence of both ubiquitin- and SUMO-binding motifs suggests that the segregase complex may also integrate SUMO- and ubiquitin-dependent signals similar to human RAP80. This protein, via tandem SIM/UIM motifs, preferentially binds RNF4-synthesized hybrid SUMO-ubiquitin chains, thereby promoting BRCA1 recruitment to DNA damage sites (Guzzo et al., 2012).

Taken together, protein group SUMOylation not only targets protein pools already engaged in their respective functions, possibly explaining why the SUMOylated fraction of a given substrate is typically very small, but it also simultaneously marks these pools for subsequent action by other SIM-containing factors that ensure the dynamic nature of SUMO modification and offer extensive possibilities for the regulation of the SUMO-SIM-assisted protein assemblies. It is attractive to speculate, that similar to ULPs or STUbLs, other enzymatic activities (e.g., phosphorylation, methylation, acetylation) could be recruited by SIM-harboring proteins to the SUMOylated substrates, further expanding the versatility of the SUMO pathway.

V. MATERIALS AND METHODS

Unless otherwise mentioned, chemicals and reagents were purchased from Amersham-Pharmacia, Applied Biosystems, Biomol, Biorad, Difco, Fluka, Invitrogen, Merck, New England Biolabs, Promega, Roth, Roche, Riedel de Haen, Serva, Sigma, and Thermo Scientific. The following microbiological, molecular biological and biochemical methods are based on standard techniques (Ausubel, 2001; Sambrook and Russell, 2001) or on the instructions of the manufacturer. For all methods described, de-ionized sterile water, sterile solutions and sterile flasks were used.

V.1 Computational Analyses

For database searches (sequence search and comparison, physical and genetic interactions, phenotypes, literature search) electronic services were used provided by the *Saccharomyces Genome Database* (<http://www.yeastgenome.org/>), the *National Center for Biotechnology Information* (<http://www.ncbi.nlm.nih.gov/>) and the *Universal Protein Resource* (<http://www.uniprot.org/>). Most of the protein sequence analyses were performed using software programs from *ExpASY Proteomics Server* (<http://www.expasy.org/>). For the prediction of SUMOylation consensus sites and SUMO-binding motifs the software packages SUMOsp 2.0 and GPS-SBM 1.0 from the *CUCKOO Workgroup* (<http://www.biocuckoo.org/>) were used. DNA sequence analyses (DNA restriction enzyme maps, DNA sequencing analyses, DNA primer design) were done with DNA Star software (DNA Star Inc.). For assessment of protein domain composition the program *SMART* (<http://smart.embl-heidelberg.de/>) was used. Protein 3D-structure coordinates obtained by X-ray crystallography and NMR analysis were downloaded from the protein databank (<http://www.rcsb.org/pdb/>) and structures were visualized using the PyMOL Molecular Graphics System (<http://www.pymol.org/>).

Chemiluminescence signals of immunoblots were detected by a CCD camera (LAS 3000, Fujifilm), quantified using ImageJ software (<http://rsb.info.nih.gov/ij/>) and processed with Adobe Photoshop (Adobe Systems Inc.). For the presentation of text, tables, graphs and figures, software programs of the Microsoft Office package 2008 (Microsoft Corp.) were used, as well as GraphPad Prism version 5.0 for Mac OS X (<http://www.graphpad.com/>).

V.2 Microbiological and Genetic Techniques

V.2.1 *E. coli* techniques

<i>E. coli</i> strains	Genotype	Source
XL1-Blue	hsd R17 rec A1 end A1 gyrA46 thi-1 sup E44 relA1 lac [F' pro AB lacI ^q Z ΔM15 Tn10 (Tet ^r)]	Stratagene
BL21(DE3)/RIL	B F ⁻ ompT hsdS (rB ⁻ mB ⁻) dcm ⁺ Tet ^r gal (DE3) EndA Hte [argU ileY leuW Cam ^r]	Stratagene
Rosetta 2(DE3) pLysS	F ⁻ ompT hsdS _B (rB mB) gal dcm (DE3) pLysSRARE2 (Cam ^r)	Novagen

MATERIALS AND METHODS

<i>E. coli</i> vectors	Purpose	Source
pQE30	Expression with N-terminal 6xHis-tag	Qiagen
pET28a(+)	Expression with N-terminal 6xHis-tag	Novagen

E. coli plasmids

pQE30- and pET28a(+)-versions of Siz2 (Nfi1) (full-length) were created by cloning the PCR-amplified open reading frame (ORF) from DF5 yeast genomic DNA extracts. pET28a(+)-siz2- Δ SAP and pET28a(+)-siz2-SAP variants were generated by site-directed mutagenesis of pET28a(+)-Siz2.

E. coli media:

LB-medium/[plates]: 1% Tryptone (Difco)
 0.5% yeast extract (Difco)
 1% NaCl
 [1.5% agar]
 sterilized by autoclaving

Cultivation and storage of bacteria cells

Liquid cultures were grown in LB media at 37°C (or 18°C and 30°C for expression experiments) with constant shaking. Cultures on agar plates were incubated at 37°C. For the selection of transformed bacteria, ampicillin (50 μ g/ml) and kanamycin (50-100 μ g/ml) were added to the media. The culture density was determined by measuring the absorbance at a wavelength of 600nm (OD₆₀₀). Cultures on solid media were stored at 4°C for up to 5 days. For long-term storages, stationary cultures were frozen in 15% (v/v) glycerol solutions at -80°C.

Preparation of competent bacteria cells

DNA plasmids were transformed into *E. coli* competent cells either by electroporation or by calcium chloride transformation. For the preparation of competent cells, 1l liquid LB medium was inoculated with 10ml of an overnight (ON) culture derived from a single colony and grown to an OD₆₀₀ of 0.8 at 37°C. After cooling the culture flask on ice for 30-60min, cells were harvested by centrifugation (10min, 4000g, 4°C). All following steps were performed with pre-cooled sterile materials and solutions at 4°C. For the preparation of electro-competent *E. coli*, the pellets were washed once with 1l ice-cold water, centrifuged and washed once again with 0.5l ice-cold water containing 10% (v/v) glycerol. After another sedimentation, the cells were finally resuspended in 3ml 10% (v/v) glycerol and stored in 100 μ l aliquots at -80°C. For the preparation of chemically competent bacteria, sedimented cells were first carefully resuspended in 200ml MgCl₂ solution (100mM), then pelleted again by centrifugation, resuspended second time in 400ml CaCl₂ solution (100mM) and incubated on ice for 30 min. Finally, the competent cells were re-pelleted by centrifugation, suspended in 15 ml 100mM CaCl₂ solution containing 10% (v/v) glycerol and stored at -80°C in 150 μ l aliquots after freezing the cells in liquid nitrogen.

MATERIALS AND METHODS

Transformation of plasmid DNA into competent *E. coli* cells

Shortly prior to transformation, electro-competent cells were thawed on ice. For the electroporation, 20-40 μ l electro-competent cells were mixed with 2 μ l of ligation sample dialyzed against water or 10ng plasmid DNA. The suspension was electroporated in a pre-chilled 0.1cm electrode gap Gene Pulser cuvette (Biorad) with a pulse of 1.8kV and 25 μ F at a resistance of 200 Ω . After addition of 1ml pre-warmed LB medium (without antibiotics), the suspension was incubated for 1h on a shaker at 37°C to recover the cells. Selection of transformants was subsequently carried out on antibiotic-containing LB agar plates ON at 37°C. For chemical transformation, 50 μ l competent cells were mixed with 10ng of *E. coli* vector DNA and incubated on ice for 15 min. Then, a 42°C heat-shock was performed for 45s, followed by a 2 min incubation on ice. For recovery, the cells were resuspended in 1ml pre-warmed LB medium lacking antibiotics and incubated at 37°C on a shaker for 1h prior to ON selection on LB agar plates containing proper antibiotics.

Expression of recombinant proteins in *E. coli* cells

For the overexpression of recombinant proteins, the *E. coli* strains BL21(DE3)/RIL and Rosetta 2(DE3)pLysS were used. Liquid LB medium containing proper antibiotics was inoculated at an OD₆₀₀ of 0.2 with an ON culture of a freshly transformed colony grown at 37°C. Cultures were incubated at 30°C until they reach an OD₆₀₀ of 0.4. Then cells were grown at room temperature for 1h and protein expression was induced by addition of IPTG to a 1mM final concentration. Cells were subsequently grown at room temperature (or 18°C) with constant shaking and harvested 3-12h after IPTG addition by centrifugation (15min, 4000g, 4°C), washed in ice-cold PBS and stored at -80°C after freezing in liquid nitrogen. Expression of the protein of interest was confirmed by analyzing samples taken before and after IPTG-induction using SDS-PAGE and Coomassie blue staining (Thermo Scientific PageBlue protein staining solution).

V.2.2 *S. cerevisiae* techniques

<i>S. cerevisiae</i> vectors	Purpose	Reference
pYCplac33, pYCplac22, pYCplac111	CEN plasmids	(Gietz and Sugino, 1988)
pYEplac195, pYEplac112, pYEplac181	2 μ m plasmids	(Gietz and Sugino, 1988)
pYIplac211, pYIplac204, pYIplac128	INT plasmids	(Gietz and Sugino, 1988)
pGAD-C1-3, pGBD-C1-3	Two-hybrid	(James et al., 1996)

S. cerevisiae plasmids

All yeast two-hybrid constructs generated in this study were based on pGAD-C1-3 vectors for the AD N-terminal fusions and pGBD-C1-3 vectors for the BD N-terminal fusions. The respective ORFs (full-length or fragments) were amplified by PCR from genomic DNA of DF5 yeast extracts using specific primers and compatible restriction enzyme sites. Truncations and mutations were introduced by site-directed mutagenesis using specific primer pairs. Phusion and PFU Turbo high-fidelity polymerases were used for all PCR reactions and restriction enzymes were purchased from NEB.

MATERIALS AND METHODS

Integrative plasmids were based on the Ylplac vector series. For the expression of studied proteins at their endogenous levels, the full-length ORFs plus sequences of the upstream promoter and downstream terminator were cloned into integrative plasmids. All *rfa1*, *rfa2*, *rfa3*, *rad52*, *rad59*, *siz2* mutant plasmids were constructed by site-directed mutagenesis using specific primer pairs.

Yeast pYCplac111 centromeric plasmids expressing *EXO1* and *exo1-ND* (*D173A*) were designed by Grzegorz Sienski, while *exo1-SA* (*S372A,S567A,S586A,S692A*) was generated by mutagenesis of YCplac111-Exo1 in this study. Centromeric plasmid expressing *HO* under the control of a *GAL10* promoter (pGAL-*HO*) was obtained from the Jackson laboratory (Downs et al., 2000).

^{His}SUMO constructs under the control of its endogenous and *ADH1* promoters were used in previous studies in the Jentsch laboratory. A ^{His}SUMO-KRall construct with all lysine residues of Smt3 (SUMO) replaced by arginine residues was generated by Oliver Gassner. All ^{His}SUMO constructs were integrated either into the *URA3/LEU2* loci by cutting the plasmid with *EcoRV* or into *SMT3* locus by cutting with *BglII* and expression levels were tested by Western blot analysis.

S. cerevisiae strains

Chromosomally tagged yeast strains and mutants used in this study were constructed by a PCR-based strategy, by genetic crosses and standard techniques (Janke et al., 2004; Knop et al., 1999). Strains expressing mutant proteins with SUMO-acceptor lysine residues replaced by arginine residues were constructed by a pop-in/pop-out allele replacement method (Scherer and Davis, 1979).

Strain	Relevant Genotype	Reference
DF5	<i>trp1-1 ura3-52 his3 200 leu2-3,11 lys2-801 CAN1 BAR1</i>	(Ulrich and Jentsch, 2000)
IP503	<i>lys1::natNT2 arg4::hphNT1 pADH-HisSMT3::URA3</i>	This study
IP698	<i>pADH-HisSMT3::LEU2</i>	This study
Y1094	<i>pADH-HisSMT3::SMT3</i>	SJ strain collection library
Y2203	<i>RFA1^{6HA}::kITRP1</i>	SJ strain collection library
Y2204	<i>RFA2^{6HA}::kITRP1</i>	SJ strain collection library
Y2205	<i>RFA3^{6HA}::kITRP1</i>	SJ strain collection library
IP046	<i>RFA1^{6HA}::kITRP1 pADH-HisSMT3::URA3</i>	This study
IP047	<i>RFA2^{6HA}::kITRP1 pADH-HisSMT3::URA3</i>	This study
IP048	<i>RFA3^{6HA}::kITRP1 pADH-HisSMT3::URA3</i>	This study
IP423	<i>RAD59^{6HA}::hphNT1 lys1::natNT2</i>	This study
IP349	<i>RAD59^{6HA}::hphNT1 pADH-HisSMT3::URA3</i>	This study
IP164	<i>Mre11^{3HA}::kITRP1 RFA2^{9MYC}::kITRP</i>	This study
IP166	<i>Mre11^{3HA}::kITRP1 RFA2^{9MYC}::kITRP1 pADH-HisSMT3::SMT3</i>	This study
IP760	<i>RAD50^{6HA}::HIS3MX6</i>	This study
IP762	<i>RAD50^{6HA}::HIS3MX6 pADH-HisSMT3::LEU2</i>	This study
IP778	<i>SAE2^{6HA}::HIS3MX6</i>	This study
IP780	<i>SAE2^{6HA}::HIS3MX6 pADH-HisSMT3::LEU2</i>	This study
IP809	<i>RAD9^{6HA}::HIS3MX6</i>	This study
IP811	<i>RAD9^{6HA}::HIS3MX6 pADH-HisSMT3::LEU2</i>	This study
IP904	<i>MRC1^{9MYC}::HIS3MX6</i>	This study
IP905	<i>MRC1^{9MYC}::HIS3MX6 pADH-HisSMT3::LEU2</i>	This study
IP782	<i>MEC1^{6HA}::HIS3MX6</i>	This study
IP783	<i>MEC1^{6HA}::HIS3MX6 pADH-HisSMT3::LEU2</i>	This study

MATERIALS AND METHODS

Strain	Relevant Genotype	Reference
IP784	<i>TEL1^{6HA}::HIS3MX6</i>	This study
IP785	<i>TEL1^{6HA}::HIS3MX6 pADH-HisSMT3::LEU2</i>	This study
Y2200	<i>RFA1^{9MYC}::kITRP1 pADH-HisSMT3::SMT3</i>	SJ strain collection library
Y2201	<i>RFA2^{9MYC}::kITRP1 pADH-HisSMT3:: SMT3</i>	SJ strain collection library
Y2202	<i>RFA3^{9MYC}::kITRP1 pADH-HisSMT3:: SMT3</i>	SJ strain collection library
IP231	<i>RAD59^{9MYC}::kanMX4 pADH-HisSMT3::SMT3</i>	This study
IP775	<i>bar1::HIS3MX6 pADH-HisSMT3::URA3</i>	This study
IP773	<i>bar1::HIS3MX6 exo1::natNT2 pADH-HisSMT3::URA3</i>	This study
IP787	<i>bar1::HIS3MX6 exo1::natNT2 pADH-HisSMT3::URA3 YCplac111 (empty)</i>	This study
IP788	<i>bar1::HIS3MX6 exo1::natNT2 pADH-HisSMT3::URA3 YCplac111-Exo1</i>	This study
IP789	<i>bar1::HIS3MX6 exo1::natNT2 pADH-HisSMT3::URA3 YCplac111-exo1-D173A</i>	This study
IP790	<i>bar1::HIS3MX6 exo1::natNT2 pADH-HisSMT3::URA3 YCplac111-exo1-S372A, S567A, S586A, S692A</i>	This study
IP902	<i>pol32::kITRP1 pADH-HisSMT3::LEU2</i>	This study
IP733	<i>sml1::HIS3MX6 pADH-HisSMT3::LEU2</i>	This study
IP734	<i>mec1::hphNT1 sml1::HIS3MX6 pADH-HisSMT3::LEU2</i>	This study
IP099	<i>ddc2::natNT2 sml1::HIS3MX6 pADH-HisSMT3::SMT3</i>	This study
IP754	<i>rad9::URA3 pADH-HisSMT3::LEU2</i>	This study
Y2325	<i>pSMT3-HisSMT3::SMT3</i>	SJ strain collection library
Y2333	<i>rad17::kanMX4 pSMT3-HisSMT3::SMT3</i>	SJ strain collection library
Y2334	<i>mec3::kanMX4 pSMT3-HisSMT3::SMT3</i>	SJ strain collection library
Y2340	<i>rad24::natNT2 pSMT3-HisSMT3::SMT3</i>	SJ strain collection library
IP735	<i>mec1::hphNT1 sml1::HIS3MX6 pADH-HisSMT3::LEU2 exo1::natNT2</i>	This study
IP746	<i>mec1::hphNT1 sml1::HIS3MX6 pADH-HisSMT3::LEU2 sgs1::kanMX4</i>	This study
IP736	<i>mec1::hphNT1 sml1::HIS3MX6 pADH-HisSMT3::LEU2 exo1::natNT2 sgs1::kanMX4</i>	This study
IP681	<i>mec1::hphNT1 sml1::HIS3MX6 pADH-HisSMT3::LEU2 rad50::kanMX4</i>	This study
IP253	<i>siz2::HIS3MX6 RAD59^{9MYC}::kanMX4 pADH-HisSMT3::SMT3</i>	This study
IP871	<i>ura3-52::natNT2::pCUP1-siz2-SAP^{9MYC}::hphNT1::URA3 siz2::HIS3MX6 pADH-HisSMT3::LEU2</i>	This study
IP057	<i>rad51::HIS3MX6 RFA1^{9MYC}::kITRP1 pADH-HisSMT3::SMT3</i>	This study
IP042	<i>rad51::HIS3MX6 RFA2^{9MYC}::kITRP1 pADH-HisSMT3::SMT3</i>	This study
IP044	<i>rad52:: natNT2 RFA2^{9MYC}::kITRP1 pADH-HisSMT3::SMT3</i>	This study
IP064	<i>RFA2^{9MYC}::kITRP1 mec1::hphNT1 sml1::HIS3MX6</i>	This study
IP088	<i>siz2::HIS3MX4 RFA2^{9MYC}::kITRP1 pADH-HisSMT3::SMT3</i>	This study
IP658	<i>Δhml::ADE1 MATα Δhmr::ADE1 ade1-100 leu2-3,112 lys5 trp1::hisG' ura3-52 ade3::GAL::HO pADH-HisSMT3::LEU2</i>	This study
IP659	<i>HMLα MATα Δhmr::ADE1 ade1-100 leu2-3,112 lys5 trp1::hisG' ura3-52 ade3::GAL::HO pADH-HisSMT3::LEU2</i>	This study
IP717	<i>mre11::hphNT1 pADH-HisSMT3::LEU2</i>	This study
IP719	<i>rad50::natNT2 pADH-HisSMT3::LEU2</i>	This study
IP701	<i>xrs2::kanMX4 pADH-HisSMT3::LEU2</i>	This study
IP849	<i>sae2::kanMX4 pADH-HisSMT3::LEU2</i>	This study
IP670	<i>exo1::natNT2 sgs1::kanMX4 pADH-HisSMT3::LEU2</i>	This study
IP671	<i>exo1::natNT2 pADH-HisSMT3::LEU2</i>	This study

MATERIALS AND METHODS

Strain	Relevant Genotype	Reference
IP672	<i>sgs1::kanMX4 pADH-HisSMT3::LEU2</i>	This study
IP845	<i>mre11::hphNT1 sae2::kanMX4 pADH-HisSMT3::LEU2</i>	This study
IP865	<i>mre11::hphNT1 sae2::kanMX4 pADH-HisSMT3::LEU2 Ylplac211-Mre11::URA3</i>	This study
IP866	<i>mre11::hphNT1 sae2::kanMX4 pADH-HisSMT3::LEU2 Ylplac211-mre11-H125N::URA3</i>	This study
IP828	<i>yku70::hphNT1 bar1::HIS3MX6 pADH-HisSMT3::URA3</i>	This study
IP829	<i>yku70::hphNT1 bar1::HIS3MX6 pADH-HisSMT3::URA3 exo1::natNT2</i>	This study
IP870	<i>cdc13ts pADH-HisSMT3::LEU2</i>	This study
IP496	<i>lys1::natNT2 arg4::hphNT1 pADH-HisSMT3::URA3 siz1::HIS3MX6</i>	This study
IP497	<i>lys1::natNT2 arg4::hphNT1 pADH-HisSMT3::URA3 siz2::HIS3MX4</i>	This study
IP525	<i>lys1::natNT2 arg4::hphNT1 pADH-HisSMT3::URA3 mms21-11::natNT2</i>	This study
IP676	<i>siz2::HIS3MX4 pADH-HisSMT3::URA3</i>	This study
IP1009	<i>siz2::HIS3MX4 pADH-HisSMT3::LEU2</i>	This study
IP850	<i>siz2::HIS3MX4 pADH-HisSMT3::LEU2 Ylplac211-Siz2^{9MYC}::hphNT1::URA3</i>	This study
IP852	<i>siz2::HIS3MX4 pADH-HisSMT3::LEU2 Ylplac211-siz2-SAP^{9MYC}::hphNT1::URA3</i>	This study
IP885	<i>siz2::HIS3MX4 pADH-HisSMT3::LEU2 Ylplac211-siz2-Siz1SAP^{9MYC}::hphNT1::URA3</i>	This study
IP235	<i>rad59::hphNT1 pADH-HisSMT3::LEU2</i>	This study
IP299	<i>rfa2-K199R</i>	This study
IP314	<i>rfa3-K46R</i>	This study
IP324	<i>rfa2-K199R rfa3-K46R</i>	This study
IP364	<i>rfa2-K199R pADH-HisSMT3::URA3</i>	This study
IP365	<i>rfa2-K199R rfa3-K46R pADH-HisSMT3::URA3</i>	This study
IP269	<i>smt3::HIS3MX6 Ylplac211-smt3-KRall::URA3</i>	This study
IP372	<i>smt3::HIS3MX6 Ylplac211-smt3-KRall::URA3 RFA3^{6HA}::kITRP1</i>	This study
IP374	<i>rfa2-K199R rfa3-K46R^{6HA}::kITRP1 pADH-HisSMT3::URA3</i>	This study
IP376	<i>rfa1-K170R,K427R rfa2-K199R rfa3-K46R</i>	This study
IP385	<i>rfa1-K170R,K427R rfa2-K199R rfa3-K46R pADH-HisSMT3::URA3</i>	This study
IP391	<i>rfa1-K133R,K170R,K427R rfa2-K199R rfa3-K46R</i>	This study
IP396	<i>rfa1-K133R,K170R,K427R rfa2-K199R rfa3-K46R pADH-HisSMT3::URA3</i>	This study
IP350	<i>rad59-K228R^{6HA}::hphNT1 pADH-HisSMT3::URA3</i>	This study
IP383	<i>rad59-K228R,K238R^{6HA}::kITRP1 pADH-HisSMT3::URA3</i>	This study
IP387	<i>rad59-K207R,K228R,K238R^{6HA}::kITRP1 pADH-HisSMT3::URA3</i>	This study
IP434	<i>rad59-K207R,K228R,K238R</i>	This study
IP422	<i>rfa1-K133R,K170R,K427R rfa2-K199R rfa3-K46R rad59-K207R,K228R,K238R</i>	This study
IP444	<i>rfa1-K133R,K170R,K427R rfa2-K199R rfa3-K46R rad52-K10R,K11R,K220R rad59-K207R,K228R,K238R</i>	This study
IP445	<i>rad52-K10R,K11R,K220R</i>	This study
IP461	<i>rad52-K10R,K11R,K220R rad59-K207R,K228R,K238R</i>	This study
YMS258/Y2011	<i>rad52::kanMX6</i>	(Sacher et al., 2006)

MATERIALS AND METHODS

Strain	Relevant Genotype	Reference
YMS417/Y2012	<i>rad50::HIS3MX6</i>	(Sacher et al., 2006)
Y1136	<i>siz2::HIS3MX4</i>	SJ strain collection library
IP895	<i>rfa1-K133R,K170R,K427R rfa2-K199R rfa3-K46R rad52-K10R,K11R,K220R rad59-K207R,K228R,K238R siz2::HIS3MX6</i>	This study
Y0710	<i>his1-1/his1-7</i>	(Pfander et al., 2005)
IP639	<i>his1-1/his1-7 rad52::natNT2/rad52::natNT2</i>	This study
IP643	<i>rfa1-K133R,K170R,K427R/rfa1-K133R,K170R,K427R rfa2-K199R/rfa2-K199R rfa3-K46R/rfa3-K46R rad52-K10R,K11R,K220R/rad52-K10R,K11R,K220R rad59-K207R,K228R,K238R/rad59-K207R,K228R,K238R his1-1/his1-7</i>	This study
IP678	<i>his1-1/his1-7 siz2::kanMX6/siz2::hphNT1</i>	This study
IP224	<i>Δhml::ADE1 MATα Δhmr::ADE1 ade1-100 leu2-3,112 lys5 trp1::hisG' ura3-52 ade3::GAL::HO RFA1^{9MYC}::natNT2</i>	This study
IP283	<i>Δhml::ADE1 MATα Δhmr::ADE1 ade1-100 leu2-3,112 lys5 trp1::hisG' ura3-52 ade3::GAL::HO RFA1^{9MYC}::natNT2 siz2::hphNT1</i>	This study
IP1015	<i>siz2ΔCterm^{9MYC}::hphNT1 pADH-HisSMT3::LEU2</i>	This study
IP1023	<i>siz2::HIS3MX4 pADH-HisSMT3::LEU2 Ylplac211-siz2-Gal4^{9MYC}DBD^{9MYC}::hphNT1::URA3</i>	This study
IP1024	<i>siz2::HIS3MX4 pADH-HisSMT3::LEU2 siz1-siz2Cterm^{9MYC}::hphNT1::URA3</i>	This study
IP1025	<i>siz2-VV720,721AA^{9MYC}::hphNT1 pADH-HisSMT3::LEU2</i>	This study
IP1031	<i>siz2::HIS3MX4 pADH-HisSMT3::LEU2 Ylplac211-siz2-II472,473AA^{9MYC}::hphNT1::URA3</i>	This study
IP1067	<i>siz2::HIS3MX4 pADH-HisSMT3::LEU2 Ylplac211-siz2-Siz1^{9MYC}PINIT^{9MYC}::hphNT1::URA3</i>	This study
IP1072	<i>Siz2^{9MYC}::kanMX4 pADH-HisSMT3::LEU2</i>	This study

All strains are isogenic to DF5, except for IP224, IP283, IP658, which are derived from JKM179 (Lee et al., 1998), and IP659, which is a derivative of JKM161 (Sugawara et al., 2003).

S. cerevisiae media and solutions

YPD/YPGal [plates]: 1% yeast extract (Difco)
2% bacto-peptone (Difco)
2% D-(+)-glucose or galactose
[2% agar]
sterilized by autoclaving

YP-Lactate: 1% yeast extract (Difco)
2% bacto-peptone (Difco)
3% lactic acid
(adjust pH to 5.5 with NaOH)
sterilized by autoclaving

YPD G418/NAT/Hph plates: YPD medium containing 2% agar was autoclaved and cooled to 50°C prior to addition of G418 (geneticine disulfate; Sigma), NAT (noursethricin, HKI Jena) or Hph (hygromycin B, PAA Laboratories) to 200mg/l, 100mg/l or 500mg/l, respectively.

MATERIALS AND METHODS

SC-media [plates]:	0.67% yeast nitrogen base (Difco) 0.2% drop out amino acid mix (according to the requirements) 2% carbon source (glucose, galactose or raffinose) [2% agar] sterilized by autoclaving
SC-Lactate:	0.67% yeast nitrogen base (Difco) 0.2% amino acid drop out mix (according to the requirements) 3% lactic acid (adjust pH to 5.5 with NaOH) sterilized by autoclaving
SC-5'FOA plates:	0.67% yeast nitrogen base (Difco) 0.2% amino acid drop out mix (according to the requirements) 3% adenine 3% uracil 2% glucose 2% agar After autoclaving, the mixture is cooled to 50°C prior to 5'FOA addition to the final concentration of 0,1%.
Drop out amino acid mix:	30 mg Arg, Tyr, Leu, Lys 50 mg Phe 100 mg Glu, Asp 150 mg Val 200 mg Thr 400 mg Ser
Sporulation medium:	2% (w/v) potassium acetate (in sterile water)
Zymolase 100T solution:	0.9 M sorbitol 0.1 M Tris-HCl, pH 8.0 0.2 M EDTA, pH 8.0 50 mM DTT 0.5 mg/ml Zymolase 100T (Seikagaku Corp., Japan)
SORB:	100 mM LiOAc 10 mM Tris-HCl, pH 8.0 1 mM EDTA, pH 8.0 1 M sorbitol sterilized by filtration
PEG:	100 mM LiOAc 10 mM Tris-HCl, pH 8.0 1 mM EDTA, pH 8.0 40 % (w/v) PEG-3350 sterilized by filtration, stored at 4°C

Cultivation and storage of *S. cerevisiae*

Liquid cultures were inoculated with a single yeast colony from freshly streaked plates and grown ON at 30°C with constant shaking. In general, from this preculture the main culture was inoculated to an OD₆₀₀ of 0.1-0.2 and incubated in baffled-flasks (size ≥ 5x liquid culture volume) on a shaking platform (150-220 rpm) at 30°C until mid-log phase growth had been reached (equals to OD₆₀₀ of 0.6-0.9). The culture density was determined photometrically (OD₆₀₀ of 1 is equal to 1.5x10⁷ cells/ml). Cultures on agar plates were stored at 4°C up to 1-2 months. For long-term storage, stationary cultures were frozen in 15% (v/v) glycerol solutions at -80°C.

Preparation of competent yeast cells

Yeast cells from a mid-log phase growing culture (generally, 50 ml at OD₆₀₀ of 0.5-0.7) were harvested by centrifugation (500g, 3 min, room temperature), washed first with 1/2 volume sterile water, then with 1/10 volume SORB solution, pelleted and suspended again in 360µl SORB solution. After addition of 40µl carrier DNA (heat denatured salmon sperm DNA, 10mg/ml, Invitrogen) and further resuspension, competent cells were stored in 50µl aliquots at -80°C.

Transformation of yeast cells

For transformation, 200ng of circular or 2µg of linearized plasmid DNA/PCR product were mixed with 10µl or 50µl competent yeast cells, respectively. Six volumes of PEG solution were added and the cell suspension was incubated at 30°C for 30min. Subsequently, DMSO (final concentration 10%) was added and a heat-shock performed at 42°C for 15 min. Cells were sedimented by centrifugation (500g for 3min at room temperature), resuspended in 100µl sterile water and plated on the respective SC medium plates. If antibiotics were used for selection, the transformed cells were first incubated for 3h in 1 ml liquid YPD medium prior to plating. Selection of transformants was carried out for 2-3 days at 30°C (or 23°C for temperature sensitive strains). If necessary, the transformants were replica-plated on selection plates to remove the background of false-positive colonies.

Genomic integration by homologous recombination

The YIplac vector series was used for stable integration of DNA into the yeast genome. Because these plasmids do not contain autonomous replication elements, only stably integrated vectors are propagated in yeast. The ORFs of the respective genes were cloned into YIplac vectors including the endogenous, constitutive (e.g., the *ADH1* promoter for overexpression) or inducible promoter (e.g., *CUP1* or *GAL10* promoter) and terminator elements. Before transformation, vectors were linearized by a restriction enzyme that specifically cuts within the auxotrophy marker gene. These linearized plasmids are then integrated into the genome by homologous recombination with the endogenous locus of the marker gene. Alternatively, the constructs can be targeted to the endogenous loci of studied genes, if the plasmids are specifically cut within the cloned gene sequence.

A similar approach was used in order to delete, truncate, C-/N-terminally tag endogenous genes with epitopes (Janke et al., 2004; Knop et al., 1999; Longtine et al., 1998) or generate point mutants/fusions. For this method, PCR products were used to transform competent yeast cells. To allow homologous recombination with the endogenous locus of a gene, PCR products were generated using primers that contain sequences for amplification of special cassettes or regions of interest in the genome (including the marker gene for selection) as well as sequences

MATERIALS AND METHODS

complementary to the gene of interest required for proper integration. For gene deletions, the forward primer contains 55bp of the promoter sequence 5' of the start codon of the respective gene, while the reverse primer includes 55bp of the terminator sequence 3' of the stop codon. For C-terminal epitope tagging of a gene, a forward primer containing 55bp 5' of the stop codon were used instead. In a similar fashion, gene truncations, fusions, point mutations were introduced through homologous recombination. Generally, PCR products were purified and concentrated after amplification using ethanol precipitation, and competent yeast cells transformed and plated on selection plates. The correct recombination was confirmed by yeast colony PCR, Western blot analysis (if applicable) and sequencing of the modified genomic loci.

Strains expressing mutant proteins with SUMO-acceptor lysine residues replaced by arginine residues (*KR*) were constructed by a pop-in/pop-out allele replacement method (Scherer and Davis, 1979). Briefly, pYIplac211 *URA3*-based integrative plasmid containing mutagenized gene of interest was linearized by cutting within the cloned gene and targeted to its endogenous chromosomal locus. This creates a gene duplication containing the wild-type copy and the mutant copy separated by the *URA3* marker and plasmid sequences. Finally, the integrated cassette is excised through pop-out recombination by selecting on 5'FOA plates and the 5'FOA-resistant colonies are sequenced. Crossovers that take place on the appropriate side of the mutated site replace the WT chromosomal site with mutant sequences specifically introducing chromosomal point mutations.

PCR screening of genomic recombination events (“yeast colony-PCR”)

For the verification of chromosomal gene disruptions, correct recombination events were identified by “yeast colony-PCR”. The screening strategy is based on oligonucleotide probes, which anneal upstream/downstream of altered chromosomal locus (primer 1) and within the introduced selection marker gene (primer 2). Prior to the PCR, a single yeast colony from a selection plate was resuspended in 50µl of 0.02M NaOH and incubated at 95°C for 5min with rigorous shaking (1400rpm). Next, the solution was briefly centrifuged (13000rpm at room temperature) and 4.0µl of the supernatant was directly used as a template for PCR. DNA oligonucleotides for PCR were custom-made by Eurofins MWG Operon.

PCR reaction mix: 4.0 µl template DNA
5.0 µl 10x Thermopol buffer (NEB)
2.0 µl dNTP-Mix (10 mM each; New England Biolabs)
0.5 µl primer 1 (100 µM)
0.5 µl primer 2 (100 µM)
0.5 µl *Taq* DNA polymerase
37.5 µl dH₂O

Cycling parameters (30 amplification cycles):

PCR step	T (°C)	Time
Initial denaturation	94	5 min
Denaturation	94	30 s
Annealing	50	30 s
Elongation	72	1 min/kb
Final elongation	72	10 min
Cooling	4	∞

MATERIALS AND METHODS

Mating type analysis of haploid yeast strains

The tester strains RC634a and RC75-7 α were used for the identification of yeast mating types. These strains are hypersensitive to the pheromone secreted by yeast strains of the opposite mating type. 500 μ l of a dense suspension of a tester strain in sterile water was mixed with 50ml of molten agar (1% w/v water, pre-cooled to 40°C) and 5ml were poured over each YPD plate. Plates containing cultures to be analyzed were either replica-plated on the a- and α -tester plates, or single colonies of unknown mating type were streaked on each tester plate. The tester strains cannot grow in proximity of colonies of different mating type, thereby generating a so-called “halo” of clear agar. Therefore, after 1-2 days of incubation at 30°C, a halo appears around a haploid colony, if the mating type of the strain is different. The diploid cells do not secrete any mating type pheromones and therefore do not give halos on both mating type tester plates.

Mating of haploid yeast strains

Freshly streaked haploid strains of opposite mating types (*MATa*, *MAT α*) were mixed and spotted together on YPD plates ON at 30°C to allow mating. Cells were then either streaked on respective selection plates to identify diploids or mating type analysis was performed for individual colonies.

Sporulation and tetrad analysis of diploid yeast strains

500 μ l of diploid stationary phase yeast cells were harvested by centrifugation (500g, 3min, room temperature), washed 2 times with sterile water and resuspended in 4ml sporulation medium (2% potassium acetate). After incubation on a shaker at room temperature for 3-7 days, 10 μ l of the culture was mixed with 10 μ l Zymolase 100T solution and incubated at room temperature for 10min. The spores were dissected in tetrads with a micromanipulator (Singer MSM Systems) and grown on YPD plates at 30°C for 2-3 days. Subsequently, tetrads were analyzed genotypically by replica plating on selection plates or by their phenotypes, where applicable.

Analysis of protein-protein interactions using the two-hybrid system

The full-length ORFs, fragments and mutant variants of proteins used for yeast two-hybrid assays in this study were fused to the C-terminus of the DNA-binding domain (BD) or activation domain (AD) of the Gal4 transcription factor by cloning them into pGBD-C1 or pGAD-C1 vectors, respectively. The expression constructs were used to transform PJ69-7A cells (James et al., 1996). Physical interaction between BD- and AD-fusion proteins leads to reconstitution of the Gal4 transcription factor, which induces expression of *HIS3* and *ADE2* reporter genes and allows cell growth on the respective selection plates. White colony color is indicative of better growth. Images were usually taken after growth for 3 days at 30°C.

Synchronization by a-factor (G1 arrest)

Treatment of *MATa* cells with the α -factor pheromone results in cell cycle arrest at the G1 phase. For such cell cycle synchronization, mid-log phase *MATa BAR1* cell cultures were supplemented with 10 μ M α -factor (stock solution in DMSO) and incubated at 30°C with constant shaking. After 2-3h, the arrest efficiency was determined microscopically (typically >90%) or by FACS analysis. Cells were released into the cell cycle by washing one time in sterile water and one time in fresh YPD at room temperature to remove α -factor. For *MATa Δ bar1* cells, α -factor was

MATERIALS AND METHODS

used at 200nM and release was achieved by addition of pronase (25 µg/ml; Calbiochem).

Phenotypic analysis of yeast mutants, growth and cell survival assays

Nonessential gene knockout strains and mutants were tested for growth impairments and DNA-damage sensitivity by spotting equal amounts of cells in serial dilutions onto solid YPD media containing DNA-damage inducing agents such as MMS, Zeocin, HU or 4NQO. For all growth and cell survival analyses, overnight cultures were harvested and resuspended in sterile water. After dilution to $OD_{600}=0.5-1$, ten-fold serial dilutions were prepared and spotted onto the respective plates. Plates were incubated for 2-3 days at 30°C and images were obtained.

When not indicated otherwise, growing cell cultures were incubated for 90 min at 30°C in the presence of MMS (0.2%), Zeocin (0.2 mg/ml), HU (100 mM) or 4NQO (1 µg/ml). Cells irradiated with UV-light (80 J/m²) in the irradiation chamber BS-03 (Dr. Gröbel UV-Elektronik GmbH) were harvested 30 min after irradiation and incubation in the dark. *cdc13ts* cells were grown at permissive conditions (24°C) and were subsequently shifted to 37°C for 3 hrs before harvesting. $\Delta pol32$ cells were grown at 30°C and subsequently shifted to 14°C for overnight incubation before harvesting. To induce the *CUP1* promoter, CuSO₄ (100 µM) was added to YPD-medium.

For qualitative analysis of MMS sensitivity, cells from overnight cultures were inoculated into 200 µl fresh YPD liquid medium containing MMS (0.02%) at a final $OD_{600}=0.2$. A Type FP-1100-C Bioscreen C machine (Thermo Labsystems) was used to measure growth every 15 min at 30°C for 48 hours with constant shaking. All physiological studies were done in triplicates.

Measuring the interchromosomal recombination rates

Spontaneous interchromosomal recombination rates between the heteroalleles *his1-1* and *his1-7* in diploid cells were determined by fluctuation analysis as previously described (Pfander et al., 2005). Briefly, individual colonies were used to inoculate twelve parallel cultures in non-selective YPD medium for each studied yeast strain. The cultures were then grown to saturation at 30°C overnight with constant shaking to obtain equal cell densities. After making appropriate dilutions in sterile water with extensive vortexing steps in between, the cells were then plated (2 plates per independent parallel culture) onto SC-His plates to obtain the number of recombinants, and dilutions were also plated onto YPD plates to calculate the total number of viable cells. The number of recombination events was determined by the MSS-maximum likelihood estimator method. The program FALCOR was used to assist the analysis. Averages were obtained from at least three independent experiments. MMS-induced interchromosomal recombination rates were assayed by inoculating appropriate dilutions of cells onto SC-His plates and YPD plates containing given concentrations of MMS. Colonies were counted after 3 days incubation at 30°C.

FACS / Flow cytometry analysis

For flow cytometry analysis, approximately 7×10^6 cells for each time-point were collected, washed in sterile water, and permeabilized in 70% ethanol. Cells were suspended in 10 mM Tris pH 7.5 buffer, and RNA together with proteins were removed by RNaseA (0.4 mg/ml final concentration) and proteinase K (1 mg/ml) treatment. Subsequently, cells were stained with PI (propidium iodide 50 µg/ml). Cell

MATERIALS AND METHODS

cycle profiles were obtained at the FL1 channel (voltage 520) using a FACSCalibur system operated via the CELLQuest software (Becton Dickinson). Data was analyzed quantitatively with FlowJo (Tree Star).

V.3 Molecular Biology Techniques

General molecular biology and cloning techniques such as DNA amplification/site-directed mutagenesis by PCR, restriction digest, ligation or analysis of DNA by agarose gel electrophoresis were performed according to standard (Sambrook and Russell, 2001) or manufacturer's protocols.

General buffers and solutions

TE buffer:	10 mM Tris-HCl, pH 8.0 1 mM EDTA sterilized by autoclaving
TBE buffer 5x:	90 mM Tris 90 mM boric acid 2.5 mM EDTA, pH 8.0 sterilized by autoclaving
DNA loading buffer 6x:	0.5% SDS 0.25% (w/v) bromophenol blue 0.25% glycerol 25 mM EDTA, pH 8.0

V.3.1 Isolation of DNA

Isolation of plasmid DNA from *E. coli*

LB medium (5 ml) containing appropriate antibiotic was inoculated with a single *E. coli* colony carrying the DNA plasmid of interest and incubated overnight at 37°C. Plasmids were isolated using the AccuPrep plasmid extraction kit (Bioneer Corp.) according to the manufacturer's instructions. The yield of isolated DNA was determined photometrically.

Isolation of 2 μ m plasmid DNA from *S. cerevisiae*

For isolation of 2 μ m plasmid DNA from the transformed yeast strains the yeast plasmid isolation kit (GE Healthcare) was used according to the manufacturer's instructions.

Isolation of chromosomal DNA from *S. cerevisiae*

Breaking buffer:	2% Triton X-100 1% SDS 100 mM NaCl 10 mM Tris-HCl, pH 8.0 1 mM EDTA, pH 8.0
------------------	---

MATERIALS AND METHODS

Yeast genomic DNA was isolated for further use as a template for amplification of genes via PCR. Cells from a stationary culture (10ml) were pelleted by centrifugation (1500g, 5 min), washed once in 0.5ml water and resuspended in 200µl breaking buffer. Subsequently, 200µl phenol/chloroform/isoamyl alcohol (24:24:1 v/v/v) and 300mg acid-washed glass beads (425-600µm; Sigma) were added, and the mixture was vortexed for 5 min. The lysate was mixed with 200µl TE buffer, centrifuged for 5 min at 14000rpm at 23°C and the supernatant transferred to a microcentrifuge tube. DNA was precipitated by addition of 1ml ethanol (absolute) followed by centrifugation at 14000rpm for 3 min at room temperature. The pellet was resuspended in 0.4ml TE buffer and RNA contaminants were destroyed by treatment with 30µl of DNase-free RNase A (1 mg/ml) for 5 min at 37°C. Afterwards, DNA was reprecipitated by mixing with 10µl ammonium acetate (3M) and 1ml ethanol (absolute). After a brief centrifugation at 14000rpm, the pellet was resuspended in 100µl TE buffer.

Alternatively, yeast genomic DNA was isolated using the MasterPure yeast DNA purification kit (Epicentre) according to the manufacturer's instructions.

Precipitation of DNA

For ethanol precipitation, 1/10 volume sodium acetate (3M, pH 4.8) and 2.5 volumes ethanol (absolute) were added to the DNA solution and incubated at -20 °C for 30min. The mixture was centrifuged (13000rpm, 15min) and the pellet was washed once with 0.5ml of 70% ethanol. Finally, the DNA pellet was air-dried and resuspended in TE buffer or sterile water.

Determination of DNA concentration

The DNA concentration was photometrically determined by measuring the absorbance at a wavelength of 260nm (OD_{260}) using the NanoDrop ND-1000 spectrophotometer (PeqLab). An OD_{260} of 1 equals to a concentration of 50µg/ml double-stranded DNA.

V.3.2 Molecular cloning

Digestion of DNA with restriction enzymes

The sequence-specific cleavage of DNA with restriction enzymes was performed according to standard protocols (Sambrook and Russell, 2001) and the instructions of the manufacturer (NEB). In general, 5 to 10 units of the respective restriction enzyme were used for digesting 1µg DNA. Typically, the reaction samples were incubated for 2 hours in the appropriate buffers (NEB) at the recommended temperature. To avoid re-circulation of linearized vectors, the 5' end of the vector DNA was dephosphorylated by incubation at 37°C for 1h with 1µl of the Calf Intestinal Phosphatase (CIP; NEB).

Separation of DNA by agarose gel electrophoresis

To isolate DNA fragments, DNA samples were mixed with 6x DNA loading buffer and subjected to electrophoresis using 1.5% agarose gels containing 0.5µg/ml ethidium bromide at 120V in TBE buffer. Separated DNA fragments were visualized using an UV transilluminator (324 nm), due to intercalation of ethidium bromide into DNA. The size of the fragments was estimated using standard size markers (1kb DNA ladder, Invitrogen).

MATERIALS AND METHODS

Isolation of DNA fragments from agarose gels

After separation by gel electrophoresis, DNA fragments were excised from the agarose gel using a sterile razor blade. DNA was then extracted from the agarose block using kits from Qiagen (QIAquick Gel Extraction Kit) or Bioneer (AccuPrep Gel Purification Kit) according to manufacturer's instructions and eluted with an appropriate volume of sterile water.

Ligation of DNA fragments

The amounts of the linearized vector and insert required for the ligation reaction were estimated by gel electrophoresis of the purified fragments. A ratio of 1:3–1:10 of vector to insert was used. The 10µl ligation reaction sample contained 100ng of vector DNA and 10 units of T4 DNA ligase (NEB). The ligation was performed at 16°C for 4-12h. Prior to electroporation of the ligation products into electro-competent *E. coli*, the sample was dialyzed against deionized water for 15 min using a nitrocellulose filter (pore size 0,05µm, Millipore).

DNA sequencing

The DNA sequencing reactions were carried out by the Core Facility of the Max Planck Institute of Biochemistry using the ABI-Prism 3730 DNA sequencer (Applied Biosystems Inc.). The 10µl samples contained 1µg DNA and 5pmol primer. The sequencing reactions and the subsequent sample preparation steps were done with the DYEnamic ET terminator cycle sequencing kit (GE Healthcare), according to the instructions of the manufacturer.

V.3.3 Polymerase chain reaction

To specifically amplify DNA fragments from small amounts of DNA templates the polymerase chain reaction (PCR) techniques were used. PCR was applied for amplification of DNA fragments for subsequent cloning, amplification of yeast targeting cassettes (e.g., for chromosomal gene disruptions), screening/sequencing of genomic recombination events, site-directed mutagenesis and quantitative real-time PCR.

Amplification of genomic DNA fragments

For the generation of genomic DNA fragments for subsequent cloning/direct yeast transformation/sequencing, full-length ORFs or selected sequences were amplified from genomic DNA using the *Phusion* High-Fidelity DNA polymerase (NEB). PCR reactions were prepared in 0.2 ml tubes (Biozym) on ice, in a volume of 50-100µl for preparative PCR. A PCR Mastercycler (Eppendorf) was used for the reaction.

PCR reaction mix: 200 ng genomic DNA
 10 µl 5x HF/GC buffer
 2.0 µl dNTP-Mix (10 mM each; NEB)
 0.5 µl forward primer (100 µM)
 0.5 µl reverse primer (100 µM)
 0.5 µl *Phusion* DNA polymerase
 adjust to 50 µl with dH₂O

MATERIALS AND METHODS

Cycling parameters (30 amplification cycles):

PCR step	T (°C)	Time
Initial denaturation	98	30 s
Denaturation	98	30 s
Annealing	55-58	30 s
Elongation	72	30 s/kb
Final elongation	72	10 min
Cooling	4	∞

Amplification of chromosomal targeting cassettes

Chromosomal gene deletions/epitope tagging and other alterations of the yeast genome were performed by a PCR strategy based on the targeted introduction of heterologous DNA sequences into genomic locations via homologous recombination (Janke et al., 2004; Knop et al., 1999). Targeting cassettes were amplified by PCR using primers containing homology to the genomic target locus. The 100 μ l PCR reactions were prepared as indicated below, whereas cycling conditions were described previously (Janke et al., 2004). After amplification, PCR products were concentrated by ethanol precipitation, dissolved in 25 μ l of sterile water and 5 μ l were directly used for the transformation of competent yeast cells, while the remaining DNA was stored at -20°C .

PCR reaction mix: 400 ng genomic DNA/ 100 ng plasmid DNA
10 μ l 10x Thermopol buffer (NEB)
4.0 μ l dNTP-Mix (10 mM each; NEB)
1 μ l forward primer (100 μ M)
1 μ l reverse primer (100 μ M)
3.2 μ l *Taq* DNA polymerase
1.6 μ l *Vent* DNA polymerase (NEB)
adjust to 100 μ l with dH₂O

Site-directed mutagenesis

To introduce specific point mutations, insertions or deletions in plasmid DNA sequences, a PCR-based strategy was developed based on the Quick-change protocol (Stratagene). This method uses two complementary oligonucleotide primers with the codon/region to be mutated in the middle of the sequence flanked by at least 15-20 additional nucleotides, each corresponding to the target sequence. For this technique the *Pfu Turbo* DNA polymerase (Stratagene) has proven to be the enzyme of choice. Alternatively, the *Phusion High-Fidelity* DNA polymerase (NEB) was used according to the manufacturer's instructions. DNA oligonucleotides for PCR (up to 120 nucleotides-long) were custom-made by Eurofins MWG Operon.

PCR reaction mix: 50-100 ng plasmid DNA
5 μ l 10x *Pfu* buffer (Stratagene)
2.0 μ l dNTP-Mix (10 mM each; NEB)
0.5 μ l forward mutagenesis primer (100 μ M)
0.5 μ l reverse mutagenesis primer (100 μ M)
1 μ l *Pfu Turbo* DNA polymerase
adjust to 50 μ l with dH₂O

MATERIALS AND METHODS

Cycling parameters (25 amplification cycles):

PCR step	T (°C)	Time
Initial denaturation	95	5 min
Denaturation	95	30 s
Annealing	45-55	45 s
Elongation	72	1 min/kb
Final elongation	72	20 min
Cooling	4	∞

To eliminate template plasmid DNA that does not harbor the mutation, 45µl of the PCR reaction were treated with 2µl of *DpnI* endonuclease (and 5µl of the respective buffer) for 1-2 hours at 37°C. *DpnI* endonuclease is specific for methylated and hemimethylated DNA and as most plasmid DNA from *E. coli* is methylated, *DpnI* treatment of the PCR product leads to the selective digestion of the parental DNA template. After digestion, the PCR product carrying the mutation was purified using the QIAquick PCR purification kit (Qiagen), eluted with water and directly used for *E. coli* transformation. Mutated plasmids were identified by DNA sequencing.

V.4 Biochemistry Techniques

General buffers and solutions

HU sample buffer:	8 M Urea 5% SDS 1 mM EDTA 1.5% DTT 1% bromphenol blue
Laemmli sample buffer:	2% SDS 20% glycerol 100 mM Tris base 60 mM EDTA 1% bromophenol blue
MOPS running buffer:	50 mM MOPS 50 mM Tris base 3.5 mM SDS 1 mM EDTA
Transfer buffer:	250 mM Tris base 1.92 M glycine 0.1% SDS 20% methanol
TBST:	25 mM Tris-HCl, pH 7,5 137 mM NaCl 2.6 mM KCl 0.1% Tween 20

MATERIALS AND METHODS

V.4.1 Preparation of yeast protein extracts

Preparation of denatured protein extracts (TCA-precipitation)

To preserve post-translational modifications, yeast cells were in most cases lysed under denaturing conditions. For preparation of denatured protein extracts, yeast cultures grown to an $OD_{600}=0.7-1$ were pelleted by centrifugation (4000rpm, 4min, 4°C) and immediately frozen in liquid nitrogen. After thawing on ice, the pellets were lysed by addition of denaturing lysis buffer (1.85M NaOH, 7.5% β -mercaptoethanol) for 15min on ice. For the cell pellet of an $OD_{600}=1$ typically 150 μ l of lysis buffer was used. To precipitate the proteins, the lysate was subsequently mixed with an equal volume (150 μ l in case of $OD_{600}=1$) of 55% (w/v) trichloroacetic acid (TCA) and further incubated on ice for 15min. The precipitated material was recovered by two sequential centrifugation steps (13000rpm, 4°C, 15min). Pelleted denatured proteins were then either directly resuspended in sample buffer (50 μ l per $OD_{600}=1$) and stored at -20°C, or used for downstream processing, e.g., Ni-NTA pull-downs of His-tagged SUMO conjugates.

Preparation of native protein extracts

Native protein extracts were used for co-immunoprecipitation (co-IP) studies. To avoid protein degradation and loss of PTMs, the samples were handled as close to 4°C as possible and protease inhibitors were used. The logarithmically growing yeast cells (typically 100-200 OD) were harvested by centrifugation (4000rpm, 4min, 4°C), washed once with pre-cooled PBS and resuspended either in an equal volume of lysis buffer (Tris-HCl, pH 7.5, 150mM NaCl), or alternatively, in PBS supplemented with 10% glycerol, containing protease inhibitors: EDTA-complete inhibitor cocktail (Roche), Pefabloc SC (Roche), and 20mM NEM. After adding 0.5mm zirconia/silica beads (BioSpec Products, Inc.) the cells were lysed at 4°C using a multitube bead-beater (MM301 from Retsch GmbH) 6x 1min (frequency 30/s), with 5min cooling intervals on ice in between. To remove glass beads, lysates were transferred to new tubes by piggyback method (1000rpm, 2min, 4°C). Collected extracts were then incubated with 0.5% NP40 for 30min at 4°C and cleared by centrifugation (5000rpm, 5min, 4°C). Next, the protein concentration of the extracts was determined by the colorimetric analysis following the Bradford method (Bio-Rad Laboratories GmbH), appropriate aliquots for input control were taken, and the remaining extracts were directly used for co-IPs.

As an alternative to cell disruption by bead-beating, the grinding of centrifuged cells in liquid nitrogen was used. To this end, a cell pellet obtained from 100-200 OD of log-phase yeast culture was broken under liquid nitrogen with a ceramic mortar and pestle. 800 μ l of lysis buffer (PBS, 10% glycerol, 0.5% NP40, protease inhibitors) was added to the frozen powder of broken cells, thawed and suspension was then transferred to fresh 2ml tube. After incubation of protein extracts for 30min at 4°C and clearing by centrifugation (5000rpm, 5min, 4°C), the obtained supernatants further served as inputs for co-IPs.

V.4.2 Gel electrophoresis and immunoblot techniques

SDS-polyacrylamide gel electrophoresis (SDS-PAGE)

For separation of proteins, SDS-PAGE was performed using self-poured (see recipe below) or pre-cast 4-12% gradient NuPAGE Bis-Tris polyacrylamide gels (Invitrogen). These gels allow resolution of proteins over a large range of different

MATERIALS AND METHODS

molecular weights (10-200kDa) and do not require stacking gels (gradient mixer chamber is used instead). Generally, samples were prepared in Laemmli or HU sample buffer and denatured by heating for 5min at 95°C or 10min at 65 °C, respectively. Next, electrophoresis was carried out at a constant voltage of 140V using MOPS running buffer. The All Blue Precision Plus protein pre-stained standard (Bio-Rad) was used as a molecular weight marker. The gels were subsequently subjected to Coomassie blue staining (Thermo Scientific PageBlue protein staining solution applied for 1h to overnight at 4°C with subsequent background destaining in dH₂O) or immunoblotting.

Solutions for pouring 4-12% Bis-Tris SDS-PAGE gradient gels using gradient mixer:

	4% solution	12% solution
30% acrylamide / 0.8% bis-acrylamide (ProtoGel; National diagnostics)	2.2 ml	6.6 ml
2.5 M Bis-Tris-HCl, pH 7.5	2.4 ml	2.4 ml
65% sucrose	—	1.2 ml
10% SDS	82.5 µl	82.5 µl
10% ammonium persulfate	82.5 µl	82.5 µl
TEMED (Sigma)	16.5 µl	16.5 µl
dH ₂ O	11.85 ml	6.2 ml

Western blot analysis

For western blot analysis, proteins separated by PAGE were transferred to polyvinylidene fluoride (PVDF) membranes (Immobilon-P, 0.45µm pore size; Millipore) using a wet tank blot system (Hoefer). The blotting was performed in fresh transfer buffer at a constant voltage of 70V for 90min at 4°C. Subsequently, membranes were blocked for 30min using 5% skim milk powder (Fluka) dissolved in TBST and further incubated ON with primary antibody at 4°C with constant shaking. After two washes with TBST (5min each), blots were incubated with the respective horseradish peroxidase (HRP)-coupled secondary antibody (Dianova; 1:5000 dilution) for 2h in TBST at room temperature. After four further washes with TBST (5min each), the signals were obtained by chemiluminescence using ECL, ECL-Plus or ECL advanced kits (Amersham/GE Healthcare) according to the manufacturer's instructions. Signal detection was performed using a luminescent image analyzer LAS-3000 (Fujifilm) equipped with a high-sensitivity CCD camera.

Peptide array immunoblotting

Peptide arrays were synthesized automatically using SPOT technology with the MultiPep instrument from INTAVIS Bioanalytical Instruments AG as previously described (Brandt et al., 2003). 12-mer peptides harboring predicted SUMO-interacting motif (SIM) with endogenous flanking sequences or mutated SIM version with two hydrophobic residues replaced by alanines were produced in quadruplicates. The peptide array membrane was blocked with 5% skim milk in TBST for 1h at room temperature, then poly-SUMO-3 chains (ULC-310) from BostonBiochem were added to a final concentration of 1 µg/ml and incubated ON at 4°C. The membrane was then washed extensively with TBST before the monoclonal SUMO-2/3 antibody (1E7; MBL) was added. The membrane was incubated with the antibody at room temperature for another 2h prior to standard chemiluminescent detection.

Primary antibodies

Polyclonal antibodies against Rad52 are described (Sacher et al., 2006), polyclonal antibodies against *S. cerevisiae* RFA (AS07 214) were obtained from Agrisera, polyclonal antibodies against Rad51 (y-180), Rad53 (yC-19) and Exo1 (yD-17), and the monoclonal antibody against the HA-epitope (F-7) were purchased from Santa Cruz Biotechnology, monoclonal antibody against the MYC-epitope (9E10) was from SIGMA, and monoclonal Pgk1 antibody (22C5) was from Invitrogen. Polyclonal antibodies directed against Histone H3 trimethylated at lysine 4 (H3K4me3) were from Diagenode (pAb-003-050), monoclonal Dpm1 antibody (5C5A7) was from Molecular Probes, and monoclonal SUMO-2/3 antibody (1E7) was from MBL.

V.4.3 Protein purification and binding experiments

Purification of recombinant proteins from *E. coli*

His-tagged recombinant proteins were overexpressed in BL21(DE3)/RIL or Rosetta 2(DE3)pLysS *E. coli* strains and purified by Ni-NTA affinity chromatography either under native, or denaturing conditions (with subsequent protein refolding during dialysis steps). For purification under native conditions, cell pellets collected from 1l bacterial culture were resuspended in Ni-NTA lysis buffer (100mM NaCl, 5mM MgCl₂, 40mM Tris-HCl, pH 7.5, 20mM imidazole), lysed using the Emulsiflex C5 cell disruptor (Avestin) and sonicated for 2min using a Sonopuls HD2200 sonicator (Bandelin). After centrifugation (23000g, 30min, 4°C) the supernatant was incubated for 2h with 600µl of a Ni-NTA Agarose (Qiagen) 50% slurry at 4°C with constant rotation. The agarose was subsequently packed into 5ml polypropylene column, washed several times with the Ni-NTA washing buffer (100mM NaCl, 5mM MgCl₂, 40mM Tris-HCl, pH 7.5, 50mM imidazole) and bound proteins were eluted by repeated incubations with the Ni-NTA elution buffer (100mM NaCl, 5mM MgCl₂, 40mM Tris-HCl, pH 7.5, 250mM imidazole). The eluted protein fractions were analyzed by PAGE and Coomassie blue staining for purity, pooled together and dialyzed ON against PBS at 4°C. For purification under denaturing conditions, the protein pellet after cell lysis and centrifugation steps was further resuspended in urea-containing buffer (8M urea, 100mM NaH₂PO₄, 10mM Tris-HCl, pH 6.3, 20mM imidazole). Following purification and elution from Ni-NTA agarose, the dialysis of denatured recombinant protein was performed against buffers with reducing urea concentrations (6M, 4M, 2M urea) and finally against PBS in a sequential manner in order to promote protein refolding. Because purified Siz2 (Nfi1) contains an SP-RING zinc-finger domain, 100mM ZnCl₂ was added to the buffers during refolding. After dialysis the protein concentration was quantified by measuring the absorption at 280nm in an ND1000 spectrophotometer (Nanodrop Technologies), the protein aliquots were frozen in liquid nitrogen and stored at -80°C for downstream applications, e.g., EMSA.

Ni-NTA chromatography of HisSUMO conjugates from denatured yeast extracts

For isolation of *in vivo* SUMOylated substrates from yeast cells expressing N-terminally His-tagged Smt3, denatured protein extracts were prepared and Ni-NTA chromatography was carried out as described previously (Hoegel et al., 2002; Sacher et al., 2005). In general, 200 OD of logarithmically growing cells were harvested by centrifugation (4000rpm, 4min, 4°C), washed with pre-chilled water, transferred to 50ml falcon tube and lysed with 6ml of 1.85M NaOH / 7.5% β-mercaptoethanol for 15min on ice. The proteins were precipitated by adding 6ml of 55% TCA and another 15min incubation on ice (TCA-precipitation, described above). Next, the precipitate

MATERIALS AND METHODS

was pelleted by centrifugation (3500rpm, 15min, 4°C), washed twice with water and finally resuspended in buffer A (6M guanidine hydrochloride, 100mM NaH₂PO₄, 10mM Tris-HCl, pH 8.0, 20mM imidazole) containing 0.05% Tween-20. After incubation for 1h on a roller at room temperature with subsequent removal of insoluble aggregates by centrifugation (23000g, 20min, 4°C), the protein solution was incubated ON at 4°C with 50µl of Ni-NTA magnetic agarose beads (Qiagen) in the presence of 20mM imidazole. After ON incubation, the beads were washed three times with buffer A containing 0.05% Tween-20 and five times with buffer C (8M urea, 100mM NaH₂PO₄, 10mM Tris-HCl, pH 6.3) with 0.05% Tween-20. His-SUMO conjugates bound to the beads were finally eluted by incubation with 30µl of 1% SDS at 65°C for 10min, dried in a SpeedVac (Eppendorf) for 30min and heated at 65°C for 10min in 25µl of HU sample buffer for subsequent analysis by SDS-PAGE and immunoblotting. To control for pull-down efficiency, SUMOylated Pkg1 species were detected by Western blot analysis using an anti-Pkg1 antibody.

Co-immunoprecipitation (co-IP) of proteins from native yeast extracts

Protein-protein interactions from native yeast protein extracts were analyzed by co-IPs. In general, native extracts of yeast strains expressing C-terminally HA-/Myc-epitope-tagged proteins of interest under the control of their endogenous promoters (or an untagged version as a control) were incubated with 25µl of the respective anti-HA affinity matrix (Roche Diagnostics GmbH) or anti-MYC agarose conjugate (SIGMA-ALDRICH) for 2 hours at 4°C with head-over-tail rotation. Background binding to the beads was removed by stringent washing: 5 times with 1ml lysis buffer (PBS, 10% glycerol, 0.5% NP40, protease inhibitors) and 3 times with lysis buffer lacking detergent. After extensive washing, the beads were dried by aspiration (0.4mm needle) and bound precipitated protein complexes were eluted from the beads by incubation for 10min at 65°C in 30µl of HU sample buffer. Proteins were then resolved on NuPAGE 4%-12% gradient gels (Invitrogen), and analyzed by standard immunoblotting techniques. Western blots were quantified with ImageJ software.

Detecting protein-DNA interactions by electrophoretic mobility shift assays

N-terminally His-tagged wild-type Siz2 protein and its SAP domain mutant variants were cloned into *pET28a(+)* (Novagen), overexpressed in *E. coli* and affinity purified using Ni-NTA Agarose (Qiagen). Protein-DNA binding interactions were characterized by electrophoretic mobility shift assays (EMSA) using the Thermo Scientific LightShift Chemiluminescent EMSA Kit according to the manufacturer's instructions. Biotin-TEG 5'-end-labeled oligos were synthesized by Eurofins MWG Operon and 20 fmol were used for each binding reaction. DNA structures, representing replication forks or 3'-end ssDNA overhangs, were pre-assembled *in vitro* by first heating appropriate complementary oligos to 95°C and then slowly cooling the mix to 22°C allowing the annealing to take place.

V.4.4 Chromatin immunoprecipitation, binding and related assays

HO-endonuclease-mediated DSB induction

Strains containing the *HO* gene under the control of a *GAL* promoter (either chromosomally integrated or expressed from a centromeric *pGAL-HO* plasmid) were grown in YP-lactate, and HO expression was induced by the addition of 2% galactose. DSB formation at *MAT* locus could be monitored by real time quantitative

MATERIALS AND METHODS

PCR with primers flanking the HO-induced cut site. Time-course experiments were essentially done as described (Lee et al., 1998; Sugawara et al., 2003). Samples for ChIP and DSB repair efficiency measurements were taken at indicated time points and processed as described below.

Chromatin immunoprecipitation (ChIP)

ChIP was performed as described (Aparicio et al., 2005; Kalocsay et al., 2009). Chromatin was sheared to an average length of 300-500 bp by water bath sonication (Bioruptor UCD-200, Diagenode). Polyclonal antibodies against Rad51 (y-180) from Santa Cruz Biotechnology and the monoclonal antibody against the MYC-epitope (9E10) from SIGMA were used. Quantitative PCR was performed on a Light Cycler LC480 System (Roche) using the following primer pairs: 0.2 kb and 5.7 kb distal to the DSB $P_{+0.2}$ and $P_{+5.7}$ as described (Sugawara et al., 2003), P_{MAT} spanning the DSB (5'-gagcatattactcacagtttgctc-3', 5'-ggatagctatactgacaacattcag-3'), and control locus primers P_{MDV1} (5'-gcggtgcctggtcacaggttcatacgcac-3', 5'-tcatacggcccaaatatttacgccc-3'). Signals distal to the DSB were normalized to an unaffected control locus (MDV1) using the formula: Fold enrichment = (IP[test]/input[test])/(IP[control]/input[control]). All signals were finally normalized to 1 for the signal before HO induction to visualize protein factor recruitment after the DSB induction. The efficiency of DSB induction was measured by quantitative PCR with primers P_{MAT} spanning the break.

Real-time (RT)-PCR quantification

Quantitative real-time (RT)-PCR was performed on a Light Cycler LC480 System using the Light Cycler 480 SYBR Green I Master hot-start reaction mix (Roche Diagnostics GmbH). 18 μ l master-mix containing primers, SYBR Green I Master and H₂O was pipetted into 384-well Light Cycler plates and either 2 μ l ChIP sample (undiluted) or 2 μ l input sample (diluted 1:10) was added. Reactions were done in triplicates, and pipetting was carried out using a CAS-1200 automated PCR setup robot (Corbett Lifescience). DNA concentrations were quantified from the second derivative maximum of the Light Cycler PCR amplification curves using the input sample dilution series as a standard for each primer pair. Amplification was followed by a melting curve analysis, which served as quality control to ensure that primers were specific and only single PCR product was amplified per reaction.

Light Cycler parameters for ChIP RT-PCR (45 amplification cycles):

PCR step	T (°C)	Time
Initial denaturation	95	10 min
Denaturation	95	10 s
Annealing	55	10 s
Elongation	72	16 s
Melting curve analysis		
Cooling	4	∞

Monitoring of DSB repair kinetics by RT-PCR

The speed of HO-induced DSB repair by homologous recombination (yeast mating type switching) was monitored by quantitative real-time (RT)-PCR using the primer pair: P_A (5'-gcagcacggaatatgggact-3') and P_B (5'-atgtgaaccgcatgggcagt-3'), which prime distal to *MAT* and within *HML-Y α* (Holmes and Haber, 1999; White and Haber, 1990). RT-PCR was performed on genomic DNA samples isolated using MasterPure Yeast DNA Purification Kit from Epicentre Biotechnologies. The only difference to the ChIP RT-PCR protocol described above was that the annealing temperature for the

MATERIALS AND METHODS

P_A/P_B primer pair was 57°C. The signals were normalized to an unaffected control locus (MDV1) on chromosome X and the WT 3h time-point was set to 100%.

Chromatin fractionation

The chromatin binding assay was adapted from previously published protocols with some modifications (Liang and Stillman, 1997; Wang et al., 2009). Briefly, for large scale chromatin fractionation, native yeast protein extract was prepared from 200 OD of logarithmically growing culture by grinding the cells under liquid nitrogen in chromatin isolation buffer and subsequently cleared from cell debris by mild centrifugation (1800g, 10min, 4°C) without pelleting the chromatin fraction (verified by isolation of DNA and agarose gel electrophoresis). The resulting whole cell extract (WCE) was carefully applied on top of the 30% sucrose cushion of equal volume and centrifuged for 30min at 20000g at 4°C. The supernatant containing soluble protein fraction (SOL) was carefully collected from the top of the cushion, sucrose aspirated and the pellet containing the chromatin fraction (CHR) was either directly resuspended in HU sample buffer for subsequent SDS-PAGE and Western blot analysis, or collected for downstream assays, e.g., denaturing Ni-NTA pull-downs of chromatin enriched ^{His}SUMO conjugates. To control for chromatin fractionation efficiency, the levels of histone H3 lysine-4 tri-methylation and the ER-membrane protein Dpm1 were detected in collected fractions.

V.5 Mass Spectrometry Analyses

SILAC-based mass spectrometry

For the detection of SUMO-conjugates enriched upon MMS- and UV-light treatment stable isotope labeling with amino acids in cell culture (SILAC) was used. Yeast cells deficient in biosynthesis of lysine and arginine ($\Delta lys1 \Delta arg4$) expressing His-tagged Smt3 (^{His}SUMO) were grown for at least 10 divisions in SC media supplemented either with unlabeled (Lys0, Arg0; Light) or heavy isotope labeled amino acids (Lys8, Arg10; Heavy) from Cambridge Isotope Laboratories. Exponentially dividing cells grown in heavy media were treated with 0.2% MMS for 90 minutes, harvested and combined with equal amount of untreated cells grown in light media. Alternatively, cells grown in heavy media were UV-irradiated (80 J/m²) instead of MMS-treatment. Then, ^{His}SUMO conjugates were isolated using denaturing Ni-NTA pull-down, separated on 4-12% Bis-Tris gel, the whole lane was excised in 10 slices, proteins were digested with trypsin and analyzed by LC-MS/MS at the Core Facility of the Max Planck Institute of Biochemistry using LTQ-Orbitrap mass spectrometer. SILAC ratios for quantified proteins were plotted against the sum of the relevant peptide intensities using the GraphPad Prism version 5.0 for Mac OS X, and the proteins were colored according to values of MaxQuant Significance(B).

Detection of SUMOylation sites

For the detection of SUMOylation sites, proteins were digested with trypsin (Shevchenko et al., 1996) or thermolysin. Extracted peptides were analyzed by Orbitrap mass spectrometry (Olsen et al., 2005) and identified using MaxQuant software (Cox and Mann, 2008). The dataset was searched for peptides harboring extra masses on lysines (branched peptides) corresponding to proteolytic remnants of the C-terminal tail of SUMO. In case of trypsin digestion, extra masses corresponding to a SUMO remnant with the sequence EQIGG were expected; in case of thermolysin, with the sequence IGG.

VI. LITERATURE

- Altmannova, V., Eckert-Boulet, N., Arneric, M., Kolesar, P., Chaloupkova, R., Damborsky, J., Sung, P., Zhao, X., Lisby, M., and Krejci, L. (2010). Rad52 SUMOylation affects the efficiency of the DNA repair. *Nucleic Acids Res* 38, 4708-4721.
- Andrews, E.A., Palecek, J., Sergeant, J., Taylor, E., Lehmann, A.R., and Watts, F.Z. (2005). Nse2, a component of the Smc5-6 complex, is a SUMO ligase required for the response to DNA damage. *Mol Cell Biol* 25, 185-196.
- Aparicio, O., Geisberg, J.V., Sekinger, E., Yang, A., Moqtaderi, Z., and Struhl, K. (2005). Chromatin immunoprecipitation for determining the association of proteins with specific genomic sequences in vivo. *Curr Protoc Mol Biol Chapter 21*, Unit 21 23.
- Aravind, L., and Koonin, E.V. (2000). SAP - a putative DNA-binding motif involved in chromosomal organization. *Trends Biochem Sci* 25, 112-114.
- Armstrong, A.A., Mohideen, F., and Lima, C.D. (2012). Recognition of SUMO-modified PCNA requires tandem receptor motifs in Srs2. *Nature* 483, 59-63.
- Ausubel, F.M., Brent, R., Kingston, R. E., Moore, D. D., Seidman, J. G., Smith, J. A., Struhl, K., ed. (2001). *Current Protocols in Molecular Biology* (John Wiley & Sons, Inc.).
- Barlow, J.H., Lisby, M., and Rothstein, R. (2008). Differential regulation of the cellular response to DNA double-strand breaks in G1. *Mol Cell* 30, 73-85.
- Bartek, J., and Lukas, J. (2007). DNA damage checkpoints: from initiation to recovery or adaptation. *Curr Opin Cell Biol* 19, 238-245.
- Bergink, S., Ammon, T., Kern, M., Schermelleh, L., Leonhardt, H., and Jentsch, S. (2013). Role of Cdc48/p97 as a SUMO-targeted segregase curbing Rad51-Rad52 interaction. *Nat Cell Biol* 15, 526-532.
- Bergink, S., and Jentsch, S. (2009). Principles of ubiquitin and SUMO modifications in DNA repair. *Nature* 458, 461-467.
- Bernardi, R., and Pandolfi, P.P. (2007). Structure, dynamics and functions of promyelocytic leukaemia nuclear bodies. *Nat Rev Mol Cell Biol* 8, 1006-1016.
- Bernier-Villamor, V., Sampson, D.A., Matunis, M.J., and Lima, C.D. (2002). Structural basis for E2-mediated SUMO conjugation revealed by a complex between ubiquitin-conjugating enzyme Ubc9 and RanGAP1. *Cell* 108, 345-356.
- Bianchi, V., Pontis, E., and Reichard, P. (1986). Changes of Deoxyribonucleoside Triphosphate Pools Induced by Hydroxyurea and Their Relation to DNA-Synthesis. *J Biol Chem* 261, 6037-6042.
- Bohm, S., Lamberti, G., Fernandez-Saiz, V., Stapf, C., and Buchberger, A. (2011). Cellular functions of Ufd2 and Ufd3 in proteasomal protein degradation depend on Cdc48 binding. *Mol Cell Biol* 31, 1528-1539.
- Bonilla, C.Y., Melo, J.A., and Toczyski, D.P. (2008). Colocalization of sensors is sufficient to activate the DNA damage checkpoint in the absence of damage. *Mol Cell* 30, 267-276.
- Brandt, O., Feldner, J., Stephan, A., Schroder, M., Schnolzer, M., Arlinghaus, H.F., Hoheisel, J.D., and Jacob, A. (2003). PNA microarrays for hybridisation of unlabelled DNA samples. *Nucleic Acids Res* 31, e119.
- Branzei, D., and Foiani, M. (2008). Regulation of DNA repair throughout the cell cycle. *Nat Rev Mol Cell Biol* 9, 297-308.
- Branzei, D., Sollier, J., Liberi, G., Zhao, X., Maeda, D., Seki, M., Enomoto, T., Ohta, K., and Foiani, M. (2006). Ubc9- and mms21-mediated sumoylation counteracts recombinogenic events at damaged replication forks. *Cell* 127, 509-522.

LITERATURE

- Bruderer, R., Tatham, M.H., Plechanovova, A., Matic, I., Garg, A.K., and Hay, R.T. (2011). Purification and identification of endogenous polySUMO conjugates. *EMBO Rep* 12, 142-148.
- Bugreev, D.V., Mazina, O.M., and Mazin, A.V. (2006). Rad54 protein promotes branch migration of Holliday junctions. *Nature* 442, 590-593.
- Capili, A.D., and Lima, C.D. (2007). Taking it step by step: mechanistic insights from structural studies of ubiquitin/ubiquitin-like protein modification pathways. *Curr Opin Struct Biol* 17, 726-735.
- Cejka, P., Plank, J.L., Bachrati, C.Z., Hickson, I.D., and Kowalczykowski, S.C. (2010). Rmi1 stimulates decatenation of double Holliday junctions during dissolution by Sgs1-Top3. *Nat Struct Mol Biol* 17, 1377-1382.
- Chapman, J.R., Taylor, M.R.G., and Boulton, S.J. (2012). Playing the End Game: DNA Double-Strand Break Repair Pathway Choice. *Mol Cell* 47, 497-510.
- Chen, H., Lisby, M., and Symington, L.S. (2013). RPA Coordinates DNA End Resection and Prevents Formation of DNA Hairpins. *Mol Cell* 50, 589-600.
- Chen, Z.C., Yang, H.J., and Pavletich, N.P. (2008). Mechanism of homologous recombination from the RecA-ssDNA/dsDNA structures. *Nature* 453, 489-U483.
- Cheng, C.H., Lo, Y.H., Liang, S.S., Ti, S.C., Lin, F.M., Yeh, C.H., Huang, H.Y., and Wang, T.F. (2006). SUMO modifications control assembly of synaptonemal complex and polycomplex in meiosis of *Saccharomyces cerevisiae*. *Genes Dev* 20, 2067-2081.
- Choi, J.H., Lindsey-Boltz, L.A., Kemp, M., Mason, A.C., Wold, M.S., and Sancar, A. (2010). Reconstitution of RPA-covered single-stranded DNA-activated ATR-Chk1 signaling. *Proc Natl Acad Sci USA* 107, 13660-13665.
- Connolly, B., White, C.I., and Haber, J.E. (1988). Physical monitoring of mating type switching in *Saccharomyces cerevisiae*. *Mol Cell Biol* 8, 2342-2349.
- Cook, C.E., Hochstrasser, M., and Kerscher, O. (2009). The SUMO-targeted ubiquitin ligase subunit Slx5 resides in nuclear foci and at sites of DNA breaks. *Cell Cycle* 8, 1080-1089.
- Cox, J., and Mann, M. (2008). MaxQuant enables high peptide identification rates, individualized p.p.b.-range mass accuracies and proteome-wide protein quantification. *Nat Biotechnol* 26, 1367-1372.
- Cremona, C.A., Sarangi, P., Yang, Y., Hang, L.E., Rahman, S., and Zhao, X. (2012). Extensive DNA damage-induced sumoylation contributes to replication and repair and acts in addition to the mec1 checkpoint. *Mol Cell* 45, 422-432.
- Daley, J.M., Palmbo, P.L., Wu, D.L., and Wilson, T.E. (2005). Nonhomologous end joining in yeast. *Annu Rev Genet* 39, 431-451.
- Dantuma, N.P., and Hoppe, T. (2012). Growing sphere of influence: Cdc48/p97 orchestrates ubiquitin-dependent extraction from chromatin. *Trends Cell Biol* 22, 483-491.
- Davis, A.P., and Symington, L.S. (2003). The Rad52-Rad59 complex interacts with Rad51 and replication protein A. *DNA Repair* 2, 1127-1134.
- de Carvalho, C.E., and Colaiacovo, M.P. (2006). SUMO-mediated regulation of synaptonemal complex formation during meiosis. *Genes Dev* 20, 1986-1992.
- de Laat, W.L., Jaspers, N.G.J., and Hoeijmakers, J.H.J. (1999). Molecular mechanism of nucleotide excision repair. *Genes Dev* 13, 768-785.
- Desterro, J.M., Rodriguez, M.S., and Hay, R.T. (1998). SUMO-1 modification of I κ B α inhibits NF- κ B activation. *Mol Cell* 2, 233-239.
- Dikic, I., Wakatsuki, S., and Walters, K.J. (2009). Ubiquitin-binding domains - from structures to functions. *Nat Rev Mol Cell Biol* 10, 659-671.

LITERATURE

- Dou, H., Huang, C., Singh, M., Carpenter, P.B., and Yeh, E.T.H. (2010). Regulation of DNA repair through deSUMOylation and SUMOylation of replication protein A complex. *Mol Cell* 39, 333-345.
- Dou, H., Huang, C., Van Nguyen, T., Lu, L.S., and Yeh, E.T. (2011). SUMOylation and deSUMOylation in response to DNA damage. *FEBS Lett* 585, 2891-2896.
- Downs, J.A., Lowndes, N.F., and Jackson, S.P. (2000). A role for *Saccharomyces cerevisiae* histone H2A in DNA repair. *Nature* 408, 1001-1004.
- Eichinger, C.S., and Jentsch, S. (2010). Synaptonemal complex formation and meiotic checkpoint signaling are linked to the lateral element protein Red1. *Proc Natl Acad Sci USA* 107, 11370-11375.
- Emili, A. (1998). MEC1-dependent phosphorylation of Rad9p in response to DNA damage. *Mol Cell* 2, 183-189.
- Felberbaum, R., and Hochstrasser, M. (2008). Ulp2 and the DNA damage response: desumoylation enables safe passage through mitosis. *Cell Cycle* 7, 52-56.
- Ferreira, H.C., Luke, B., Schober, H., Kalck, V., Lingner, J., and Gasser, S.M. (2011). The PIAS homologue Siz2 regulates perinuclear telomere position and telomerase activity in budding yeast. *Nat Cell Biol* 13, 867-874.
- Filippo, J.S., Sung, P., and Klein, H. (2008). Mechanism of eukaryotic homologous recombination. *Annu Rev Biochem* 77, 229-257.
- Finkbeiner, E., Haindl, M., and Muller, S. (2011a). The SUMO system controls nucleolar partitioning of a novel mammalian ribosome biogenesis complex. *EMBO J* 30, 1067-1078.
- Finkbeiner, E., Haindl, M., Raman, N., and Muller, S. (2011b). SUMO routes ribosome maturation. *Nucleus* 2, 527-532.
- Finley, D. (2009). Recognition and processing of ubiquitin-protein conjugates by the proteasome. *Annu Rev Biochem* 78, 477-513.
- Freemont, P.S. (2000). Ubiquitination: RING for destruction? *Curr Biol* 10, R84-R87.
- Galanty, Y., Belotserkovskaya, R., Coates, J., and Jackson, S.P. (2012). RNF4, a SUMO-targeted ubiquitin E3 ligase, promotes DNA double-strand break repair. *Genes Dev* 26, 1179-1195.
- Galanty, Y., Belotserkovskaya, R., Coates, J., Polo, S., Miller, K.M., and Jackson, S.P. (2009). Mammalian SUMO E3-ligases PIAS1 and PIAS4 promote responses to DNA double-strand breaks. *Nature* 462, 935-939.
- Gareau, J.R., and Lima, C.D. (2010). The SUMO pathway: emerging mechanisms that shape specificity, conjugation and recognition. *Nat Rev Mol Cell Biol* 11, 861-871.
- Garvik, B., Carson, M., and Hartwell, L. (1995). Single-stranded DNA arising at telomeres in *cdc13* mutants may constitute a specific signal for the RAD9 checkpoint. *Mol Cell Biol* 15, 6128-6138.
- Geiss-Friedlander, R., and Melchior, F. (2007). Concepts in sumoylation: a decade on. *Nat Rev Mol Cell Biol* 8, 947-956.
- Gellert, M. (1992). V(D)J Recombination Gets a Break. *Trends Genet* 8, 408-412.
- Geoffroy, M.C., and Hay, R.T. (2009). An additional role for SUMO in ubiquitin-mediated proteolysis. *Nat Rev Mol Cell Biol* 10, 564-568.
- Giannattasio, M., Follonier, C., Tourriere, H., Puddu, F., Lazzaro, F., Pasero, P., Lopes, M., Plevani, P., and Muzi-Falconi, M. (2010). Exo1 competes with repair synthesis, converts NER intermediates to long ssDNA gaps, and promotes checkpoint activation. *Mol Cell* 40, 50-62.

LITERATURE

- Gietz, R.D., and Sugino, A. (1988). New yeast-*Escherichia coli* shuttle vectors constructed with in vitro mutagenized yeast genes lacking six-base pair restriction sites. *Gene* 74, 527-534.
- Gilbert, C.S., Green, C.M., and Lowndes, N.F. (2001). Budding yeast Rad9 is an ATP-dependent Rad53 activating machine. *Mol Cell* 8, 129-136.
- Gravel, S., Chapman, J.R., Magill, C., and Jackson, S.P. (2008). DNA helicases Sgs1 and BLM promote DNA double-strand break resection. *Genes Dev* 22, 2767-2772.
- Guzzo, C.M., Berndsen, C.E., Zhu, J., Gupta, V., Datta, A., Greenberg, R.A., Wolberger, C., and Matunis, M.J. (2012). RNF4-dependent hybrid SUMO-ubiquitin chains are signals for RAP80 and thereby mediate the recruitment of BRCA1 to sites of DNA damage. *Sci Signal* 5, ra88.
- Haber, J.E. (1999). DNA recombination: the replication connection. *Trends Biochem Sci* 24, 271-275.
- Haindl, M., Harasim, T., Eick, D., and Muller, S. (2008). The nucleolar SUMO-specific protease SENP3 reverses SUMO modification of nucleophosmin and is required for rRNA processing. *EMBO Rep* 9, 273-279.
- Hang, L.E., Liu, X., Cheung, I., Yang, Y., and Zhao, X. (2011). SUMOylation regulates telomere length homeostasis by targeting Cdc13. *Nat Struct Mol Biol* 18, 920-926.
- Harper, J.W., and Elledge, S.J. (2007). The DNA damage response: Ten years after. *Mol Cell* 28, 739-745.
- Hershko, A., and Ciechanover, A. (1998). The ubiquitin system. *Annu Rev Biochem* 67, 425-479.
- Heun, P. (2007). SUMO organization of the nucleus. *Curr Opin Cell Biol* 19, 350-355.
- Hickey, C.M., Wilson, N.R., and Hochstrasser, M. (2012). Function and regulation of SUMO proteases. *Nat Rev Mol Cell Biol* 13, 755-766.
- Ho, J.C., Warr, N.J., Shimizu, H., and Watts, F.Z. (2001). SUMO modification of Rad22, the *Schizosaccharomyces pombe* homologue of the recombination protein Rad52. *Nucleic Acids Res* 29, 4179-4186.
- Hochstrasser, M. (2001). SP-RING for SUMO: new functions bloom for a ubiquitin-like protein. *Cell* 107, 5-8.
- Hoege, C., Pfander, B., Moldovan, G.L., Pyrowolakis, G., and Jentsch, S. (2002). RAD6-dependent DNA repair is linked to modification of PCNA by ubiquitin and SUMO. *Nature* 419, 135-141.
- Hoeijmakers, J.H. (2001). Genome maintenance mechanisms for preventing cancer. *Nature* 411, 366-374.
- Holmes, A., and Haber, J.E. (1999). Physical monitoring of HO-induced homologous recombination. *Methods Mol Biol* 113, 403-415.
- Hopfner, K.P., Craig, L., Moncalian, G., Zinkel, R.A., Usui, T., Owen, B.A., Karcher, A., Henderson, B., Bodmer, J.L., McMurray, C.T., *et al.* (2002). The Rad50 zinc-hook is a structure joining Mre11 complexes in DNA recombination and repair. *Nature* 418, 562-566.
- Husnjak, K., and Dikic, I. (2012). Ubiquitin-Binding Proteins: Decoders of Ubiquitin-Mediated Cellular Functions. *Annu Rev Biochem* 81, 291-322.
- Ira, G., Malkova, A., Liberi, G., Foiani, M., and Haber, J.E. (2003). Srs2 and Sgs1-Top3 suppress crossovers during double-strand break repair in yeast. *Cell* 115, 401-411.
- Ivanov, E.L., Sugawara, N., White, C.I., Fabre, F., and Haber, J.E. (1994). Mutations in XRS2 and RAD50 delay but do not prevent mating-type switching in *Saccharomyces cerevisiae*. *Mol Cell Biol* 14, 3414-3425.

LITERATURE

- Jackson, S.P., and Bartek, J. (2009). The DNA-damage response in human biology and disease. *Nature* *461*, 1071-1078.
- Jackson, S.P., and Durocher, D. (2013). Regulation of DNA Damage Responses by Ubiquitin and SUMO. *Mol Cell* *49*, 795-807.
- Jakobs, A., Koehnke, J., Himstedt, F., Funk, M., Korn, B., Gaestel, M., and Niedenthal, R. (2007). Ubc9 fusion-directed SUMOylation (UFDS): a method to analyze function of protein SUMOylation. *Nat Methods* *4*, 245-250.
- James, P., Halladay, J., and Craig, E.A. (1996). Genomic libraries and a host strain designed for highly efficient two-hybrid selection in yeast. *Genetics* *144*, 1425-1436.
- Janke, C., Magiera, M.M., Rathfelder, N., Taxis, C., Reber, S., Maekawa, H., Moreno-Borchart, A., Doenges, G., Schwob, E., Schiebel, E., *et al.* (2004). A versatile toolbox for PCR-based tagging of yeast genes: new fluorescent proteins, more markers and promoter substitution cassettes. *Yeast* *21*, 947-962.
- Jentsch, S. (1992). The ubiquitin-conjugation system. *Annu Rev Genet* *26*, 179-207.
- Jentsch, S., and Rumpf, S. (2007). Cdc48 (p97): a "molecular gearbox" in the ubiquitin pathway? *Trends Biochem Sci* *32*, 6-11.
- Johnson, E.S. (2004). Protein modification by sumo. *Annu Rev Biochem* *73*, 355-382.
- Johnson, E.S., and Blobel, G. (1997). Ubc9p is the conjugating enzyme for the ubiquitin-like protein Smt3p. *J Biol Chem* *272*, 26799-26802.
- Johnson, E.S., and Blobel, G. (1999). Cell cycle-regulated attachment of the ubiquitin-related protein SUMO to the yeast septins. *J Cell Biol* *147*, 981-994.
- Johnson, E.S., and Gupta, A.A. (2001). An E3-like factor that promotes SUMO conjugation to the yeast septins. *Cell* *106*, 735-744.
- Johnson, E.S., Schwienhorst, I., Dohmen, R.J., and Blobel, G. (1997). The ubiquitin-like protein Smt3p is activated for conjugation to other proteins by an Aos1p/Uba2p heterodimer. *EMBO J* *16*, 5509-5519.
- Kalocsay, M., Hiller, N.J., and Jentsch, S. (2009). Chromosome-wide Rad51 spreading and SUMO-H2A.Z-dependent chromosome fixation in response to a persistent DNA double-strand break. *Mol Cell* *33*, 335-343.
- Karras, G.I., and Jentsch, S. (2010). The RAD6 DNA damage tolerance pathway operates uncoupled from the replication fork and is functional beyond S phase. *Cell* *141*, 255-267.
- Keeney, S., Giroux, C.N., and Kleckner, N. (1997). Meiosis-specific DNA double-strand breaks are catalyzed by Spo11, a member of a widely conserved protein family. *Cell* *88*, 375-384.
- Kerscher, O. (2007). SUMO junction-what's your function? New insights through SUMO-interacting motifs. *EMBO Rep* *8*, 550-555.
- Kerscher, O., Felberbaum, R., and Hochstrasser, M. (2006). Modification of proteins by ubiquitin and ubiquitin-like proteins. *Annu Rev Cell Dev Biol* *22*, 159-180.
- Klein, U.R., Haindl, M., Nigg, E.A., and Muller, S. (2009). RanBP2 and SENP3 function in a mitotic SUMO2/3 conjugation-deconjugation cycle on Borealin. *Mol Biol Cell* *20*, 410-418.
- Knop, M., Siegers, K., Pereira, G., Zachariae, W., Winsor, B., Nasmyth, K., and Schiebel, E. (1999). Epitope tagging of yeast genes using a PCR-based strategy: more tags and improved practical routines. *Yeast* *15*, 963-972.
- Koegl, M., Hoppe, T., Schlenker, S., Ulrich, H.D., Mayer, T.U., and Jentsch, S. (1999). A novel ubiquitination factor, E4, is involved in multiubiquitin chain assembly. *Cell* *96*, 635-644.
- Kolli, N., Mikolajczyk, J., Drag, M., Mukhopadhyay, D., Moffatt, N., Dasso, M., Salvesen, G., and Wilkinson, K.D. (2010). Distribution and paralogue specificity of mammalian deSUMOylating enzymes. *Biochem J* *430*, 335-344.

LITERATURE

- Komander, D., and Rape, M. (2012). The Ubiquitin Code. *Annu Rev Biochem* 81, 203-229.
- Kroetz, M.B., Su, D., and Hochstrasser, M. (2009). Essential role of nuclear localization for yeast Ulp2 SUMO protease function. *Mol Biol Cell* 20, 2196-2206.
- Kulathu, Y., and Komander, D. (2012). Atypical ubiquitylation - the unexplored world of polyubiquitin beyond Lys48 and Lys63 linkages. *Nat Rev Mol Cell Biol* 13, 508-523.
- Lallemand-Breitenbach, V., Jeanne, M., Benhenda, S., Nasr, R., Lei, M., Peres, L., Zhou, J., Zhu, J., Raught, B., and de The, H. (2008). Arsenic degrades PML or PML-RARalpha through a SUMO-triggered RNF4/ubiquitin-mediated pathway. *Nat Cell Biol* 10, 547-555.
- Lee, J.H., and Paull, T.T. (2005). ATM activation by DNA double-strand breaks through the Mre11-Rad50-Nbs1 complex. *Science* 308, 551-554.
- Lee, M.T., Bakir, A.A., Nguyen, K.N., and Bachant, J. (2011). The SUMO Isopeptidase Ulp2p Is Required to Prevent Recombination-Induced Chromosome Segregation Lethality following DNA Replication Stress. *Plos Genet* 7, e1001355.
- Lee, S.E., Moore, J.K., Holmes, A., Umezu, K., Kolodner, R.D., and Haber, J.E. (1998). *Saccharomyces* Ku70, mre11/rad50 and RPA proteins regulate adaptation to G2/M arrest after DNA damage. *Cell* 94, 399-409.
- Li, S.J., and Hochstrasser, M. (2000). The yeast ULP2 (SMT4) gene encodes a novel protease specific for the ubiquitin-like Smt3 protein. *Mol Cell Biol* 20, 2367-2377.
- Li, S.J., and Hochstrasser, M. (2003). The Ulp1 SUMO isopeptidase: distinct domains required for viability, nuclear envelope localization, and substrate specificity. *J Cell Biol* 160, 1069-1082.
- Li, X., Stith, C.M., Burgers, P.M., and Heyer, W.D. (2009). PCNA Is Required for Initiation of Recombination-Associated DNA Synthesis by DNA Polymerase delta. *Mol Cell* 36, 704-713.
- Liang, C., and Stillman, B. (1997). Persistent initiation of DNA replication and chromatin-bound MCM proteins during the cell cycle in *cdc6* mutants. *Genes Dev* 11, 3375-3386.
- Lin, D.Y., Huang, Y.S., Jeng, J.C., Kuo, H.Y., Chang, C.C., Chao, T.T., Ho, C.C., Chen, Y.C., Lin, T.P., Fang, H.I., *et al.* (2006). Role of SUMO-interacting motif in Daxx SUMO modification, subnuclear localization, and repression of sumoylated transcription factors. *Mol Cell* 24, 341-354.
- Lin, X., Sun, B.H., Liang, M., Liang, Y.Y., Gast, A., Hildebrand, J., Brunicardi, F.C., Melchior, F., and Feng, X.H. (2003). Opposed regulation of corepressor CtBP by SUMOylation and PDZ binding. *Mol Cell* 11, 1389-1396.
- Lisby, M., Barlow, J.H., Burgess, R.C., and Rothstein, R. (2004). Choreography of the DNA damage response: spatiotemporal relationships among checkpoint and repair proteins. *Cell* 118, 699-713.
- Liu, J., Renault, L., Veaute, X., Fabre, F., Stahlberg, H., and Heyer, W.D. (2011). Rad51 paralogues Rad55-Rad57 balance the antirecombinase Srs2 in Rad51 filament formation. *Nature* 479, 245-248.
- Lois, L.M., and Lima, C.D. (2005). Structures of the SUMO E1 provide mechanistic insights into SUMO activation and E2 recruitment to E1. *EMBO J* 24, 439-451.
- Longtine, M.S., McKenzie, A., 3rd, Demarini, D.J., Shah, N.G., Wach, A., Brachat, A., Philippsen, P., and Pringle, J.R. (1998). Additional modules for versatile and economical PCR-based gene deletion and modification in *Saccharomyces cerevisiae*. *Yeast* 14, 953-961.
- Lopes, M., Cotta-Ramusino, C., Pelliccioli, A., Liberi, G., Plevani, P., Muzi-Falconi, M., Newlon, C.S., and Foiani, M. (2001). The DNA replication checkpoint response stabilizes stalled replication forks. *Nature* 412, 557-561.
- Lukas, J., Lukas, C., and Bartek, J. (2011). More than just a focus: The chromatin response to DNA damage and its role in genome integrity maintenance. *Nat Cell Biol* 13, 1161-1169.

LITERATURE

- Luo, K., Zhang, H., Wang, L., Yuan, J., and Lou, Z. (2012). Sumoylation of MDC1 is important for proper DNA damage response. *EMBO J* 31, 3008-3019.
- Maeda, D., Seki, M., Onoda, F.T., Branzei, D., Kawabe, Y., and Enomoto, T. (2004). Ubc9 is required for damage-tolerance and damage-induced interchromosomal homologous recombination in *S. cerevisiae*. *DNA Repair* 3, 335-341.
- Majka, J., Binz, S.K., Wold, M.S., and Burgers, P.M. (2006). Replication protein A directs loading of the DNA damage checkpoint clamp to 5'-DNA junctions. *J Biol Chem* 281, 27855-27861.
- Makhnevych, T., Ptak, C., Lusk, C.P., Aitchison, J.D., and Wozniak, R.W. (2007). The role of karyopherins in the regulated sumoylation of septins. *J Cell Biol* 177, 39-49.
- Mann, M. (2006). Functional and quantitative proteomics using SILAC. *Nat Rev Mol Cell Biol* 7, 952-958.
- Matic, I., Schimmel, J., Hendriks, I.A., van Santen, M.A., van de Rijke, F., van Dam, H., Gnad, F., Mann, M., and Vertegaal, A.C.O. (2010). Site-Specific Identification of SUMO-2 Targets in Cells Reveals an Inverted SUMOylation Motif and a Hydrophobic Cluster SUMOylation Motif. *Mol Cell* 39, 641-652.
- Matsuoka, S., Ballif, B.A., Smogorzewska, A., McDonald, E.R., Hurov, K.E., Luo, J., Bakalarski, C.E., Zhao, Z.M., Solimini, N., Lerenthal, Y., *et al.* (2007). ATM and ATR substrate analysis reveals extensive protein networks responsive to DNA damage. *Science* 316, 1160-1166.
- Mazin, A.V., Mazina, O.M., Bugreev, D.V., and Rossi, M.J. (2010). Rad54, the motor of homologous recombination. *DNA Repair (Amst)* 9, 286-302.
- Mazon, G., Mimitou, E.P., and Symington, L.S. (2010). SnapShot: Homologous Recombination in DNA Double-Strand Break Repair. *Cell* 142.
- Meister, P., Taddei, A., Vernis, L., Poidevin, M., Gasser, S.M., and Baldacci, G. (2005). Temporal separation of replication and recombination requires the intra-S checkpoint. *J Cell Biol* 168, 537-544.
- Mimitou, E.P., and Symington, L.S. (2008). Sae2, Exo1 and Sgs1 collaborate in DNA double-strand break processing. *Nature* 455, 770-774.
- Mimitou, E.P., and Symington, L.S. (2011). DNA end resection-Unraveling the tail. *DNA Repair* 10, 344-348.
- Minty, A., Dumont, X., Kaghad, M., and Caput, D. (2000). Covalent modification of p73alpha by SUMO-1. Two-hybrid screening with p73 identifies novel SUMO-1-interacting proteins and a SUMO-1 interaction motif. *J Biol Chem* 275, 36316-36323.
- Mohideen, F., Capili, A.D., Bilimoria, P.M., Yamada, T., Bonni, A., and Lima, C.D. (2009). A molecular basis for phosphorylation-dependent SUMO conjugation by the E2 UBC9. *Nat Struct Mol Biol* 16, 945-952.
- Moldovan, G.L., Pfander, B., and Jentsch, S. (2006). PCNA controls establishment of sister chromatid cohesion during S phase. *Mol Cell* 23, 723-732.
- Moldovan, G.L., Pfander, B., and Jentsch, S. (2007). PCNA, the maestro of the replication fork. *Cell* 129, 665-679.
- Morin, I., Ngo, H.P., Greenall, A., Zubko, M.K., Morrice, N., and Lydall, D. (2008). Checkpoint-dependent phosphorylation of Exo1 modulates the DNA damage response. *EMBO J* 27, 2400-2410.
- Morris, J.R., Boutell, C., Keppler, M., Densham, R., Weekes, D., Alamshah, A., Butler, L., Galanty, Y., Pangon, L., Kiuchi, T., *et al.* (2009). The SUMO modification pathway is involved in the BRCA1 response to genotoxic stress. *Nature* 462, 886-890.
- Nagai, S., Davoodi, N., and Gasser, S.M. (2011). Nuclear organization in genome stability: SUMO connections. *Cell Res* 21, 474-485.

LITERATURE

- Nagai, S., Dubrana, K., Tsai-Pflugfelder, M., Davidson, M.B., Roberts, T.M., Brown, G.W., Varela, E., Hediger, F., Gasser, S.M., and Krogan, N.J. (2008). Functional targeting of DNA damage to a nuclear pore-associated SUMO-dependent ubiquitin ligase. *Science* 322, 597-602.
- Naiki, T., Wakayama, T., Nakada, D., Matsumoto, K., and Sugimoto, K. (2004). Association of Rad9 with double-strand breaks through a Mec1-dependent mechanism. *Mol Cell Biol* 24, 3277-3285.
- Namanja, A.T., Li, Y.J., Su, Y., Wong, S., Lu, J.J., Colson, L.T., Wu, C.G., Li, S.S.C., and Chen, Y. (2012). Insights into High Affinity Small Ubiquitin-like Modifier (SUMO) Recognition by SUMO-interacting Motifs (SIMs) Revealed by a Combination of NMR and Peptide Array Analysis. *J Biol Chem* 287, 3231-3240.
- Nicolette, M.L., Lee, K., Guo, Z., Rani, M., Chow, J.M., Lee, S.E., and Paull, T.T. (2010). Mre11-Rad50-Xrs2 and Sae2 promote 5' strand resection of DNA double-strand breaks. *Nat Struct Mol Biol* 17, 1478-1485.
- Nie, M., Aslanian, A., Prudden, J., Heideker, J., Vashisht, A.A., Wohlschlegel, J.A., Yates, J.R., 3rd, and Boddy, M.N. (2012). Dual recruitment of Cdc48 (p97)-Ufd1-Npl4 ubiquitin-selective segregase by small ubiquitin-like modifier protein (SUMO) and ubiquitin in SUMO-targeted ubiquitin ligase-mediated genome stability functions. *J Biol Chem* 287, 29610-29619.
- Ohuchi, T., Seki, M., Branzei, D., Maeda, D., Ui, A., Ogiwara, H., Tada, S., and Enomoto, T. (2008). Rad52 sumoylation and its involvement in the efficient induction of homologous recombination. *DNA Repair* 7, 879-889.
- Ohuchi, T., Seki, M., Kugou, K., Tada, S., Ohta, K., and Enomoto, T. (2009). Accumulation of sumoylated Rad52 in checkpoint mutants perturbed in DNA replication. *DNA Repair* 8, 690-696.
- Olsen, J.V., de Godoy, L.M.F., Li, G.Q., Macek, B., Mortensen, P., Pesch, R., Makarov, A., Lange, O., Horning, S., and Mann, M. (2005). Parts per million mass accuracy on an orbitrap mass spectrometer via lock mass injection into a C-trap. *Mol Cell Proteomics* 4, 2010-2021.
- Ong, S.E., Blagoev, B., Kratchmarova, I., Kristensen, D.B., Steen, H., Pandey, A., and Mann, M. (2002). Stable isotope labeling by amino acids in cell culture, SILAC, as a simple and accurate approach to expression proteomics. *Mol Cell Proteomics* 1, 376-386.
- Palvimo, J.J. (2007). PIAS proteins as regulators of small ubiquitin-related modifier (SUMO) modifications and transcription. *Biochem Soc Trans* 35, 1405-1408.
- Panse, V.G., Kressler, D., Pauli, A., Petfalski, E., Gnadig, M., Tollervey, D., and Hurt, E. (2006). Formation and nuclear export of preribosomes are functionally linked to the small-ubiquitin-related modifier pathway. *Traffic* 7, 1311-1321.
- Papouli, E., Chen, S., Davies, A.A., Huttner, D., Krejci, L., Sung, P., and Ulrich, H.D. (2005). Crosstalk between SUMO and ubiquitin on PCNA is mediated by recruitment of the helicase Srs2p. *Mol Cell* 19, 123-133.
- Parker, J.L., and Ulrich, H.D. (2012). A SUMO-interacting motif activates budding yeast ubiquitin ligase Rad18 towards SUMO-modified PCNA. *Nucleic Acids Res* 40, 11380-11388.
- Parrilla-Castellar, E.R., Arlander, S.J., and Karnitz, L. (2004). Dial 9-1-1 for DNA damage: the Rad9-Hus1-Rad1 (9-1-1) clamp complex. *DNA Repair (Amst)* 3, 1009-1014.
- Perry, J.J., Tainer, J.A., and Boddy, M.N. (2008). A SIM-ultaneous role for SUMO and ubiquitin. *Trends Biochem Sci* 33, 201-208.
- Petukhova, G., Stratton, S., and Sung, P. (1998). Catalysis of homologous DNA pairing by yeast Rad51 and Rad54 proteins. *Nature* 393, 91-94.
- Pfander, B., Moldovan, G.L., Sacher, M., Hoege, C., and Jentsch, S. (2005). SUMO-modified PCNA recruits Srs2 to prevent recombination during S phase. *Nature* 436, 428-433.

LITERATURE

- Pfeiffer, P., Goedecke, W., and Obe, G. (2000). Mechanisms of DNA double-strand break repair and their potential to induce chromosomal aberrations. *Mutagenesis* 15, 289-302.
- Pfleger, C.M., and Kirschner, M.W. (2000). The KEN box: an APC recognition signal distinct from the D box targeted by Cdh1. *Genes Dev* 14, 655-665.
- Pichler, A., Knipscheer, P., Oberhofer, E., van Dijk, W.J., Korner, R., Olsen, J.V., Jentsch, S., Melchior, F., and Sixma, T.K. (2005). SUMO modification of the ubiquitin-conjugating enzyme E2-25K. *Nature Struct Mol Biol* 12, 264-269.
- Potts, P.R. (2009). The Yin and Yang of the MMS21-SMC5/6 SUMO ligase complex in homologous recombination. *DNA Repair (Amst)* 8, 499-506.
- Potts, P.R., and Yu, H. (2005). Human MMS21/NSE2 is a SUMO ligase required for DNA repair. *Mol Cell Biol* 25, 7021-7032.
- Potts, P.R., and Yu, H. (2007). The SMC5/6 complex maintains telomere length in ALT cancer cells through SUMOylation of telomere-binding proteins. *Nat Struct Mol Biol* 14, 581-590.
- Praefcke, G.J., Hofmann, K., and Dohmen, R.J. (2012). SUMO playing tag with ubiquitin. *Trends Biochem Sci* 37, 23-31.
- Prakash, R., Satory, D., Dray, E., Papusha, A., Scheller, J., Kramer, W., Krejci, L., Klein, H., Haber, J.E., Sung, P., *et al.* (2009). Yeast Mph1 helicase dissociates Rad51-made D-loops: implications for crossover control in mitotic recombination. *Genes Dev* 23, 67-79.
- Prudden, J., Pebernard, S., Raffa, G., Slavin, D.A., Perry, J.J., Tainer, J.A., McGowan, C.H., and Boddy, M.N. (2007). SUMO-targeted ubiquitin ligases in genome stability. *EMBO J* 26, 4089-4101.
- Rape, M., Hoppe, T., Gorr, I., Kalocay, M., Richly, H., and Jentsch, S. (2001). Mobilization of processed, membrane-tethered SPT23 transcription factor by CDC48(UFD1/NPL4), a ubiquitin-selective chaperone. *Cell* 107, 667-677.
- Reindle, A., Belichenko, I., Bylebyl, G.R., Chen, X.L., Gandhi, N., and Johnson, E.S. (2006). Multiple domains in Siz SUMO ligases contribute to substrate selectivity. *J Cell Sci* 119, 4749-4757.
- Renkawitz, J., Lademann, C.A., Kalocsay, M., and Jentsch, S. (2013). Monitoring Homology Search during DNA Double-Strand Break Repair In Vivo. *Mol Cell* 50, 261-272.
- Richly, H., Rape, M., Braun, S., Rumpf, S., Hoege, C., and Jentsch, S. (2005). A series of ubiquitin binding factors connects CDC48/p97 to substrate multiubiquitylation and proteasomal targeting. *Cell* 120, 73-84.
- Rodriguez, M.S., Dargemont, C., and Hay, R.T. (2001). SUMO-1 conjugation in vivo requires both a consensus modification motif and nuclear targeting. *J Biol Chem* 276, 12654-12659.
- Rotin, D., and Kumar, S. (2009). Physiological functions of the HECT family of ubiquitin ligases. *Nat Rev Mol Cell Biol* 10, 398-409.
- Rouse, J., and Jackson, S.P. (2002). Lcd1p recruits Mec1p to DNA lesions in vitro and in vivo. *Mol Cell* 9, 857-869.
- Sacher, M., Pfander, B., Hoege, C., and Jentsch, S. (2006). Control of Rad52 recombination activity by double-strand break-induced SUMO modification. *Nat Cell Biol* 8, 1284-1290.
- Sacher, M., Pfander, B., and Jentsch, S. (2005). Identification of SUMO-protein conjugates. *Methods Enzymol* 399, 392-404.
- Sambrook, J., and Russell, D.W. (2001). *Molecular cloning : a laboratory manual*, 3rd edn (Cold Spring Harbor, N.Y., Cold Spring Harbor Laboratory Press).
- Sampson, D.A., Wang, M., and Matunis, M.J. (2001). The small ubiquitin-like modifier-1 (SUMO-1) consensus sequence mediates Ubc9 binding and is essential for SUMO-1 modification. *J Biol Chem* 276, 21664-21669.

LITERATURE

- Sancar, A., Lindsey-Boltz, L.A., Unsal-Kacmaz, K., and Linn, S. (2004). Molecular mechanisms of mammalian DNA repair and the DNA damage checkpoints. *Annu Rev Biochem* 73, 39-85.
- Scherer, S., and Davis, R.W. (1979). Replacement of chromosome segments with altered DNA sequences constructed in vitro. *Proc Natl Acad Sci USA* 76, 4951-4955.
- Schiestl, R.H., and Wintersberger, U. (1992). DNA Damage Induced Mating Type Switching in *Saccharomyces-Cerevisiae*. *Mutat Res* 284, 111-123.
- Shalizi, A., Gaudilliere, B., Yuan, Z., Stegmuller, J., Shirogane, T., Ge, Q., Tan, Y., Schulman, B., Harper, J.W., and Bonni, A. (2006). A calcium-regulated MEF2 sumoylation switch controls postsynaptic differentiation. *Science* 311, 1012-1017.
- Shen, T.H., Lin, H.K., Scaglioni, P.P., Yung, T.M., and Pandolfi, P.P. (2006). The mechanisms of PML-nuclear body formation. *Mol Cell* 24, 331-339.
- Shevchenko, A., Jensen, O.N., Podtelejnikov, A.V., Sagliocco, F., Wilm, M., Vorm, O., Mortensen, P., Boucherie, H., and Mann, M. (1996). Linking genome and proteome by mass spectrometry: large-scale identification of yeast proteins from two dimensional gels. *Proc Natl Acad Sci U S A* 93, 14440-14445.
- Silver, H.R., Nissley, J.A., Reed, S.H., Hou, Y.M., and Johnson, E.S. (2011). A role for SUMO in nucleotide excision repair. *DNA Repair* 10, 1243-1251.
- Song, J., Durrin, L.K., Wilkinson, T.A., Krontiris, T.G., and Chen, Y. (2004). Identification of a SUMO-binding motif that recognizes SUMO-modified proteins. *Proc Natl Acad Sci USA* 101, 14373-14378.
- Srikumar, T., Lewicki, M.C., Costanzo, M., Tkach, J.M., van Bakel, H., Tsui, K., Johnson, E.S., Brown, G.W., Andrews, B.J., Boone, C., *et al.* (2013). Global analysis of SUMO chain function reveals multiple roles in chromatin regulation. *J Cell Biol* 201, 145-163.
- Stankovic-Valentin, N., Deltour, S., Seeler, J., Pinte, S., Vergoten, G., Guerardel, C., Dejean, A., and Leprince, D. (2007). An acetylation/deacetylation-SUMOylation switch through a phylogenetically conserved psi KXEP motif in the tumor suppressor HIC1 regulates transcriptional repression activity. *Mol Cell Biol* 27, 2661-2675.
- Steinacher, R., and Schär, P. (2005). Functionality of human thymine DNA glycosylase requires SUMO-regulated changes in protein conformation. *Curr Biol* 15, 616-623.
- Stracker, T.H., and Petrini, J.H. (2011). The MRE11 complex: starting from the ends. *Nat Rev Mol Cell Biol* 12, 90-103.
- Sugawara, N., Wang, X., and Haber, J.E. (2003). In vivo roles of Rad52, Rad54, and Rad55 proteins in Rad51-mediated recombination. *Mol Cell* 12, 209-219.
- Sun, H., Levenson, J.D., and Hunter, T. (2007). Conserved function of RNF4 family proteins in eukaryotes: targeting a ubiquitin ligase to SUMOylated proteins. *EMBO J* 26, 4102-4112.
- Svendsen, J.M., and Harper, J.W. (2010). GEN1/Yen1 and the SLX4 complex: Solutions to the problem of Holliday junction resolution. *Genes Dev* 24, 521-536.
- Sydorsky, Y., Srikumar, T., Jeram, S.M., Wheaton, S., Vizeacoumar, F.J., Makhnevych, T., Chong, Y.T., Gingras, A.C., and Raught, B. (2010). A novel mechanism for SUMO system control: regulated Ulp1 nucleolar sequestration. *Mol Cell Biol* 30, 4452-4462.
- Symington, L.S., and Gautier, J. (2011). Double-Strand Break End Resection and Repair Pathway Choice. *Annu Rev Genet* 45, 247-271.
- Szostak, J.W., Orrweaver, T.L., Rothstein, R.J., and Stahl, F.W. (1983). The Double-Strand-Break Repair Model for Recombination. *Cell* 33, 25-35.
- Takahashi, Y., Iwase, M., Strunnikov, A.V., and Kikuchi, Y. (2008). Cytoplasmic sumoylation by PIAS-type Siz1-SUMO ligase. *Cell Cycle* 7, 1738-1744.

LITERATURE

- Takahashi, Y., Kahyo, T., Toh, E.A., Yasuda, H., and Kikuchi, Y. (2001). Yeast Ull1/Siz1 is a novel SUMO1/Smt3 ligase for septin components and functions as an adaptor between conjugating enzyme and substrates. *J Biol Chem* 276, 48973-48977.
- Takahashi, Y., and Kikuchi, Y. (2005). Yeast PIAS-type Ull1/Siz1 is composed of SUMO ligase and regulatory domains. *J Biol Chem* 280, 35822-35828.
- Takahashi, Y., Toh, E.A., and Kikuchi, Y. (2003). Comparative analysis of yeast PIAS-type SUMO ligases in vivo and in vitro. *J Biochem* 133, 415-422.
- Tatham, M.H., Geoffroy, M.C., Shen, L., Plechanovova, A., Hattersley, N., Jaffray, E.G., Palvimo, J.J., and Hay, R.T. (2008). RNF4 is a poly-SUMO-specific E3 ubiquitin ligase required for arsenic-induced PML degradation. *Nat Cell Biol* 10, 538-546.
- Tong, H., Hateboer, G., Perrakis, A., Bernards, R., and Sixma, T.K. (1997). Crystal structure of murine/human Ubc9 provides insight into the variability of the ubiquitin-conjugating system. *J Biol Chem* 272, 21381-21387.
- Torres-Rosell, J., Sunjevaric, I., De Piccoli, G., Sacher, M., Eckert-Boulet, N., Reid, R., Jentsch, S., Rothstein, R., Aragon, L., and Lisby, M. (2007). The Smc5-Smc6 complex and SUMO modification of Rad52 regulates recombinational repair at the ribosomal gene locus. *Nat Cell Biol* 9, 923-931.
- Ulrich, H.D. (2008). The Fast-Growing Business of SUMO Chains. *Mol Cell* 32, 301-305.
- Ulrich, H.D. (2009). The SUMO system: an overview. *Methods Mol Biol* 497, 3-16.
- Ulrich, H.D., and Jentsch, S. (2000). Two RING finger proteins mediate cooperation between ubiquitin-conjugating enzymes in DNA repair. *EMBO J* 19, 3388-3397.
- Uzunova, K., Gottsche, K., Miteva, M., Weisshaar, S.R., Glanemann, C., Schnellhardt, M., Niessen, M., Scheel, H., Hofmann, K., Johnson, E.S., *et al.* (2007). Ubiquitin-dependent proteolytic control of SUMO conjugates. *J Biol Chem* 282, 34167-34175.
- van Gent, D.C., Hoeijmakers, J.H.J., and Kanaar, R. (2001). Chromosomal stability and the DNA double-stranded break connection. *Nat Rev Genet* 2, 196-206.
- Veaute, X., Jeusset, J., Soustelle, C., Kowalczykowski, S.C., Le Cam, E., and Fabre, F. (2003). The Srs2 helicase prevents recombination by disrupting Rad51 nucleoprotein filaments. *Nature* 423, 309-312.
- Verma, R., Oania, R., Fang, R., Smith, G.T., and Deshaies, R.J. (2011). Cdc48/p97 mediates UV-dependent turnover of RNA Pol II. *Mol Cell* 41, 82-92.
- Visintin, R., Prinz, S., and Amon, A. (1997). CDC20 and CDH1: A family of substrate-specific activators of APC-dependent proteolysis. *Science* 278, 460-463.
- Wang, A.Y., Schulze, J.M., Skordalakes, E., Gin, J.W., Berger, J.M., Rine, J., and Kobor, M.S. (2009). Asf1-like structure of the conserved Yaf9 YEATS domain and role in H2A. Z deposition and acetylation. *Proc Natl Acad Sci U S A* 106, 21573-21578.
- Wasch, R., and Cross, F.R. (2002). APC-dependent proteolysis of the mitotic cyclin Clb2 is essential for mitotic exit. *Nature* 418, 556-562.
- Weiffenbach, B., and Haber, J.E. (1981). Homothallic mating type switching generates lethal chromosome breaks in rad52 strains of *Saccharomyces cerevisiae*. *Mol Cell Biol* 1, 522-534.
- Weissman, A.M. (2001). Themes and variations on ubiquitylation. *Nat Rev Mol Cell Biol* 2, 169-178.
- Welchman, R.L., Gordon, C., and Mayer, R.J. (2005). Ubiquitin and ubiquitin-like proteins as multifunctional signals. *Nat Rev Mol Cell Biol* 6, 599-609.
- Werner, A., Flotho, A., and Melchior, F. (2012). The RanBP2/RanGAP1*SUMO1/Ubc9 complex is a multisubunit SUMO E3 ligase. *Mol Cell* 46, 287-298.
- Westman, B.J., and Lamond, A.I. (2011). A role for SUMOylation in snoRNP biogenesis revealed by quantitative proteomics. *Nucleus* 2, 30-37.

LITERATURE

- Westman, B.J., Verheggen, C., Hutten, S., Lam, Y.W., Bertrand, E., and Lamond, A.I. (2010). A proteomic screen for nucleolar SUMO targets shows SUMOylation modulates the function of Nop5/Nop58. *Mol Cell* 39, 618-631.
- White, C.I., and Haber, J.E. (1990). Intermediates of recombination during mating type switching in *Saccharomyces cerevisiae*. *EMBO J* 9, 663-673.
- Woodsmith, J., Jenn, R.C., and Sanderson, C.M. (2012). Systematic Analysis of Dimeric E3-RING Interactions Reveals Increased Combinatorial Complexity in Human Ubiquitination Networks. *Mol Cell Proteomics* 11, M111 016162.
- Wu, L., and Hickson, I.D. (2003). The Bloom's syndrome helicase suppresses crossing over during homologous recombination. *Nature* 426, 870-874.
- Xie, Y., Rubenstein, E.M., Matt, T., and Hochstrasser, M. (2010). SUMO-independent in vivo activity of a SUMO-targeted ubiquitin ligase toward a short-lived transcription factor. *Genes Dev* 24, 893-903.
- Yang, S.H., Galanis, A., Witty, J., and Sharrocks, A.D. (2006). An extended consensus motif enhances the specificity of substrate modification by SUMO. *EMBO J* 25, 5083-5093.
- Yin, Y., Seifert, A., Chua, J.S., Maure, J.F., Golebiowski, F., and Hay, R.T. (2012). SUMO-targeted ubiquitin E3 ligase RNF4 is required for the response of human cells to DNA damage. *Genes Dev* 26, 1196-1208.
- Yunus, A.A., and Lima, C.D. (2009). Structure of the Siz/PIAS SUMO E3 ligase Siz1 and determinants required for SUMO modification of PCNA. *Mol Cell* 35, 669-682.
- Zhang, Z.M., and Buchman, A.R. (1997). Identification of a member of a DNA-dependent ATPase family that causes interference with silencing. *Mol Cell Biol* 17, 5461-5472.
- Zhao, X., and Blobel, G. (2005). A SUMO ligase is part of a nuclear multiprotein complex that affects DNA repair and chromosomal organization. *Proc Natl Acad Sci U S A* 102, 4777-4782.
- Zhao, X.L., Muller, E.G.D., and Rothstein, R. (1998). A suppressor of two essential checkpoint genes identifies a novel protein that negatively affects dNTP pools. *Mol Cell* 2, 329-340.
- Zheng, G., and Yang, Y.C. (2004). ZNF76, a novel transcriptional repressor targeting TATA-binding protein, is modulated by sumoylation. *J Biol Chem* 279, 42410-42421.
- Zhou, B.B., and Elledge, S.J. (2000). The DNA damage response: putting checkpoints in perspective. *Nature* 408, 433-439.
- Zhu, Z., Chung, W.H., Shim, E.Y., Lee, S.E., and Ira, G. (2008). Sgs1 helicase and two nucleases Dna2 and Exo1 resect DNA double-strand break ends. *Cell* 134, 981-994.
- Zou, L., and Elledge, S.J. (2003). Sensing DNA damage through ATRIP recognition of RPA-ssDNA complexes. *Science* 300, 1542-1548.

Abbreviations

μ	micro
ψ	aliphatic amino acid
4-NQO	4-nitroquinoline 1-oxide
5'-FOA	5'-fluoroorotic acid
53BP1	p53 binding protein 1
aa	amino acid
AD	Gal4 Activation Domain
Ade	adenine
Amp	ampicillin
APC/C	Anaphase Promoting Complex / Cyclosome
APS	Ammonium peroxodisulfate
Arg, R	arginine
ATM	ataxia-telangiectasia mutated
ATP	adenosine 5'-triphosphate
ATR	ATM and Rad3-related
ATRIP	ATR interacting protein
BD	Gal4 DNA Binding Domain
BER	base excision repair
bp	base pairs
BRCA	BReast CAncer
BSA	bovine serum albumin
CDC	cell division cycle
cDNA	complementary DNA
ChIP	chromatin immunoprecipitation
Chr	chromosome
CPD	cyclobutane pyrimidine dimer
CPT	Camptothecin
C-terminal	carboxy-terminal
Cys, C	cysteine
D	Aspartic acid
D-box	Destruction box
D-loop	displacement loop
DBD	DNA Binding Domain
DDR	DNA Damage Response
dHJ	DNA double Holliday Junction
DMSO	dimethylsulfoxide
DNA	deoxyribonucleic acid
DNAase	deoxyribonuclease
dNTP	deoxynucleoside triphosphate
DSB	DNA double-strand break
dsDNA	double-stranded DNA
DTT	dithiothreitol
E	Glutamic acid
E1	Ubiquitin/SUMO activating enzyme
E2	Ubiquitin/SUMO conjugating enzyme
E3	Ubiquitin/SUMO ligase
EDTA	ethylenediaminetetraacetic acid
EMSA	electrophoretic mobility shift assay
EtBr	ethidium bromide
g	gram; gravitational constant
G1	gap 1 phase of the cell cycle
G2	gap 2 phase of the cell cycle (pre-mitotic phase)
G418	geneticine disulfate
GCR	gross chromosomal rearrangement

Abbreviations

GFP	green fluorescent protein
Gly, G	glycine
h	hour
H2B	histone 2B
HA	human influenza hemagglutinin epitope: YPYDVPDYA
HCSM	N-terminal hydrophobic cluster SUMO motif
HECT	homologous to E6-AP C-terminus
His	histidine
HJ	DNA Holliday junction
HO	HO endonuclease
HR	homologous recombination
HRP	horse radish peroxidase
HU	hydroxyurea
IP	immunoprecipitation
IPTG	isopropyl- β -D-1-thiogalactopyranoside
k	kilo
Kan	kanamycine
kb	kilo base pairs
kDa	kilo Daltons
l	liter
LC-MS/MS	Liquid Chromatography Tandem Mass Spectrometry
LB	Luria-Bertani
Lys, K	lysine
m	milli
M	molar
MAT	mating type
min	minute
MMR	mismatch repair
MMS	methyl methanesulfonate
MOPS	3-N-morpholinopropane sulfonic acid
mRNA	messenger RNA
MRX	yeast DSB-sensing Mre11/Rad50/Xrs2 complex
MW	molecular weight
Myc	human c-Myc protein derived epitope: EQKLISEEDL
n	nano
NAT	noursethricin
NDSM	negatively charged amino acid-dependent SUMO motif
NEM	N-ethylmaleimide
NER	nucleotide excision repair
NHEJ	non-homologous end-joining
Ni PD	Ni-nitrilotriacetic acid (NTA) pull-down
NPC	nuclear pore complex
nt	nucleotide
N-terminal	aminoterminal
OD	optical density
ON	overnight
ORF	open reading frame
PAGE	polyacrylamide gel electrophoresis
PBS	phosphate-buffered saline
PCNA	proliferating cell nuclear antigen
PDSM	phosphorylation-dependent SUMO motif
PCR	polymerase chain reaction
PEG	polyethylene glycol
PI3K	phosphoinositide 3-kinase
PIAS	protein inhibitor of activated STAT
PIP	PCNA-Interacting protein
PML bodies	promyelocytic bodies

Abbreviations

PMSF	phenylmethylsulfonyl fluoride
POL	polymerase
PrtA	protein A
PTM	posttranslational modification
qPCR	quantitative PCR
RFC	replication factor C
RING	Really Interesting New Gene
RNase	ribonuclease
RNR	ribonucleotide reductase
RPA	replication protein A
rpm	rounds per minute
RT	room temperature
s	seconds
S	sedimentation coefficient (Svedberg)
S-phase	DNA synthesis phase of the cell cycle
SAP domain	DNA binding domain after <u>S</u> AF-A/B, <u>A</u> cinus and <u>P</u> IAS
SC	synaptonemal complex
SC media	synthetic complete media
SCE	sister chromatid exchange
SD	standard deviation
SDS	sodium dodecylsulfate
SDSA	synthesis-dependent strand annealing
SEM	standard error of the mean
SENP	SUMO/Sentrin-specific protease
SIM	SUMO-interacting motif
SILAC	Stable Isotope Labelling with Amino Acids in Cell Culture
SIZ	SAP and mIZ-finger domain containing protein
SMC	Structural Maintenance of Chromosomes
SP-RING	Siz/PIAS-RING
ssDNA	single-stranded DNA
SSB	DNA single-strand break
STUbL	SUMO-targeted ubiquitin ligase
STR	Sgs1-Top3-Rmi1 complex
SUMO	Small Ubiquitin-like Modifier
SWI/SNF	SWItch/Sucrose NonFermentable
TBS	tris-buffered saline
TCA	trichloro acidic acid
TDG	thymine DNA glycosylase
TEMED	N,N,N,N'-tetramethylethylene diamine
Tris	Tris (hydroxymethyl) aminomethane
U	unit
Ub	ubiquitin
Uba	ubiquitin-activating
Ubc	ubiquitin-conjugating
UBD	ubiquitin-binding domain
Ubl	ubiquitin-like
UBP	ubiquitin-specific protease
UBZ	ubiquitin-binding zinc finger domain
ULP	ubiquitin-like protein (SUMO)-specific protease
UPS	ubiquitin-proteasome system
UV	ultraviolet light
V	Volt
v/v	volume per volume
w/v	weight per volume
WT	wild-type
YPD	yeast bactopectone dextrose

Acknowledgements

I would like to sincerely thank my research advisor, Stefan Jentsch, for his continuous support and trust in my work. I have been fortunate to have a thoughtful and open-minded mentor, who not only inspired me with new ideas and insightful advice, but also gave me the freedom to explore on my own and encouraged me at times when my attempts failed. Stefan's kindness, generosity and enthusiasm create a great working environment making his laboratory an exceptional place to do research. I am grateful that I got an opportunity to be a part of the Jentsch team.

I would also like to kindly acknowledge all the members of my doctoral thesis committee for dedicating their time to read and evaluate the manuscript, and in particular Prof. Dr. Peter Becker for kindly accepting to co-referee this work.

I would like to express my sincere gratitude to all my colleagues in the Jentsch lab for their constant help, fruitful discussions and for the great pleasure it has been to work with them. My special thanks go to Georgios, Sandrine, Christian, Marian and Steven for their kind advice and care right from the beginning of my studies. I would also like to thank Kenji, Qin, Florian, Kefeng, Tim, Sean, Joerg, Max, Ramazan, Greg and Matthias for their good moods and cheerful times we spent together.

Moreover, I would like to express my special thanks to Alex, who provided excellent technical assistance and contributed a lot to the success of this work. It was a true pleasure and privilege to work together. I am also grateful to Cyril Boulegue for the great support with the mass spectrometry analyses throughout my studies. In addition, I wish to thank Jochen, Ulla, Dirk, Massimo and Klara for their care about a myriad of things in the lab.

Finally, I am deeply thankful to my parents, family and friends for their understanding, encouragement and trust in me. I owe everything to their love and care.

Curriculum Vitae

Name Ivan PSAKHYE
Address Irschenhauser Str. 17
81379, München
Date / Place of birth May 19, 1984 / Tomsk, Russia

2007 – 2013 PhD studies: *Principles of protein group SUMO modification substantiated in DNA repair.*
Supervisor: Prof. Dr. Stefan Jentsch,
Max Planck Institute of Biochemistry,
Martinsried, Germany

2006 – 2007 Master's thesis: *Development of the drug-delivery system based on the bionanocomposites "nanoparticles-cysteine protease inhibitors" for diagnostics and cancer treatment.*
Supervisor: Prof. Dr. Vladimir Serebrov,
Siberian State Medical University, Tomsk, Russia,
in cooperation with Dr. Olga Vasiljeva,
Jožef Stefan Institute, Ljubljana, Slovenia

2001 – 2007 Student of Biochemistry, Department of Biochemistry and Molecular Biology, Siberian State Medical University, Tomsk, Russia

2000 – 2001 Nansemond River High School, Suffolk, Virginia, USA,
Freedom Support Act Future Leaders Exchange (FSA FLEX) program

1990 – 2001 Academlyceum High School, Tomsk, Russia

Publications

Jentsch S. and **Psakhye I.** Control of nuclear activities by substrate-selective and protein group SUMOylation. *Annual Review of Genetics*; 2013 (47, 185-204)

Psakhye I. and Jentsch S. Protein group modification and synergy in the SUMO pathway as exemplified in DNA repair. *Cell*; 2012 (151, 4, 807-820)

Mikhaylov G, Mikac U, Magaeva AA, Itin VI, Naiden EP, **Psakhye I**, Babes L, Reinheckel T, Peters C, Zeiser R, Bogyo M, Turk V, Psakhye SG, Turk B, and Vasiljeva O. Ferri-liposomes as an MRI-visible drug-delivery system for targeting tumours and their microenvironment. *Nature Nanotechnology*; 2011 (6, 9, 594-602)